Convention on Long-range Transboundary Air Pollution

emep

Co-operative programme for monitoring and evaluation of the long-range transmission of air pollutants in Europe

STATUS REPORT 4/2008

Transboundary particulate matter in Europe

Status Report 4/2008

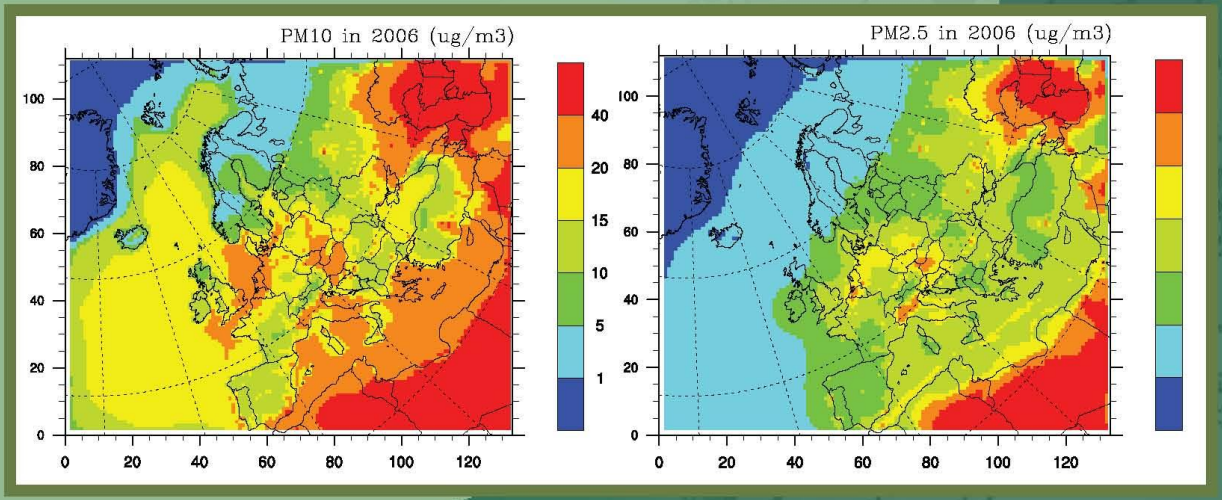

ccc & msc-w & ceip

NILU: EMEP Report 4/2008
REFERENCE: O-98134
DATE: AUGUST 2008
ISSN: 1504-6109 (print)
1504-6192 (online)

EMEP Co-operative Programme for Monitoring and Evaluation of the Long-Range Transmission of Air Pollutants in Europe

Transboundary particulate matter in Europe Status report 2008

Joint CCC, MSC-W and CEIP Report 2008

Norwegian Institute for Air Research
P.O. Box 100, NO-2027 Kjeller, Norway

Norwegian Meteorological Institute
P.O. Box 43 Blindern, NO-0313 Oslo, Norway

Umweltbundesamt GmbH
Spittelauer Lände 5, AT-1090 Vienna, Austria

List of Contributors

Karl-Espen Yttri[1], Wenche Aas[1], Kjetil Tørseth[1], Kerstin Stebel[1],
Ágnes Nyíri[2], Svetlana Tsyro[2],
Katarina Merckova[3], Robert Wankmüller[3]
Wilfried Winiwarter[4,5], Heidi Bauer[6], Alexandre Caseiro[6,7], Hans Puxbaum[6],
Thomas Holzer-Popp[8] and Marion Schroedter-Homscheidt[8]

1) Norwegian Institute for Air Research, Kjeller, Norway
2) Norwegian Meteorological Institute, Oslo, Norway
3) Umweltbundesamt, Vienna, Austria
4) International Institute for Applied Systems Analysis, Laxenburg, Austria
5) Austrian Research Centers – ARC, Vienna, Austria
6) Institute of Chemical Technologies and Analytics, Vienna University of Technology, Vienna, Austria
7) CESAM and Environment and Planning Department, University of Aveiro, Portugal
8) German Aerospace Center (DLR), German Remote Sensing Data Center (DFD), Oberpfaffenhofen, Germany

[1] EMEP Chemical Coordinating Centre
[2] EMEP Meteorological Synthesizing Centre – West
[3] EMEP Centre on Emission Inventories and Projections

Contents

Page

Executive Summary

The report presents the status of the activities undertaken under EMEP in relation to particulate matter in the European rural environment. An assessment is made on the observed chemical and physical properties at monitoring sites, an update is provided with respect to emissions of primary particles and further a model assessment of the concentration levels are given. The report also includes a special section on the importance of agricultural fires which had a significant impact on ambient particulate matter concentrations during 2006. Finally, two chapters present the comparison between model results and the comprehensive data series available from the intensive monitoring campaigns, and a comparison between satellite remote sensing data with EMEP monitoring and modelling results.

In total 49 sites have provided particulate mass observations from 2006 (47 for PM_{10} and 25 for $PM_{2.5}$) and this is an increase of 11 sites compared to 2005. There were 4 countries reporting PM mass concentration data for the first time. Still, the site density is poor in large regions of the EMEP domain, and in particular in the eastern areas and in the Mediterranean region. The lowest concentrations of PM_{10} are observed in the northern and north-western parts of Europe, while the highest levels are seen in Central-Europe. Nearly half of the sites experienced levels significantly higher than during 2005 (Scandinavia and parts of Germany), while about 43% of the sites had lower concentrations (Spain, Denmark and SW parts of Germany). The spatial trends of $PM_{2.5}$ generally resemble PM10 trends, and with the highest levels measured at Ispra in Italy. Also the increase from 2005 in Scandinavia and a decrease in SW Europe and Germany is apparent. The EU annual mean limit value of PM_{10} (40 µg m^{-3}) was not exceeded for any of the sites, however, about 40% of the sites (18 sites) experienced annual mean concentrations exceeding the Air Quality Guideline (AQG) for PM_{10} of 20 µg m^{-3}. Violation of the AQG was observed all across Europe, including parts of Scandinavia (Denmark) but was most pronounced for central Europe, southern Europe, and western Europe. The Austrian site Illmitz was the only site violating the 24 hour mean limit value for PM_{10} of 35 days exceeding 35 µg m^{-3} in 2006, reporting 37 days. Ispra was the only site exceeding the EU annual target value of $PM_{2.5}$ (25 µg m^{-3}) to be valid from 2010 with an annual mean $PM_{2.5}$ concentration of 28.5 µg m^{-3}, which is approximately 15% above the limit value. More than 50% of the sites were in exceedance of the WHO AQG for $PM_{2.5}$ of 10 µg m^{-3}. No part of Europe experience $PM_{2.5}$ levels below the targets set in the guidelines, and even Scandinavian sites, which typically report the lowest PM levels in Europe, are found to exceed the guideline. The seasonal pattern of exceedances of the WHO 24-hour air quality guideline for $PM_{2.5}$ is similar to that of PM_{10} and the EU limit value; i.e. the majority of the exceedances take place during spring and summer in the Mediterranean region and during winter for the rest of Europe.

While PM mass concentrations allow for comparing ambient concentrations with air quality limit values, it is only through the understanding the chemical composition of particles that the relationship between emissions, transport and transformations can be assessed, EMEP has thus its major focus on the chemical speciation and mass closure of PM. Historically focus has been on the secondary inorganic constituents SO_4^{2-}, NO_3^- and NH_4^+ and more recently has base cations,

sea salts and carbonaceous content become parts of the monitoring requirements. Still however, only few countries report a sufficient number of parameters to fully understand the regional particulate matter distribution and its origin. There were in total 31 sites measuring both PM_{10} and SO_4^{2-} in 2006, 25 measuring both PM while the number for PM_{10} and NO_3^- and only 12 measuring both PM_{10} and NH_4^+. SO_4^{2-} and NO_3^- contributed about equally to PM_{10}, accounting for 8-22% and 6-19% of PM_{10}, respectively. The relative contribution of NH_4^+ to PM_{10} ranged between 5-9%. SIA thus constitutes in the order of 15-45% of the aerosol mass and reductions in their precursor emissions remain essential to abate PM concentrations. In some regions, mineral dust has a significant contribution (mainly associated with dust events) but due to the low level of sites performing measurements of its constituents, further assessment is strongly impeded. It is only in coastal areas that sea-salts make a significant contribution to the aerosol mass concentrations, with levels normally not exceeding a few percent at continental sites. Potassium is associated with biomass burning, and its seasonal variation provides helpful insight to the relative contribution of different sources to ambient PM concentrations. Trends in PM mass concentrations are difficult to assess due to short time series and significant inter-annual variations caused by meteorological conditions.

There is still a general lack of comparable EC/OC data in Europe, which makes it difficult to address the spatial and temporal variation of these parameters on the regional scale. During 2006, measurements were made at in total 3 sites, and only two of those have time series extending back in time. The three sites represents very different conditions with one being located in Southern Norway (Birkenes) one in Italy (Ispra) and now also in Germany at Melpitz. The relative contribution of elemental carbon (EC) to total carbon (TC) in PM_{10} was 14% at Birkenes and 42% at Melpitz, while similar numbers for $PM_{2.5}$ was 16% and 48%. At Ispra there are no measurements of EC/OC in PM_{10} and the relative contribution of EC to TC was 23%. Total carbon mass in $PM_{2.5}$ at the sites Birkenes, Melpitz and Ispra were about 1, 4 and 11 $\mu g\ m^{-3}$ respectively.

Emissions on precursor gases and primary PM were reported for the first time this year to the newly established EMEP Center on Emission Inventories and Projections (CEIP). This implied some changes in the emission data used for modelling, that generally this year followed more closely what was reported by the Parties.This is particularly relevant for EECCA countries, for which emission expert estimates used last years were from Cofola et al. (2006) and those emissions were much higher than those used this year, as reported by the Parties. Changes in the total emissions within the EMEP area from 2005 to 2006 are generally small, with averaged reductions of -1.6% for SO_x, -1.3% for NO_x and -5.9% for NH_3. In the case of particulate matter, there are averaged reductions of -2.9% for $PM_{2.5}$ and -1% for PM_{coarse} if we consider only those countries and areas where PM emissions were available both in 2006 and 2005. The individual country emissions change more significantly from 2005 to 2006. These changes are different from country to country and region to region. For Asian areas expert estimates of PM emissions were not provided in 2005, while such data are accessible in 2006. Therefore, with the Asian areas included an increase of 0.4% is present for $PM_{2.5}$ over the EMEP area. For PM_{coarse} the increase is 8.1%

Our current knowledge about Primary Biological Aerosol Particles (PBAP), their atmospheric concentrations and emissions are rather limited, in particular for size fractions such as PM_{10} and $PM_{2.5}$ for which regulations and limit values exist. The recent advances within the use of source specific tracers have made it possible to address various sub classes of PBAP. In Chapter 2, PM_{10} concentrations of the two most common PBAP sub fractions, i.e. fungal spores and plant debris, have been quantified and presented based on the work by Winiwarter et al. (2008). Annual emissions of 233 Gg (as PM_{10}) have been derived for Europe. When scaling European emissions by land area, a global estimate of a few Tg annually are obtained, which is considerably less than the global predictions made by Penner et al. (2001) (56 Tg) and Jaenicke (2005) (1000 Tg). Even when considering the large uncertainty involved, the assessment by Winiwarter et al. (2008) tends to support the lower of the literature values available. The OC content of PBAP is found to contribute considerably (e.g. with 40% in Sweden) to the total OC emissions for selected European countries. These are countries with a low population density and where the anthropogenic emissions per area are small (e.g. the Scandinavian countries). Measurement data from a Norwegian site (Yttri et al., 2007a) confirms the emission estimate of 30% OC from PBAP presented here for Norway. Considerable progress in estimating PBAP emissions is still to be made. More specific tracers may contribute to obtain more precise emission factors. This can ultimately lead to an understanding where PBAP actually derive from, a prerequisite to investigate the release mechanism and to develop a source term of emissions.

From the combined EMEP model results and observations (Chapter 3), annual mean concentrations of regional background PM_{10} ranged from 5 to 20 μg m^{-3}, whereas the corresponding range for $PM_{2.5}$ was from 2 to 15 μg m^{-3} in 2005 over most of Europe. The regions characterized by the enhanced PM_{10} and $PM_{2.5}$ pollution, with concentrations exceeding 20 μg m^{-3} and 15 μg m^{-3} respectively, were the Benelux countries, central and northern Italy, south of Spain, central Europe (the Czech Republic, Slovakia, Hungary) and the southern part of the Russian Federation. Model results show that SO_4^{2-} is the main SIA component, contribute to PM_{10} between 10-15% in western Europe and between 25-30% in southern European countries and Russia. The contribution of NO_3^- to PM_{10} is 15–25% in central and western Europe, exceeding 30% in the Benelux countries and Germany, and varies between 5 and 15% in the rest of Europe. The contribution of NH_4^+ to PM_{10} is fairly flat, lying around 10-14% over central and eastern Europe, while it goes down to 5-10% in northern Europe, Spain and Russia. The concentrations of PM_{10} and $PM_{2.5}$ are lower by 5 to 20% in the Alps, in Finland, in the Russian Federation and in several EECCA countries, especially Ukraine and Moldova, in the year 2006 compared to 2005. Elsewhere, PM_{10} and $PM_{2.5}$ concentrations are higher by 5 to 15% in 2006 than in 2005 over the rest of EMEP area. The changes in PM concentrations are due to both emission changes and meteorological variability in 2006 compared to 2005. It is noted that the changes in emissions and meteorological conditions appear to make opposite effects on PM concentrations. The changes in primary $PM_{2.5}$ concentrations vary from below -40% in Belarus and Moldova (and in Sweden for primary coarse PM) to 15% in southern Kazakhstan (and in Spain for coarse PPM). One of the main reasons for the differences in primary PM concentrations is that expert estimated emissions in 2006 in Turkmenistan and Uzbekistan were taken into account in the model runs

this year compared to 2005. The overall levels of SIA concentrations are lower in 2006 than in 2005 due to the minor decreases in total emissions of SO_x, NO_x and NH_3. The most pronounced decrease in SIA concentrations by 15-20% are found in Ukraine, which is due to much smaller NO_x (by 49%) and NH_3 (by 41%) emissions and despite lower by 4% SO_x emissions in 2006 compared to 2005. SIA concentrations are about 2 to 5% higher in Finland and France as a result of larger SO_x and NO_x emissions in 2006 than in 2005. The meteorological variability explains somewhat 10-30% lower annual mean concentrations of $PM_{2.5}$ and PM_{10} (and individually primary PM and SIA) over Russia and 5 to 15% higher concentrations in the countries of southern and eastern Europe for 2006 compared to 2005. Higher PM concentrations over Spain and Italy are also due to the higher concentrations of wind blown dust in 2006 than in 2005, as predicted by the model. The model underestimates annual mean PM_{10} concentrations by 28% and $PM_{2.5}$ concentrations by 23% compared to the observed values in 2006. The spatial correlations between calculated and measured concentrations, which characterise model ability of reproducing mean regional gradients, are 0.70 for PM_{10} and 0.72 for $PM_{2.5}$. Model calculated the annual mean concentrations of the individual PM components lie mostly within 15% of the measured values; however, bias for NO_3^- is larger, being 33%. The coefficients of spatial correlation between calculated and observed concentrations of PM components vary between 0.74 and 0.97 on the annual basis. The temporal correlation coefficients between calculated and measured daily PM_{10} and $PM_{2.5}$ concentrations vary mostly between 0.4 and 0.6, averaging to 0.48 and 0.49 respectively.

Model calculations show that the regional background PM_{10} concentrations were below the EU annual limit value of 40 µg m^{-3} in all of Europe in 2006, with the exception of the outmost southern areas of the model domain. The annual mean PM_{10} exceeded the WHO AQG of 20 µg m^{-3} in some parts of the Benelux countries and in the Po Valley in northern Italy. These exceedances were mainly due to anthropogenic emissions, whereas in the south of Spain and the Russian Federation, eastern parts of Ukraine, Kazakhstan and in the Caucasus, PM exceedances were also due to a large influence of windblown dust. The calculated annual mean background concentrations of $PM_{2.5}$ exceeding 10 µg m^{-3} were found in most of central and eastern Europe, the Po Valley, the south of the Russian Federation and the EECCA (eastern Europe, Caucasus, central Asia) countries. In the southern regions of the modelled domain, windblown dust contributed considerably to the $PM_{2.5}$ exceedances in 2006. Model results show that in 2006, there were several places in Europe where the EU daily limit value of 50 µg m^{-3} was exceeded by regional background PM_{10} more than 35 days. Those are the Milan region, the Moscow region, in Belgium, in eastern Ukraine and southern parts of the Russian Federation and EECCA countries. Model calculations suggest that the emissions from anthropogenic sources were responsible to a large degree for the exceedances of the WHO AQGs for PM_{10} and especially for $PM_{2.5}$ in most parts of central and eastern Europe, whereas natural dust pollution is responsible for the impairment the air quality in the south of Europe and especially in the southern parts of Russia and EECCA countries.

PM emissions from wild fires can have significant impact on ambient air quality on the European regional scale. During spring 2006, large parts of Europe experienced reduced air quality for a prolonged period of time caused by

emissions from agricultural waste burning in eastern Europe; i.e. the Baltic States, western Russia, Belarus, and the Ukraine. Of particular interest was that this episode also affected the European Arctic. The episode was initiated by the late onset of spring in eastern Europe, forcing the farmers to await burning of agricultural waste until the snow was melted in late April. These initially prescribed fires, which spread to the natural vegetation, lead to concurrent fires over a large area and caused huge PM and gaseous emissions to the atmosphere. During this event record high levels of several pollutants were recorded in the European Arctic. E.g. the hourly O_3 concentration reached 166 µg m^{-3} at the Zeppelin observatory on Spitzbergen, whereas at Storhofdi (Iceland) experienced hourly concentration of 176 µg m^{-3}. The previous highest level of O_3 recorded at Zeppelin was 122 µg m^{-3} (1989) which illustrates to magnitude of this event. Also PM levels were extreme during the event. Forest fires can also have a significant impact on the pollution levels in more populated areas including in the urban environment. An evaluation of the 2006 episode and the performance of the EMEP model during the event is given in chapter 4.

Chapter 5 provides a first analysis of the observations and model performance during the EMEP intensive campaigns. These campaigns provide an opportunity to extend on a temporary basis the monitoring capacity towards the requirements set by the monitoring strategy and the first two sampling periods were set for June 2006 and January 2007. In total 9 sites offered an extended dataset with additional chemical or physical parameters throughout the campaigns. The data is shown to represent a very valuable material for model evaluation with respect to different PM components and to distribution of such constituents between the fine and the coarse mode. The first results of the comparison between calculated and measured concentrations of PM_{10} and $PM_{2.5}$ components did however shown somewhat mixed results for different stations. The main findings concerning the model performance with respect to reproducing the intensive measurements are presented; however, a further in-depth analysis of the results is envisaged.

Chapter 6 describes ongoing attempts to use satellite for the assessment of air quality levels in Europe. The first part presents the incorporation of a module to derive aerosol optical depth (AOD) in the EMEP model. It also presents a comparison between the AOD retrievals from MODIS measurements available from satellite remote sensing with the EMEP model estimates and the results are further compared with EMEP in situ observations. While strong limitations and significant differences are evident between the three datasets, results are still encouraging considering the expected future development expected in the remote sensing capacities. For the whole of EMEP grid, the model underestimates AOD by about 53% for summer and spring months and by 11% for late autumn-winter. The temporal correlation between modelled and MODIS AOD is better over land (lying between 0.4 and 0.65 in summer months) than over ocean. Rather mixed correlation between observed surface $PM_{2.5}$ and MODIS AOD is found for EMEP stations. In general, the correlation between measured $PM_{2.5}$ and AOD is better for southern European sites, lying mostly between 0.45 and 0.7, while it is lower for central and northern Europe (between 0.2 and 0.5). The interesting result is that for many sites, the correlation between modelled and MODIS AOD is higher than the correlation between calculated and measured $PM_{2.5}$. In addition, the utilization of a particular satellite data product, so-called SYNAER, for monitoring of

aerosols in Europe has been studied. The main advantage of this product is its ability to calculate, besides aerosol optical depth, aerosol composition and concentrations of particulate matter. It is quite clear that information obtained from satellites can contribute to our understanding of PM distribution in Europe, in particular in regions with a low or lacking coverage of EMEP stations. First evaluation results show that the overall quality of the AOD and PM data products looks very promising, but further validation needs to be performed to assess the product in depth.

1 Measurement of particulate matter in the European rural environment: Status in 2006

By Karl Espen Yttri and Wenche Aas

1.1 Concentrations, exceedances and trends

1.1.1 Introduction

Ambient particulate matter constitutes a complex mixture of various chemical compounds, which originates from a wide variety of sources, and their size varies over several orders of magnitude. The physical and chemical properties of PM vary with respect to time and place and they often inhibit a seasonal variability.

Particulate matter can cause a variety of negative effects on our environment. Currently, particulate matter is considered the most severe air contaminant encountered in Europe, causing about 300 000 excess deaths in Europe on an annual basis. The recent Air Quality Guidelines from WHO underline the importance of PM as a severe air pollutant, calling for a significant decrease in the ambient PM level. PM also affects the Earth's temperature through scattering of solar radiation and absorption of solar and terrestrial radiation. In addition, aerosols influence the radiative balance indirectly by affecting the optical properties, frequencies and lifetimes of clouds.

In Europe, PM measurements are mainly performed in urban areas in order to monitor human exposure to PM, while PM measurements in rural areas is less extensive around 50 sites. Rural measurements are important, as it has been demonstrated that the concentration gap between rural and urban areas can be quite marginal for certain regions in Europe. The atmospheric lifetime of aerosols is of a magnitude allowing significant transboundary fluxes. Thus, measurement of particulate matter was specifically added to the EMEP work programme in 1998 in order to monitor long-range transport of PM in Europe and its long-term trends. It is a steady increase in the number of sites measuring particulate mass concentration in EMEP, however, a further extension eastwards is still required to obtain a more comprehensive geographical overview of the rural background PM levels in Europe.

In last year status report (EMEP report 4/2007), we urged the countries that are reporting rural background PM data to the European Union but not to EMEP to coordinate their reporting better to ensure that these data are also submitted to EMEP. The situation has improved reflected by data-submission from Great Britain and The Netherlands. However there are additional countries that should look into their reporting routines. When looking into AirBase for 2006, there are PM_{10} data from EMEP sites in Finland (FI17 Virolahti); Belgium (BE13 Houlen); Bulgaria (BG39 Rojen Peak), Portugal (PT04 Monte Velho) and Macedonia (MK07 Lazaropole) which are not reflected in the EMEP database.

1.1.2 PM mass concentrations

The annual mean concentrations of PM_{10}, $PM_{2.5}$, and PM_1 for 2006 are presented in Table 1.1, whereas the spatial coverage of sites monitoring PM_{10} and $PM_{2.5}$ are shown in Figure 1.1.

For 2006, mass concentrations are reported for 49 sites (47 for PM_{10} and 25 for $PM_{2.5}$), which are 11 more than for 2005 (9 more for PM_{10} and 3 more for $PM_{2.5}$). For the sites CH01 (Jungfraujoch), DE44 (Melpitz), GR01 (Aliartos), GR02 (Finnokalia), GB36 (Harwell), IE0031 (Mace Head), 2006 was the first time mass concentrations have been reported to EMEP. In addition, data from the Netherlands and Great Britain have now been reported both to AirBase and EMEP which was not the case in 2005. 17 countries reported mass concentrations to EMEP for 2006, which is an increase by four countries. Despite the significant increase in number of sites reporting PM_{10} in 2006 compared to 2005, large parts of the EMEP domain are still not covered. This is particularly true for eastern Europe. Though, the inclusion of the two Greek sites makes an important extension to the eastern Mediterranean region. Furthermore, the inclusion of data from the Netherlands, UK and Ireland improves the geographical coverage in the north-western parts of Europe, which previously have been poorly represented.

The lowest concentrations of PM_{10} were observed in the northern and north-western parts of Europe, i.e. the Scandinavian Peninsula and northern Ireland, and for high altitude sites (> 800 m asl) on the European mainland (Figure 1.1 and Table 1.1). This spatial distribution of PM_{10} in 2006 corresponds with that reported for previous years and reflects both population density and major anthropogenic sources. While vehicular traffic and industry are important sources for the entire European mainland, mineral dust from local sources and Saharan dust events are likely to grow more important for the countries in the Mediterranean region. The lowest annual mean concentration of PM_{10} was observed at the Jungfraujoch (CH01) (3.3 µg m^{-3}) site situated in the Swiss Alps, whereas the highest was recorded at the Cypriote site (CY02) (33.8 µg m^{-3}). For previous years the highest annual mean has always been reported for the Italian site Ispra (IT04), however this site did not report levels of PM_{10} for 2006.

46% of the sites which reported levels of PM_{10} both for 2005 and 2006 experienced higher annual mean concentrations in 2006 compared to 2005. For the majority of these sites the increase was above 10%. The most significant increase was observed at the Swedish site Aspvreten (SE12), reporting a substantial 22% increase from 2005. In fact, the four sites situated on the Scandinavian Peninsula all reported an increase in the annual mean PM_{10} concentration exceeding 10%, averaging 16 ± 5%. An increase in the PM_{10} concentration exceeding 10% was also observed for two Swiss sites, i.e. CH02 (17%) and CH03 (20%), two German sites, i.e. DE02 (17%) and DE07 (12%) and the Cypriote site CY02 (17%). The increase in PM_{10} experienced by the majority of the sites going from 2005 to 2006 was mainly attributed to $PM_{2.5}$, although at the Norwegian site (NO01) also $PM_{10\text{-}2.5}$ contributed substantially.

43% of the sites which reported levels of PM_{10} both for 2005 and 2006 experienced lower annual mean concentrations in 2006 compared to 2005. For six of the 16 sites the observed decrease was higher than 10%. The most significant

decrease was observed for the Spanish site ES11, observing a decrease of 18% compared to 2005. A reduction of 14% and 11% was observed for the Spanish sites ES13 and ES15, respectively. The three Spanish sites are all located in western Spain, close to the Portuguese border. A decrease in the annual mean PM_{10} concentration corresponding to 14% was observed for the two German sites DE03 and DE08, whereas a decrease of 13% was observed for the Danish site DK05.

For four of the sites no change in the annual mean was observed.

Table 1.1: Annual mean concentrations of PM_{10}, $PM_{2.5}$ and PM_1 at EMEP sites for 2006 (concentrations in $\mu g\ m^{-3}$).

Code	PM_{10}	$PM_{2.5}$	PM_1	Code	PM_{10}	$PM_{2.5}$	PM_1
AT0002R	25.6	20.8	14.7	ES0013R	11.1	6.9	
AT0005R	10.0			ES0014R	16.9	10.4	
AT0048R	10.0			ES0015R	13.5	8.7	
CH0001G	3.3			ES0016R	13.2	8.7	
CH0002R	23.1	17.1	11.9	GR0001R	31.7		
CH0003R	22.1			GR0002R	25.9		
CH0004R	10.8	8.2	6.2	GB0006R	11.5		
CH0005R	11.3			GB0036R	21.7	12.3	
CY0002R	33.8			GB0043R	17.6		
CZ0001R	23.6			IE0031R		8.8	
CZ0003R	19.7	17.4		IT0001R	29.2	17.3	
DE0001R	19.6			IT0004R		28.5	
DE0002R	20.7	16.4	8.8	NL0007R	27.0		
DE0003R	8.3	5.6		NL0009R	26.8		
DE0007R	15.6			NL0010R	26.5		
DE0008R	10.5			NO0001R	8.1	5.0	3.7
DE0009R	18.4			PL0005R	20.6		
DE0044R	23.6	18.7		SE0011R	17.3	13.0	
DK0005R	21.4			SE0012R	11.6	8.2	
ES0007R	20.2	10.1		SE0035R	8.6		
ES0008R	18.4	9.0		SI0008R	15.9	13.1	
ES0009R	11.9	7.6		SK0004R	15.0		
ES0010R	19.0	10.1		SK0005R	21.9		
ES0011R	15.5	8.6		SK0006R	18.8		
ES0012R	14.1	8.4					

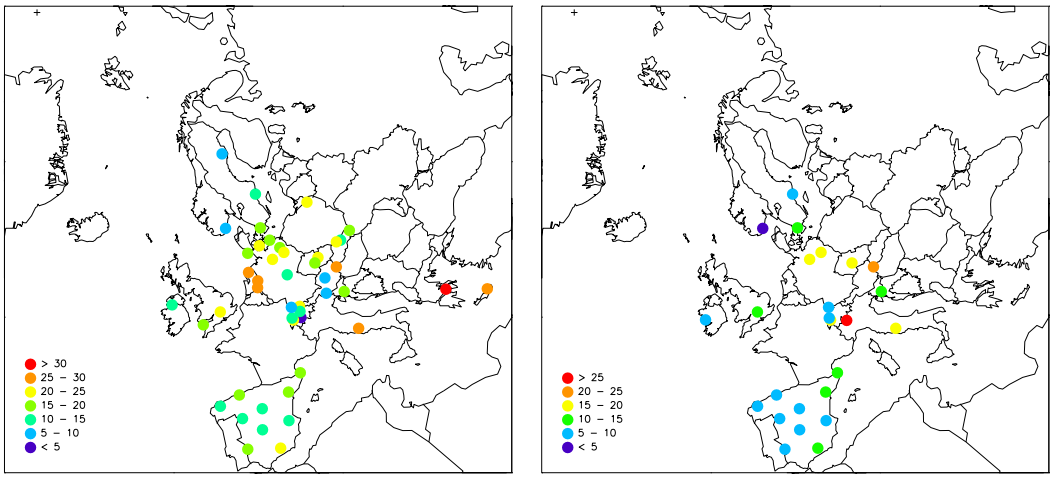

Figure 1.1: Annual mean concentrations of PM_{10} (left) and $PM_{2.5}$ (right) for 2006 ($\mu g\ m^{-3}$).

The highest annual mean concentrations of $PM_{2.5}$ were observed for sites situated in central Europe and Italy, whereas the concentrations reported for the Spanish sites were in the same range as that observed for southern Scandinavia (from Figure 1.1 and Table 1.1). The highest concentration of $PM_{2.5}$ was observed at the Italian site Ispra (IT04) (28.5 µg m^{-3}), whereas the lowest was reported for the Norwegian site Birkenes (NO01) (5.0 µg m^{-3}).

33% of the sites which reported levels of $PM_{2.5}$ both for 2005 and 2006 experienced higher annual mean concentrations in 2006 compared to 2005. For the majority of these sites the increase was above 10%, i.e. 14% on average. The most significant increase was observed at the German site Langenbrügge (DE02) and the Norwegian site Birkenes (NO01), reporting a substantial 22% increase from 2005. Also the Swedish site Vavihill (SE11) observed a significant increase of 19% in the annual mean concentration of $PM_{2.5}$.

62% of the sites which reported levels of $PM_{2.5}$ both for 2005 and 2006 experienced lower annual mean concentrations in 2006 compared to 2005. For four of the sites, the observed decrease was more than 10%. The most significant decrease was observed for the German site Schauinsland (DE03), observing a decrease of 23% compared to 2005. The remaining sites reporting reduced annual mean concentrations of $PM_{2.5}$ by 10% or more were all located in Spain i.e. ES10, ES11 and ES13. For the Spanish site ES08, the annual mean concentration of $PM_{2.5}$ was unchanged.

The annual mean concentration of PM_1 was reported for five sites, which is two more than for 2005. The two new sites reporting for 2006 were Birkenes (NO01) in Norway and Payerne (CH02) in Switzerland, thus annual mean concentrations of PM_1 are reported for four countries. The highest annual mean was reported for the Austrian site Illmitz (AT02) (14.7 µg m^{-3}), which is four times higher than that observed at the Birkenes site (3.7 µg m^{-3}), reporting the lowest annual mean. A decrease in the annual mean concentration of PM_1 of 13% was reported for the Swiss site CH04 from 2005 to 2006, whereas for the German site DE03 an

increase of 16% was observed. A decrease corresponding to 6% was observed for AT02.

1.1.3 Exceedances of limit values and guidelines

The EU annual limit value (EC, 2008) of PM_{10} (40 µg m^{-3}) was not exceeded for any of the sites reporting annual mean PM_{10} concentrations for 2006 (Table 1.1). However, about 40% of the sites (18 sites) experienced annual mean concentrations exceeding the Air Quality Guideline (AQG) for PM_{10} of 20 µg m^{-3} (WHO, 2005). Violation of the AQG was observed all across Europe, including Scandinavia (DK05), but was most pronounced for central Europe (AT02, DE02, DE44, CH02, CH03 and CZ01), southern Europe (CY02, IT01, GR01 and GR02), and western Europe (GB36, NL07, NL09 and NL10). These results show that a substantial effort is needed to cope with the guidelines in Europe, even in the rural background environment.

The number of days for which the EU daily PM_{10} limit value (50 µg m^{-3} not to be exceeded more than 35 days per year) was exceeded during 2006 is presented in Table 1.2. Note that not all the sites listed in Table 1.1 have daily or hourly measurements. 13 of the 30 sites reporting this parameter both for 2005 and 2006 observed an increase in the number of exceedances from 2005 to 2006, while 13 sites reported a decrease. For the remaining four sites no change in number of exceedances was observed. Note that for certain sites, i.e. the Czech sites, the data capture is less than 75%, thus the number of exceedances is likely underestimated.

For Spain, nine of ten sites reported a decrease or no change in the number of exceedances, while an increase was observed for the southernmost site (ES07). The number of days exceeding the limit value for the Spanish sites is closely associated with the frequency of Saharan dust intrusions. For the three non-Spanish southern European sites, a one day increase in the number of exceedances was observed for IT01, while a one day decrease was seen for SI08. For the Cypriotic site CY02, situated in the eastern Mediterranean region, the increase was more substantial, i.e. 23 in 2005 and 28 in 2006. A considerable increase in the number of exceedances was observed for selected Swiss and German sites from 2005 to 2006. For the two Swiss sites Payerne (CH02) and Tänikon (CH03) and the German sites Langenbrügge (DE02) and Neuglobsow (DE07), the number of exceedances increased by a factor of 4-6. For the two Swiss sites this corresponds to 24 more days in 2006 compared to 2005. The most severe episodes of high PM levels at these sites were observed in January and February. Filterpack measurements do not reveal any changes in the relative contribution of inorganic constituents for PM_{10} during these high PM_{10} concentration events.

Table 1.2: Number of exceedances of the daily PM_{10} limit value (50 µg m^{-3}) during 2006.

	Code	Number of exceedances of the daily limit value for PM_{10}				
		Total	Winter	Spring	Summer	Autumn
Central Europe	AT0002R	37	29			8
	AT0005R	0				
	AT0048R	0				
	CH0001G	2		1	1	
	CH0002R	29	29			
	CH0003R	30	27			3
	CH0004R	1	1			
	CH0005R	7	7			
	CZ0001R*	2		1		1
	CZ0003R*	3	3			
	DE0001R	3	1	1		1
	DE0002R	15	12	3		
	DE0003R	0				
	DE0007R	11	11			
	DE0008R	1	1			
	DE0009R	10	10			
	DE0044R	11	7	1		3
	GB0006R	0				
	GB0036R	3	1			2
	GB0043R	1			1	
	NL0007R	19	11	1		7
	NL0009R	18	8	5		5
	NL0010R	17	8		2	7
	PL0005R	12	10	2		
	SI0008R	5	5			
Southern Europe	CY0002R	28	12	6	9	1
	ES0007R	17		14		3
	ES0008R	0				
	ES0009R	1				1
	ES0010R	2	1			1
	ES0011R	1		1		
	ES0012R	0				
	ES0013R	0				
	ES0014R	2		1		1
	ES0015R	4		3		1
	ES0016R	2			2	
	IT0001R	21	8	9		4
	GR0002*	12	7	2		3
Northern Europe	DK0005R	9	4	3	1	1
	SE0011R	1	1			
	SE0012R	1		1		
	SE0035R	0				

**Data capture less than 75%*

The Austrian site Illmitz (AT02) was the only site violating the 24 hour mean limit value for PM_{10} of 35 days exceeding 50 µg m^{-3} in 2006, reporting 37 days. A minor decrease in number of exceedances was observed compared to 2005 (40 days). The number of exceedances at Illmitz in 2006 was slightly higher than the mean for the period 1999 – 2006 (34 days).

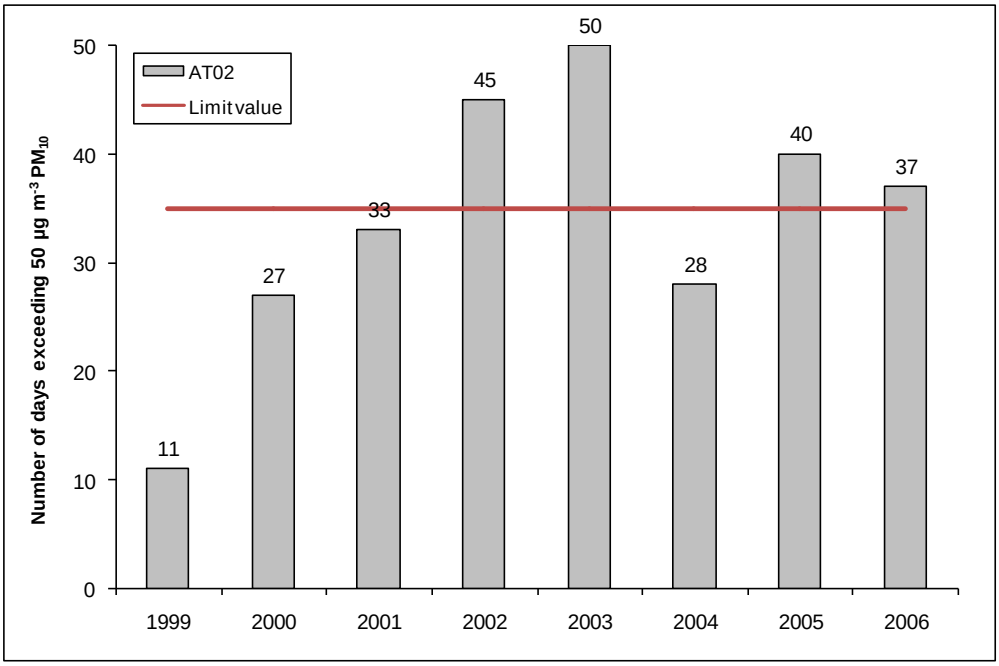

Figure 1.2: Number of days exceeding the 24-hour mean limit value for PM_{10} at the Austrian site Illmitz (AT02) for the period 1999-2006. The limit value is not to be violated more than 35 days pr year.

Table 1.2 shows the number of exceedances of the 24-hour PM_{10} limit value for each station with respect to season. Overall, the majority of the exceedances were observed in winter (more than 60%), likely reflecting increased anthropogenic emissions and unfavourable dispersion conditions. However, differences were observed for various regions of Europe. For southern Europe most (~40%) of the exceedances were observed in spring. This finding is largely influenced by the Spanish sites, which constitutes 10 of the 14 sites in the southern European region. For the other southern European sites, most exceedances were observed in winter. Interestingly, emissions from burning of agricultural waste were found to cause violation of the PM_{10} daily limit value at several sites, and in particular in northern, eastern and central parts of Europe. This topic is presented in more detail in chapter 4.

Ispra was the only site exceeding the EU annual target value of $PM_{2.5}$ (25 µg m^{-3}) to be valid from 2010 (EC, 2008) with an annual mean $PM_{2.5}$ concentration of 28.5 µg m^{-3}, which is approximately 15% above the limit value.

More than 50% of the sites reporting annual mean concentrations of $PM_{2.5}$ in 2006 exceeded the WHO AQG of 10 µg m^{-3} (WHO, 2005). No part of Europe

experience $PM_{2.5}$ levels below the targets set in the guidelines, and even Scandinavian sites, which typically report the lowest PM levels in Europe, are found to exceed the guideline. Of the ten Spanish sites, only three violated the AQG for $PM_{2.5}$ and that only by a small margin; the highest annual mean was observed at ES14 reporting an annual mean of 10.4 µg m^{-3}.

The sites violating the guideline exceeded it by more than 50% on average. At many sites, i.e. Illmitz (AT02), Payerne (CH02), Košetice (CZ03), Langenbrügge (DE02), Melpitz (DE44), Montlibretti (IT01) and Ispra (IT04), there is obviously a long way ahead before being in compliance with the WHO guideline, as they also exceed the WHO interim target three (IT-3) of 15 µg m^{-3}. The annual mean concentration of $PM_{2.5}$ at Ispra even exceeds the WHO interim target two (IT-2) of 25 µg m^{-3}. The interim targets have been defined in such a way that with successive and sustained abatement measures they will be achievable.

When comparing the daily values of $PM_{2.5}$ for 2006 with that of the WHO 24-hour guideline, *i.e.* the 99th percentile (corresponding to the fourth highest value of the year) of the distribution of daily values should not exceed 25 µg m^{-3}, 19 of 24 sites exceeded the guideline (Figure 1.3). The corresponding number for 2005 was 19 of 22, however the selection of sites are not the same for the two years. It is worth noting that the 99th percentile has increased substantially for selected sites, i.e. IT04 (by 25%), CH04 (by 31%), DE02 (by 57%) and CH02 (by 84%).

There are also three sites which fail to meet the interim target number 1 (IT-01) at 75 µg m^{-3} and these are located in central Europe and northern Europe; i.e. IT04 (99th percentile = 123 µg m^{-3}), AT02 (99th percentile = 80 µg m^{-3}) and Chaumont (99th percentile = 79 µg m^{-3}). Two more sites, DE02 (99th percentile = 66.2 µg m^{-3}) and DE44 (99th percentile = 58.2 µg m^{-3}) fail to meet the IT-2 requirement at 50 µg m^{-3}, while four more sites exceeds IT-3 (37.5 µg m^{-3}). The WHO has recommended *"that countries with areas not meeting these guideline values should take immediate action to achieve these levels in the shortest possible time."* The five sites not violating the guideline were DE03 (99th percentile = 18.9 µg m^{-3}), ES13 (99th percentile = 19.7 µg m^{-3}), ES09 (99th percentile = 20 µg m^{-3}), IE31 (99th percentile = 20.6 µg m^{-3}), and ES12 (99th percentile = 21 µg m^{-3}).

The seasonal pattern of exceedances of the WHO 24-hour air quality guideline for $PM_{2.5}$ is similar to that of PM_{10} and the EU limit value; i.e. the majority of the exceedances take place during spring and summer in the Mediterranean region and during winter for the rest of Europe.

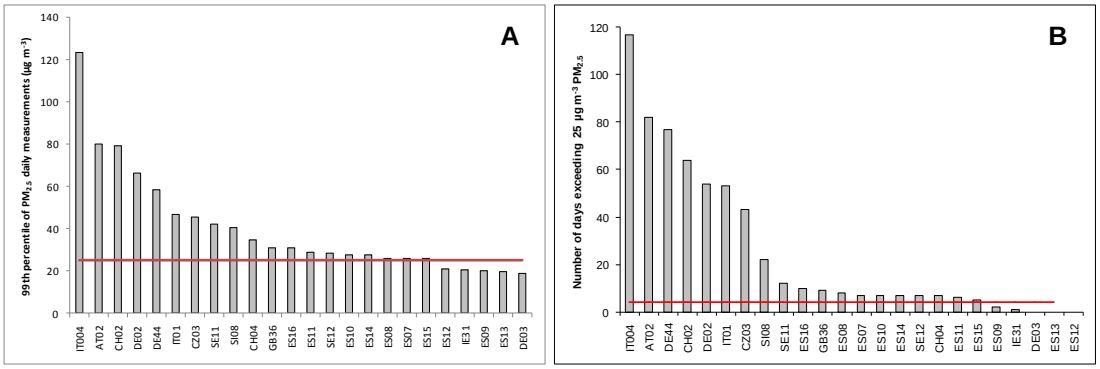

Figure 1.3: A) The 99th percentile for the annual distribution of $PM_{2.5}$ at rural background sites in 2006; (B) Number of days exceeding the WHO 24-hour air quality guideline for $PM_{2.5}$ at rural background sites in Europe.

1.1.4 Ratios

Ratios of $PM_{2.5}$ to PM_{10}, PM_1 to PM_{10}, and PM_1 to $PM_{2.5}$ for 2006 are summarized in Table 1.3 showing that sites in central Europe have rather high $PM_{2.5}/PM_{10}$ ratios (0.77 ± 0.05) compared to sites in Spain, Italy and Scandinavia (0.59 ± 0.06). This difference is probably associated with the high contribution of anthropogenic fine PM emissions to concentrations of PM_{10} in central Europe. In addition, the PM_{10} concentration in Spain and Italy is influenced by dust from semi arid regions and deserts, whereas for certain Scandinavian sites the influence by marine aerosols (sea-salt) could be important. Hence, this could be a possible explanation for why a larger fraction of the particles in southern Europe and in the Scandinavian countries is found in the $PM_{10\text{-}2.5}$ fraction, compared to central Europe.

Table 1.3: PM mass concentration ratios for 2006.

		Code	$PM_{2.5}/PM_{10}$	PM_1/PM_{10}	$PM_1/PM_{2.5}$
Southern Europe	Spain	ES07R	0.50		
		ES08R	0.49		
		ES09R	0.64		
		ES10R	0.53		
		ES11R	0.55		
		ES12R	0.59		
		ES13R	0.62		
		ES14R	0.62		
		ES15R	0.65		
		ES16R	0.66		
	Italy	IT01R	0.59		
Central Europe	Slovenia	SI08R	0.82		
	Austria	AT02R	0.81	0.57	0.70
	Switzerland	CH02R	0.74	0.53	0.70
		CH04R	0.75	0.56	0.77
	Germany	DE02R	0.79	0.42	0.54
		DE03R	0.68		
		DE44R	0.79		
Northern Europe	Norway	NO01R	0.61	0.44	0.75

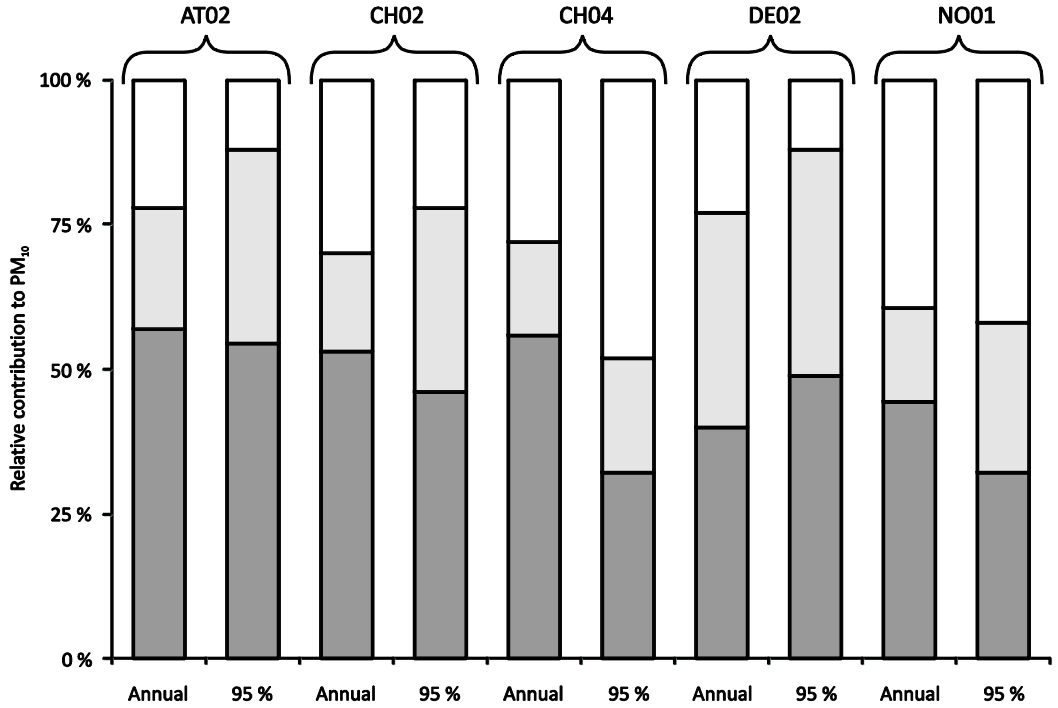

$PM_{10-2,5}$	0,22	0,12	0,30	0,22	0,28	0,48	0,23	0,12	0,39	0,42
$PM_{2,5-1}$	0,21	0,33	0,17	0,32	0,16	0,2	0,37	0,39	0,16	0,26
PM_1	0,57	0,54	0,53	0,46	0,56	0,32	0,40	0,49	0,44	0,32

Figure 1.4: Relative contribution of PM_1, $PM_{2.5-1}$ and $PM_{10-2.5}$ to PM_{10} at the sites Illmitz (AT02), Payerne (CH02), Chaumont (CH04), Langenbrügge (DE02) and Birkenes (NO01) for the year 2006 and for the 5-percent highest concentrations of PM_{10} in 2006.

PM_1 is the major fraction of PM_{10} on an annual basis for the five sites investigated, constituting between 40–55% of PM_{10}. The relative contribution is somewhat higher for the three most southerly sites (AT02, CH02, and CH04) (55%) compared to the two northern ones (DE02 and NO01) (42%). When addressing the relative contribution of $PM_{2.5}$ to PM_{10}, the four continental European sites all fall within a narrow range (70–78%), hence the $PM_{2.5-1}$ fraction nearly equals that of the PM_1 fraction at the DE02 site ($PM_{2.5-1}$ = 37 %; PM_1 = 40%). At the northern European site, $PM_{2.5}$ constitutes no more than 60% of PM_{10}. The relative contribution of the coarse fraction ($PM_{10-2.5}$) to PM_{10} ranged between 20–30% at the continental European site, while it accounted for nearly 40 % at NO01, which is just slightly less than that of the PM_1 fraction.

Distinct differences were observed when comparing the relative contribution of the various size fractions to PM_{10} for the days with the 5% highest PM_{10} concentrations at the different sites. For AT02, CH02 and DE02, 76–88% of PM_{10} could be attributed to $PM_{2.5}$, whereas more than 50% of $PM_{2.5}$ was accounted for by PM_1. Somewhat surprising, the coarse fraction of PM_{10} dominated the highest PM_{10} concentration samples at CH04 and NO01, accounting for 48% and 42%, respectively. For the Norwegian site this finding might be somewhat biased by the fact that samples was collected on a weekly frequency. For the German site, there is a poor data capture for PM_1 and $PM_{2.5}$ for those of the 5% highest PM_{10}

concentrations reported in winter, hence the mean values are schewed towards those days with high concentrations taking place in summer, which have a dominating coarse fraction.

1.1.5 Chemical composition of PM

Within EMEP speciation of particulate matter has historically been focused on the secondary inorganic constituent (SIA) formed in the atmosphere and which are known to have a long range potential, i.e. SO_4^{2-}, NO_3^- and NH_4^+. Also basecations and sea salts are part of the monitoring programmes, but with few countries reporting data. The carbonaceous content of PM is measured at a few sites only and is discussed more closely in chapter 1.2.

SO_4^{2-} is measured at a majority of the sites, while nitrate is often measured as the sum of NO_3^- and HNO_3 and ammonium as the sum of NH_4^+ and NH_3. However when using the filterpack method it is possible to report gas and particulate separately, though realizing that the gas/particles split can be biased due to evaporation of NH_4NO_3. Measurements using filterpack are typically not done with a specific size cut off, but it is commonly assumed to be around 10 µm. Secondary inorganic constituents are typically associated primarily with the fine fraction of PM_{10}.

For 2006, 31 sites reported concurrent measurements of PM_{10} and SO_4^{2-}, 25 for PM_{10} and NO_3^-, and 12 for PM_{10} and NH_4^+. This corresponds to 39%, 52% and 36% of the sites measuring SO_4^{2-}, NO_3^-, and NH_4^+, respectively. There were also some sites, 16 in total, which reported concentrations of PM_{10} for 2006, which did not have co-located measurements of SO_4^{2-}, NO_3^-, or NH_4^+ Indeed, effort should be undertaken so that such measurements are initiated at these sites in the near future.

Table 1.4 lists the relative contribution of the individual SIA to PM_{10} based on the data reported for 2006. SO_4^{2-} and NO_3^- contributed about equally to PM_{10}, accounting for 8-22% and 6-19% of PM_{10}, respectively. For those sites performing concurrent measurements of SO_4^{2-} and NO_3^-, SO_4^{2-} was typically the major constituent. The relative contribution of NH_4^+ to PM_{10} ranged between 5-9%. NH_4^+ always made a lower contribution to PM_{10} than SO_4^{2-} and NO_3^- at those sites were concurrent measurements was available.

To acquire mass closure of the PM mass typically requires analysis of the secondary inorganic constituents, the carbonaceous fraction, and the mineral dust content. For sites frequently influenced by marine air masses the sea salt contribution should also be measured. In 2006 the chemical data reported from the EMEP sites included only inorganic components, with the exception of three sites measuring the carbonaceous content. No sites reported concentrations of Silicon (Si), Aluminium (Al), and Iron (Fe), which are the most abundant constituents of mineral dust, originating from the Earth's crust. However, two sites included these measurements during the intensive period (see chapter 5). Ca was measured at eleven sites, and the relative contribution of Ca^{2+} to PM_{10} varied between 0.7% and 5%. The highest level was observed at ES09, which occasionally experience high levels of Saharan dust.

Measurements of all the major constituents of sea salt (Na^+, Cl^- and Mg^{2+}) were only reported for three sites in 2006. However, fourteen sites reported concentrations of one or two of the ions. When calculating the relative contribution of Na^+ to PM_{10} it was found to contribute less than 3.5% at all sites except at NO01, DK05 and DE01. At these three sites, which all are located quite close to the coastline, the relative contribution ranged from 5.2% and 7.9% (Table 1.4). At Birkenes, measuring all three constituents, the relative contribution was 12.1% on the annual basis.

Table 1.4: Relative contribution of SO_4^{2-}, NO_3^-, NH_4^+, Ca^{2+}, K^+, Cl^-, Mg^{2+} and Na^+ to PM_{10} at EMEP sites for 2006 (%).

Site	SO_4^{2-}/PM_{10}	NO_3^-/PM_{10}	NH_4^+/PM_{10}	Ca^{2+}/PM_{10}	K^+/PM_{10}	Cl^-/PM_{10}	Mg^+/PM_{10}	Na^+/PM_{10}
AT02	14	9	6	0.7	0.9		0.2	0.4
CH01	10							
CH02	10							
DE01	14	18	6	0.8	0.9		1.1	7.9
DE02	16	16	7	0.7	1.0		0.4	1.9
DE03	22	13	5	2.4	4.1		0.8	1.7
DE07	21	18	8	1.0	1.3		0.7	2.4
DE09	17	19	7	0.8	1.1		0.7	3.1
DE44	14	16	9	0.7	0.8	1.1	0.2	1.1
DK05	14			0.7	0.7	6.8		5.2
ES07	10	10						
ES08	21	11						
ES09	12	6		3.9	0.6		0.3	1.9
ES10	17	13						
ES11	13	8						
ES12	17	13						
ES13	16	12						
ES14	17	14						
ES15	11	10						
ES16	21	9						
GB06	11	8	5					
IT01	11	10	6					
NL09	8	13	6			2.6		
NL10	8	13	7			1.5		
NO01	20	16		1.6	0.6	5.5	1.1	5.5
PL05	12							
SE11	13							
SI08	18			1.3	0.9	0.3	0.3	0.9
SK04	20	10	9	1.0	1.1		0.1	1.3
SK05	17	12						
SK06	20	9						
Mean SD	**15 ± 4**	**12 ± 4**	**7 ± 1**	**1.3 ± 1.0**	**1.2 ± 0.9**	**3.0 ± 2.6**	**0.5 ± 0.4**	**2.8 ± 2.3**

Potassium was measured at twelve sites in 2006, typically accounting for a minor (< 1.5%) part of the mass concentration of PM_{10} on an annual basis. One exception was seen for Schauinsland (DE03), where the relative contribution was about 4%. The seasonal variation of potassium is different between the various sites (Figure 1.5). At Illmitz, levels of potassium were found to be increased by a factor of three in winter compared to summer, probably reflecting increased emissions by residential wood burning in winter. The same pattern is seen for the PM_{10}, but the relative contribution of potassium is higher during winter. At Schauinsland there are higher concentrations of potassium in summer and the relative contribution peaks in August. Increased levels of potassium during summer are usually attributed either to forest fires or biological material, *e.g.* fungal spores.

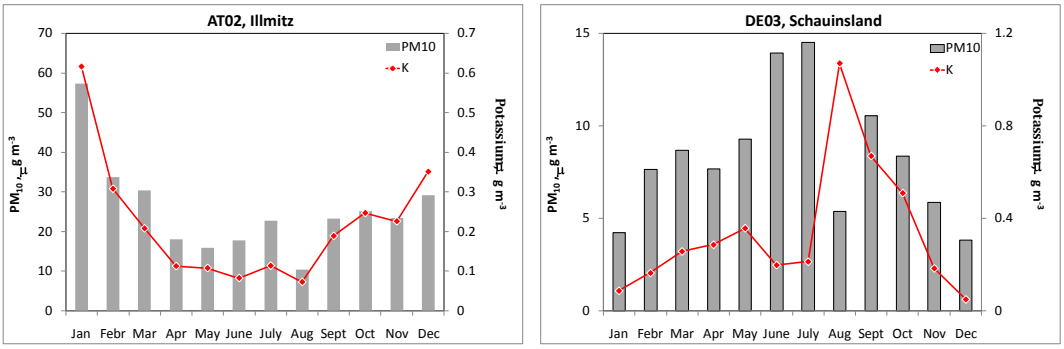

Figure 1.5: Monthly mean concentrations of potassium and PM_{10} at the Austrian site Illmitz (AT02, left) and the German site Schauinsland (DE03, right) during 2006.

1.1.6 Trends

13 of the sites reporting concentrations of PM_{10} for 2006 have time series extending more than five years. The longest time series, going back to 1997, are reported for the four Swiss sites. Six sites reporting concentrations of $PM_{2.5}$ for 2006 have time series that extend five years. The longest time series are reported for Chaumont (CH04) and Payerne (CH02), going back to 1998 and 1999, respectively. Both for PM_{10} and $PM_{2.5}$ none of these sites show a stepwise year-by-year reduction or increase in the concentration. Large inter annual variations are observed where the peak in 2003 is the most pronounced (Figure 1.6).

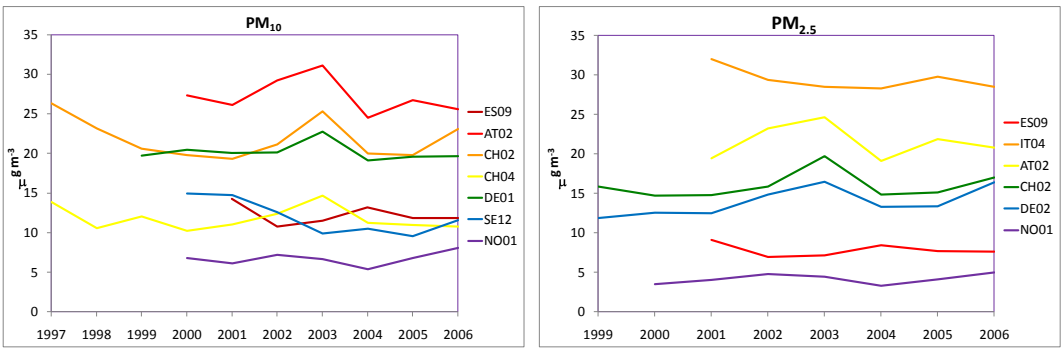

Figure 1.6: Time series of PM_{10} and $PM_{2.5}$ at selected EMEP sites.

Time series of the relative contribution of the individual SIA constituents to PM_{10} were examined for those sites reporting such data for a period of five years or more Figure 1.7. For the six sites examined with respect to SO_4^{2-}, the relative contribution was found to be rather consistent, with an exception of a few years for some of the sites (2002 for ES09 and 2003 for IT01). For NO_3^- and NH_4^+ the number of sites are so few and thus not reported.

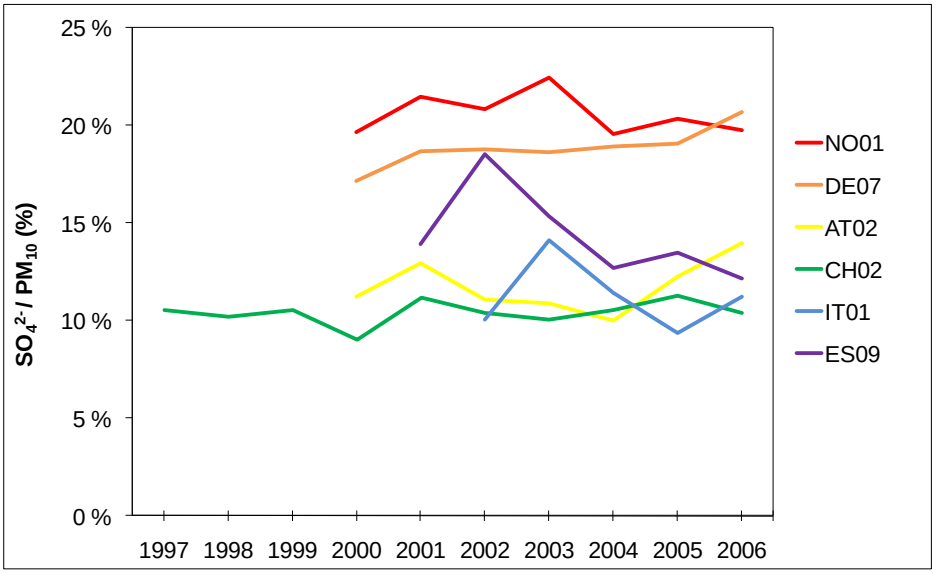

Figure 1.7: Relative contribution of SO_4^{2-} to PM_{10} for the period 1997–2006.

1.2 Monitoring of EC and OC within EMEP

1.2.1 Introduction

Long-term monitoring data of EC and OC are not yet available on the regional scale in Europe, although the importance of such data has been emphasized by e.g. Kahnert et al. (2004). Monitoring of EC and OC needs to rely on both robust and cost-efficient techniques, but at the same time a satisfactory quality of the data must be maintained. It has long been recognized that significant artefacts can be introduced during filter sampling of particulate matter for subsequent analysis of OC (McDow and Huntzicker, 1990), which can both grossly over and underestimate the samples content of OC. Furthermore, great analytical challenges are associated with splitting the aerosols content of EC from OC (Schmid et al., 2001).

A comprehensive work is currently going on within EUSAAR project (European Supersites for Atmospheric Aerosol Research, EC FP6 Infrastructures) to develop and optimise a unified protocol on artefact-free sampling of OC and thermal-optical analysis of EC and OC, for subsequent adaption by the EMEP TFMM. A status report on this work and on the first Round Robin test within EUSAAR for EC, OC and TC measurements was reported in last year's PM status report (EMEP, 2007) and will not be repeated here. Since then, the performance of the sampling train during summertime conditions have been tested and reported to EUSAAR.

In 2008, a second campaign is scheduled for testing of the sampling train's performance concerning negative sampling artefacts. With respect to the analytical protocol for quantification of the aerosol filter samples content of EC, OC and TC, testing of the first version (EUSAAR 1) revealed that inaccuracy in the split point between EC and OC could occur for selected samples at certain sites. Modifications to the protocol have been made to account for this, thus EUSAAR 2 will then hopefully be the final version. A second Round Robin test has been initiated in 2008, in which several EMEP sites are participating. Unlike the first inter comparison conducted in 2007, this second inter comparison will use the EUSAAR 2 protocol. The outcome of the second Round Robin test will give a first indication of the uncertainty range to be expected when the various laboratories starts to take the new analytical protocol into service.

1.2.2 Status of sampling and measurement, and quality of data

According to the current (2004 – 2009) EMEP monitoring strategy, quantifying the aerosols content of EC and OC is a level 2 activity. One more site (DE44) reported concentrations of EC and OC for 2006 compared to the previous years. Table 1.5 lists the three countries that reported such measurements for 2006. These sites are Birkenes (NO01) in Norway, Melpitz (DE44) in Germany, and Ispra (IT04) in Italy. At Birkenes, concentrations of EC and OC in PM_{10} and $PM_{2.5}$ have been reported since 2001, whereas at Ispra such measurements started in 2002. However, for 2006 only EC and OC concentrations for $PM_{2.5}$ were reported for Ispra. Melpitz reported levels of EC and OC for the first time in 2006, and for both PM_{10} and $PM_{2.5}$.

Table 1.5: Sites reporting EC and OC to the EMEP database, including size fractions and sampling period.

Site (Country)	EC	OC	PM_1	$PM_{2.5}$	PM_{10}	Period
Birkenes (Norway)	x	x		x	x	2001, 2002, 2003, 2004, 2005, 2006, 2007
Melpitz (Germany)	x	x		x	x	2006
Ispra (Italy)	x	x		x	x	2002[1)], 2003, 2004, 2005, 2006[2)]

1. EMEP EC/OC campaign
2. $PM_{2.5}$ fraction only.

Table 1.6 shows the sampling time and frequency, the filter face velocity, the sampling technique, and the analytical instrumentation used at the three sites. These are the most crucial parameters concerning the magnitude of the sampling artefacts of OC and the separation of EC and OC.

Similar sampling time and sampling frequency were only applied at two of the sites. Neither of the samplers operated according to a sampling technique that corrected for, or quantified, the negative artefacts, while a denuder was used to account for the positive artefact at Ispra.

Table 1.6: Sampling equipment and analytical approach used at the sites reporting EC and OC to the EMEP database.

Site (Country)	Sampling time/frequency	Filter face velocity	Sampling equipment	Analytical approach
Birkenes (Norway)	(6+1) days, weekly	54 cm s^{-1}	Single filter (no correction)	Sunset TOT (quartz. par)
Melpitz (Germany)	24 hr, daily	54 cm s^{-1}	Single filter (no correction)	VDI 2465 Part 2
Ispra (Italy)	24 hr, daily	20 cm s^{-1}	Denuder (pos. artifact)	Sunset Dual Optical Analyser

Thermal optical analysis was used to quantify the samples content of EC and OC at Birkenes and Ispra, whereas the samples collected at Melpitz were analyzed using a non-thermal system that do not account for charring of OC during analysis. According to Schmid et al. (2001) only methods that correct for charring during analysis, or that prevent charring to take place, should be recommended when it comes to splitting TC into EC and OC. Thus, any comparison of data from the three sites listed in Table 1.5 should only be based on TC. Despite that the results are not likely comparable with respect to EC and OC, they still provide valuable information concerning seasonal variation, mass closure of PM, and time-trends at the respective sites.

1.2.3 EC and OC levels in Europe

There is still a general lack of comparable EC/OC data in Europe, which makes it difficult to address the spatial and temporal variation of these parameters on the regional scale. Thus, the situation did not improve from 2005 to 2006. Currently there are only two datasets available that can be used to obtain such information, namely that of the EMEP EC/OC campaign (Yttri et al., 2007a), conducted during the period July 2002 to July 2003, and the CARBOSOL project (Pio et al., 2007), conducted during the period October 2002 – July 2004. Both datasets are comprehensive and benefits from thermal-optical analysis being used to quantify EC and OC, however, potential sampling artefacts were not accounted for. Data from these two campaigns have been used by Simpson et al. (2007) to validate the performance of the EMEP model with respect to OC and TC.

An increase in the number of countries and sites reporting levels of EC and OC are likely to increase markedly in the coming years, due to the importance and thus increased focus on such measurements and because of the ongoing development of a unified protocol for sampling and measurement of the ambient aerosol content of EC and OC.

1.2.4 EC and OC levels at the Norwegian site Birkenes (NO01)

The Birkenes atmospheric research station (58° 23'N, 8° 15'E, 190 m asl) is a joint supersite for EMEP and GAW and is situated approximately 20 km from the Skagerrak coast in the southern part of Norway. The site is often influenced by episodes of transboundary air pollution from continental Europe and has frequently been used to study long-range air pollution. The station is located in a boreal forest with mixed conifer and deciduous trees. The station has been operational since 1971.

Figure 1.8A-C shows the annual mean concentrations of EC, OC, and TC in PM_{10}, $PM_{2.5}$ and $PM_{10-2.5}$ at Birkenes for the period 2001–2007. During this period, OC in PM_{10} ranged from 0.8 µg m^{-3} to 1.2 µg m^{-3}, whereas the corresponding range for OC in $PM_{2.5}$ was 0.6–1.0 µg m^{-3}. For $PM_{10-2.5}$ the annual mean concentration of OC ranged from 0.1–0.3 µg m^{-3}. For PM_{10} and $PM_{2.5}$, the annual mean concentrations of EC ranged between 0.1–0.2 µg m^{-3} for the period in question. For $PM_{10-2.5}$ the annual mean concentration of EC did not exceed 0.05 µg m^{-3}. The mean TC concentration on the field blanks typically constitutes 10% of the annual mean TC concentration for PM_{10} and $PM_{2.5}$.

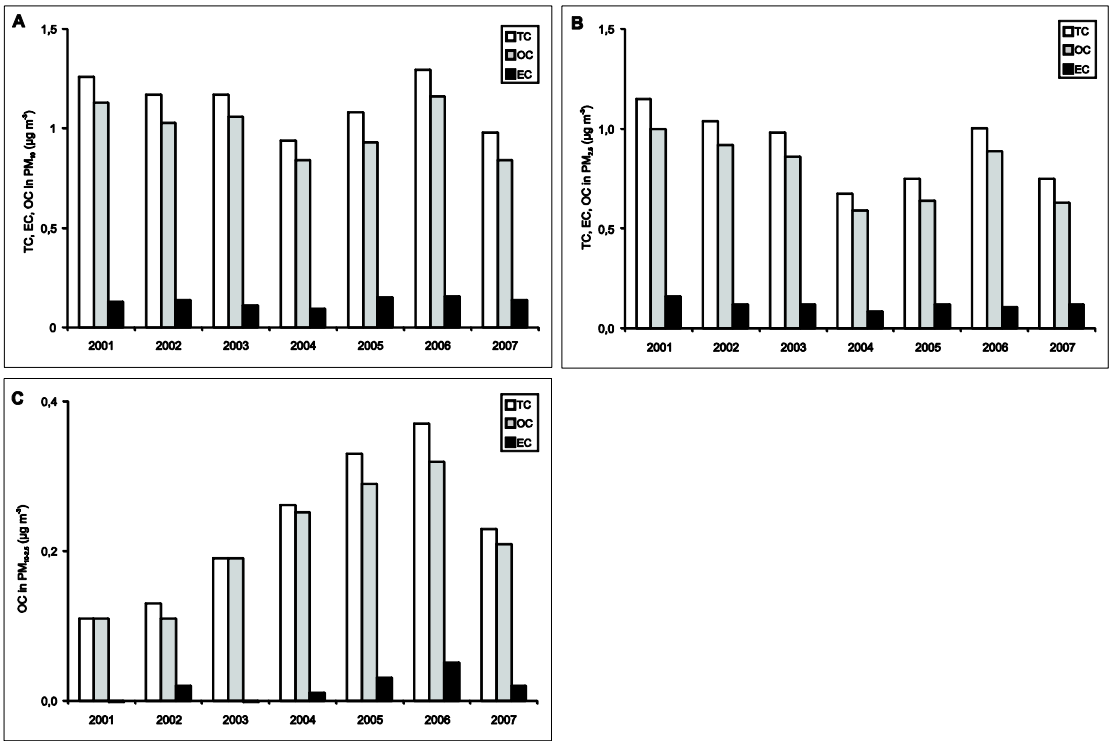

Figure 1.8: Annual mean concentrations of EC, OC and TC in PM_{10} (A), $PM_{2.5}$ (B) and $PM_{10-2.5}$ (C) at the Norwegian site Birkenes.

The concentration of OC in PM_{10} is always higher during summer compared to winter at Birkenes. This is observed for each year during the period 2001–2007. This is attributed to increased levels of $OC_{PM10-2.5}$ during summer. For $PM_{2.5}$, the increase of OC in summer is not as pronounced as for PM_{10}. For EC, the concentration tends to be higher in winter compared to summer for both PM_{10} and $PM_{2.5}$, but this is not a consistent pattern.

OC is always the dominant fraction of TC at Birkenes, regardless of size fraction (Table 1.7). In 2007, OC accounted for 86±6% of the TC fraction in PM_{10} on an annual basis, whereas the corresponding range for EC was 14±6%. Only minor differences were observed for $PM_{2.5}$ compared to PM_{10} with respect to the relative contribution of EC and OC to TC. The EC/TC ratio has an obvious seasonal variation both for PM_{10} and $PM_{2.5}$ with lower levels in summer compared to winter. This is characteristic for the entire period (2001 - 2007) during which such

measurements have been taken place (see Figure 1.11 in last year's report). This finding is particularly pronounced for PM_{10} and reflects decreased levels of EC and increased levels of OC in summer.

Table 1.7: Relative contributions of EC-to-TC and OC-to-TC for PM_{10} and $PM_{2.5}$ at the site Norwegian site Birkenes (NO01), the German site Melpitz (DE44) and at the Italian site Ispra (IT04).

Site	PM_{10}		$PM_{2.5}$	
	EC/TC (%)	OC/TC (%)	EC/TC (%)	OC/TC (%)
Birkenes (NO01)	14 ± 6	86 ± 6	16 ± 7	84 ± 7
Melpitz (DE44)	42 ± 11	58 ± 11	48 ± 14	52 ± 14
Ispra (IT04)			23 ± 7	77 ± 7

The majority of OC in PM_{10} can be attributed to the fine fraction for the period 2001 - 2007. For 2007, 76% of OC in PM_{10} could be attributed to $PM_{2.5}$. Fine OC makes a less contribution to OC in PM_{10} in summer and fall. This seems to be attributed to the impact of primary biological aerosol particles (PBAP) in summer (Yttri et al., 2007a, b), which mainly is found in the coarse fraction of PM_{10}. During summer, coarse OC may be the major fraction, accounting for more than 50% of OC in PM_{10} even on a monthly basis. This emphasizes the importance of monitoring OC in both $PM_{2.5}$ and PM_{10}.

Birkenes (NO01) has EC, OC, and TC time series of seven years (2001–2007). The decreasing concentrations of OC and TC observed from 2001–2004, was followed by a stepwise increase for the two consecutive years 2005–2006. After the rather high annual mean concentrations reported for OC and TC in 2006, the level decreased by approximately 25% for 2007. Thus, the annual mean concentrations of OC and TC are well below the mean concentration for the actual period for PM_{10} and $PM_{2.5}$, whereas for $PM_{10-2.5}$ the annual mean is equal to mean of the period 2001–2007. Concentrations of EC in PM_{10} decreased from 2006 to 2007, while for $PM_{2.5}$ the concentration increased. However, the changes are small and the levels low for EC.

For the period 2001–2007, the relative contribution of TCM-to-PM_{10} [(TCM = Total carbonaceous matter (TCM = OC x 1.7 + EC x 1.1)] at Birkenes has varied from 34% in 2001 to 26% in 2005/6 (Figure 1.9A). The relative contribution of TCM-to-$PM_{2.5}$ follows the same pattern as for TCM-to-PM_{10}, accounting for 47% in 2001 and 32% in 2006. A slight increase in TCM to both PM_{10} and $PM_{2.5}$ was observed for 2007 compared to 2006. The relative contribution of TCM to $PM_{10-2.5}$ ranged from 9–21% for the actual period. While TCM-to-$PM_{10-2.5}$ increased substantially from 2001–2004, corresponding to the major increase in the $OC_{PM10-2.5}$ concentration shown in Figure 1.8C, the relative contribution have declined slightly again from 2004 and onwards. Compared to SO_4^{2-}, NO_3^-, NH_4^+, and sea salt, TCM accounts for the greatest contribution of mass to PM_{10} at Birkenes (Figure 1.9B).

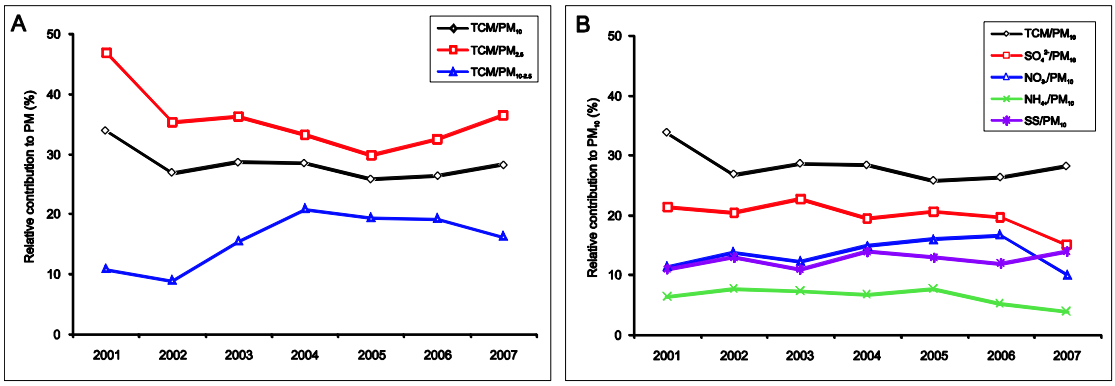

Figure 1.9: Relative contribution of TCM (Total Carbonaceous Matter) to PM_{10}, $PM_{2.5}$ and $PM_{10-2.5}$ (A) and relative contribution of TCM, SO_4^{2-}, NO_3^-, NH_4^+ and sea salt to PM_{10} (B).

1.2.5 EC and OC levels at the Italian site Ispra (IT04)

The Italian site Ispra (IT04) (45° 49'N, 8° 38'E, 209 m asl) is situated in the Po Valley in the north-western part of Italy. The site is representative for the rural parts of the densely populated central Europe and has been operational since 1985.

For 2006 the annual mean concentration of OC in $PM_{2.5}$ at Ispra was 8.8 µg m^{-3} whereas it was 2.5 µg m^{-3} for EC (Table 1.8). The annual mean concentration of TC in $PM_{2.5}$ was 11.3 µg m^{-3} $PM_{2.5}$.

Table 1.8: Annual mean concentrations of EC, OC, and TC in PM_{10}, $PM_{2.5}$ and $PM_{10-2.5}$ at the Italian site Ispra (IT04) for the years 2003-2006 (µg m^{-3}).

Year	PM_{10}			$PM_{2,5}$			$PM_{10-2.5}$		
	EC	OC	TC	EC	OC	TC	EC	OC	TC
2003	1.7	8.3	10.1	1.3	6.6	7.8	0.46	1.8	2.3
2004	1.8	9.0	10.8	1.6	8.6	10.2	0.14	0.42	0.56
2005	4.1	12.7	16.6	2.4	10.1	12.5	1.8	2.7	4.3
2006				2.5	8.8	11.3			

There were a slight reduction (~10 %) in the annual mean concentrations of OC and TC in $PM_{2.5}$ for 2006 compared to the previous year. For EC there were almost no change; i.e. 2.4 µg m^{-3} in 2004 vs 2.5 µg m^{-3} in 2006.

The carbonaceous sub fractions of $PM_{2.5}$ all have pronounced seasonal cycles, with elevated concentrations in winter compared to summer (Figure 1.10). This is in agreement with what was observed at Ispra in previous years. Indeed, the highest monthly reported for Ispra in 2006, i.e. in January, was 6–7 times higher than the lowest monthly mean, which was observed in June.

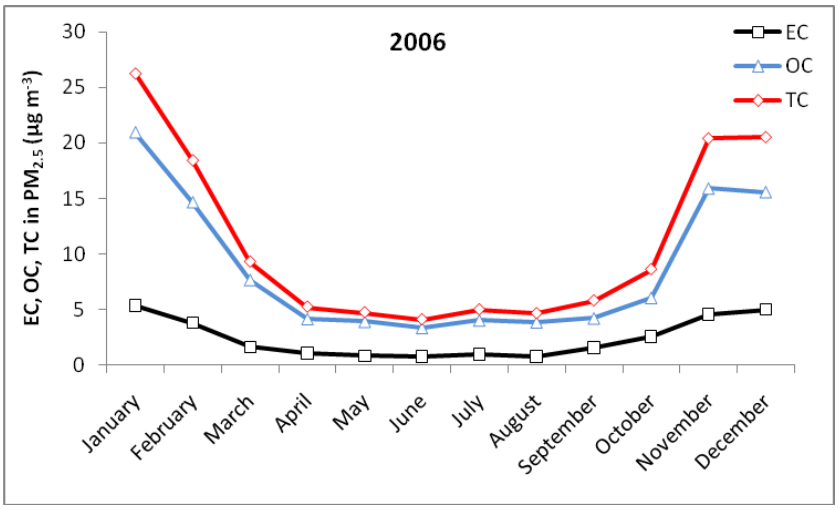

Figure 1.10: Monthly mean concentrations of EC, OC and TC in $PM_{2.5}$ at the Italian site Ispra (IT04) for 2006.

From Table 1.7 it can be seen that OC was the dominant fraction of TC at Ispra for 2006, accounting for 77±7% of TC in $PM_{2.5}$. The corresponding percentages for EC were 23±7%. A somewhat higher annual mean EC/TC ratio was observed for 2006 compared to the previous year.

For 2006 the annual mean concentration of TCM accounted for 50% of $PM_{2.5}$ (Figure 1.11). This is in accordance with the two previous years, but higher than for 2003 (37%). A conversion factor of 1.4 was used to convert OC to OM at Ispra, whereas a factor of 1.1 was used to account for hydrogen associated with EC (Kiss et al., 2002). The conversion factors for OC reported in literature range from 1.2-2.6, depending on the origin of the aerosols and to what extent they have been aged in the atmosphere (Turpin and Lim, 2001). Undoubtedly, the use of such a wide range of conversion factors might introduce a significant level of uncertainty to the TCM-to-PM estimates.

From Figure 1.11 it is apparent that the relative contribution of carbonaceous matter to $PM_{2.5}$ at Ispra is much higher than any of the single inorganic secondary constituents measured. The carbonaceous fraction is also higher than the sum of SO_4^{2-}, NO_3^- and NH_4^+ for all years considered (2003–2006).

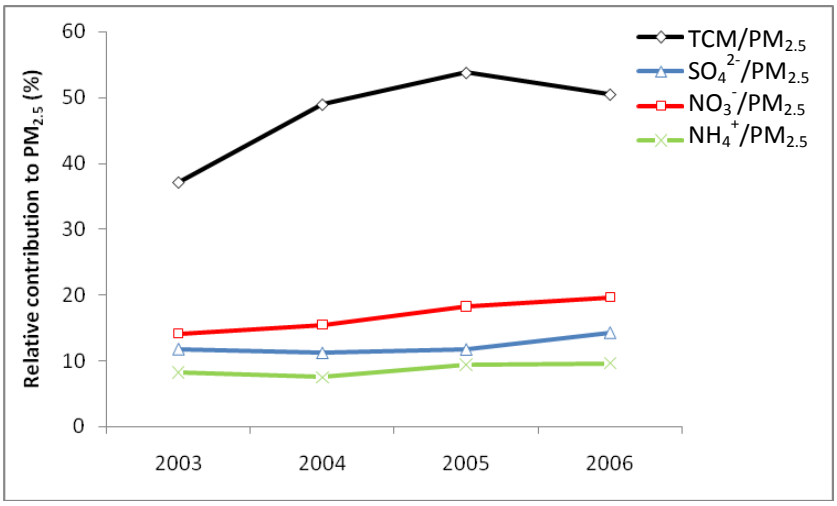

Figure 1.11: Relative contribution of TCM (Total Carbonaceous Matter) and major inorganic constituents to $PM_{2.5}$ at Ispra for the period 2003–2006.

1.2.6 EC and OC levels at the German site Melpitz (DE44)

The third site reporting levels of EC, OC and TC for 2006 was the German site Melpitz (51° 32' N, 12° 54' E, 87 m asl). As Ispra and Birkenes, Melpitz is a supersite in the EUSAAR (European Supersites for Atmospheric Aerosol Research) network. The site is situated in an agricultural area and is surrounded by meadows for fodder production.

The annual mean concentration of OC at Melpitz was 3.1 µg m^{-3} for PM_{10} and 2.1 µg m^{-3} for $PM_{2.5}$ (Table 1.9). The corresponding levels for EC were 2.3 µg m^{-3} (PM_{10}) and 1.9 µg m^{-3} for $PM_{2.5}$. The annual mean concentration of TC was 5.4 µg m^{-3} for PM_{10} and 2.0 µg m^{-3} for $PM_{2.5}$. For $PM_{10\text{-}2.5}$ the annual mean concentration of EC, OC and TC were 0.9 µg m^{-3}, 1.1 µg m^{-3}, and 2.0 µg m^{-3} respectively. Concentrations of carbonaceous sub fractions in $PM_{10\text{-}2.5}$ are calculated from the PM_{10} and $PM_{2.5}$ data. Samples providing negative concentrations for either of the three sub fractions are not included in the annual mean of EC, OC and TC in $PM_{10\text{-}2.5}$. Large variation were observed when comparing the monthly mean concentrations of TC; i.e. TC varied by more than a factor of four for PM_{10} and a factor of seven for $PM_{2.5}$.

Table 1.9: Annual mean concentrations of EC, OC, and TC in PM_{10}, $PM_{2.5}$ and $PM_{10\text{-}2.5}$ at the German site Melpitz (DE44) for 2006 (µg m^{-3}).

Year	PM_{10}			$PM_{2.5}$			$PM_{10\text{-}2.5}$ [1)]		
	EC	OC	TC	EC	OC	TC	EC	OC	TC
2006	2.3	3.1	5.4	1.9	2.1	4.0	0.9	1.1	2.0

1) Annual mean concentrations of EC, OC and TC in $PM_{10\text{-}2.5}$ are based on concurrent 24 hour measurements of EC, OC and TC in PM_{10} and $PM_{2.5}$ for which the difference between EC, OC and TC in PM_{10} and $PM_{2.5}$ is > 0.

The temporal variation of EC, OC and TC strongly resemble each other for all three size fractions, however there were no pronounced seasonal variation observed, except that EC was slightly higher in winter. OC was the major fraction of TC, however by a much less margin compared to the two other sites reporting such measurements (Table 1.7). For PM_{10}, 58% of TC was attributed to OC, whereas the corresponding percentage for $PM_{2.5}$ was 52%. These rather low OC/TC ratios can be explained by the analytical procedure used for quantification of the samples from Melpitz. The VDI protocol does not correct for charring of OC during analysis, hence artificial EC generated during the analysis is added to the initial EC and thus overestimating the true EC concentration in the sample. Despite this erroneous feature of the instrument, the results could still provide useful information concerning seasonal variation and time trends. However, it could introduce substantial uncertainties in mass closure studies.

The majority of the carbonaceous matter in PM_{10}, here measured as TC, was associated with fine aerosols. For 2006 the frequency based annual mean $PM_{2.5}/PM_{10}$ ratio for TC was 63%. This shows that a substantial amount of the carbonaceous matter actually is present in the coarse fraction of PM_{10}, which typically is associated with primary biological aerosol particles (PBAP). However, no obvious seasonal variation in this ratio was observed which could point towards an increased influence of such biogenic sources in summer and fall. Nevertheless, previous studies including measurements of odd and even numbered alkanes have shown that biogenic material contributes to the coarse fraction at this site in summer.

The relative contribution of TCM, that is the sum of organic matter (OM) and elemental matter (EM), to PM_{10} and $PM_{2.5}$ is presented in Figure 1.12. For PM_{10} 30% could be attributed to TCM, whereas the corresponding percentage for $PM_{2.5}$ was 27%. As the analytical method (VDI) used leads to an erroneous separation of EC and OC, the relative contribution of TCM to PM_{10} and $PM_{2.5}$ is underestimated. Thus, the difference between the relative contribution of the sum of the secondary inorganic constituents (SO_4^{2-}, NO_3^-, and NH_4^+) and TCM to PM_{10} and $PM_{2.5}$ is somewhat less than that predicted in Figure 1.12.

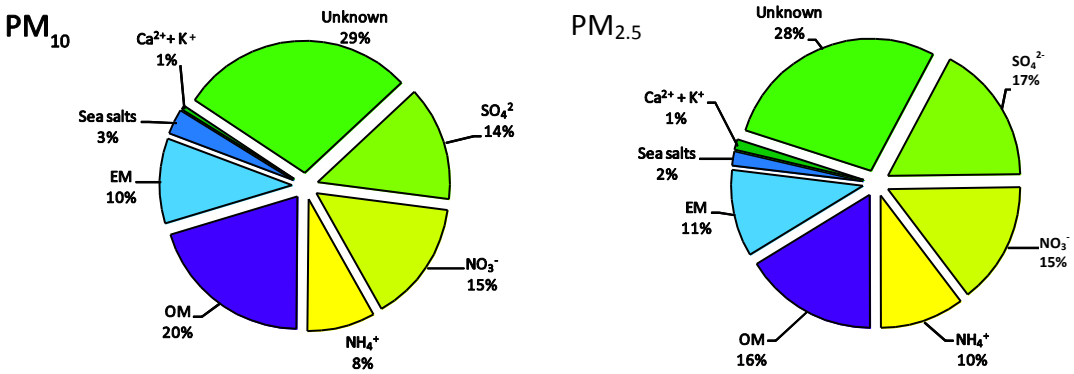

Figure 1.12: Relative contribution of TCM (Total Carbonaceous Matter = Organic matter (OM) + Elemental matter (EM)) and major inorganic constituents to PM_{10} (left) and $PM_{2.5}$ (right) at Melpitz (DE44) for 2006.

2 PM emissions, status 2006

By Ágnes Nyíri, Wilfried Winiwarter, Katarina Mareckova, Robert Wankmüller, Heidi Bauer, Alexandre Caseiro and Hans Puxbaum

2.1 Anthropogenic emissions in the official EMEP area

2.1.1 Emission data submitted in 2006

Parties to the LRTAP Convention submit annually air pollution emission data for precursor gases and primary particulate matter (SO_x, NO_x, NH_3, $PM_{2.5}$ and PM_{10}). This year the emission data was submitted for the first time to the newly constituted EMEP Centre on Emission Inventories and Projections (CEIP) and the LRTAP Convention secretariat was notified thereof. The deadline for submission of 2006 data was 15 February 2008. Parties were requested to report emission inventory data using standard formats in accordance with the EMEP reporting guidelines.

40 of the 51 Parties to the Convention submitted inventories in 2008. Of these Parties 30 reported emission data by the due date of 15th February 2008. 59% of the Parties reported on time and another ten Parties submitted data after the deadline, thus increasing the number of submissions to 78%. This is a slight increase compared with last year. Three Parties - Luxembourg, Lichtenstein and the Russian Federation - did not submit data before 30th June 2008. Data as submitted by Parties can be accessed on: http://www.ceip.at/emission-data-webdab/2008-submissions-under-clrtap/.

Gridded data and projections are parts of the five year reporting obligation and as such were not due in 2008. However, seven Parties (Estonia, Finland, Latvia, Lithuania, Portugal, Romania and Spain) submitted gridded sectoral and national total emissions and one Party (Slovakia) re-submitted gridded national total emissions. CEIP also imported late 2007 submissions of 2005 gridded data for the EC and Croatia into the database. The availability of 2005 gridded sector data used for EMEP modelling improved considerably compared to year 2000.

In 2008, 18 Parties submitted emission projections, out of which only 13 Parties submitted data for 2020. Analysis of the completeness of projections is out of the scope of this evaluation. However, one should note that projected values that were previously reported would show up as emissions for 2005 if no data is reported this year. More detailed information on data submitted by Parties is provided in the EEA/CEIP Inventory review report 2008 (Marackova et al., 2008).

2.1.2 Emission data used for modelling purposes in 2006

Before sectoral emission data can be used by modellers, missing information has to be filled in. To gap-fill missing data CEIP used three methods:

a) data submitted under the UNFCCC
b) linear extrapolation of the last five years (three as a minimum) or
c) copy of last year's emissions.

It has to be pointed out that only those sectors are gap-filled in which emissions for 2005 occurred (based on data compiled by MSC-W and published on WebDab http://www.ceip.at/emission-data-webdab/gap-filled-emissions/).

The geographical distribution and the magnitude of replacements are shown in Figure 2.1 for precursor gases and Figure 2.2 for primary particles. With a few exceptions, this year the corrections of official emissions have been done mainly for EECCA and South-Eastern European countries. The main reason to substitute official emission estimates is related to incomplete or lacking reporting in the submission by the Parties. Only data submitted before 10th April 2008 to CEIP could be included in the expert emission data set used in the modelling work. Greece, Italy, Iceland, Luxembourg, Lichtenstein and the Russian Federation submitted emission data after the above deadline, thus their 2006 emissions were also gap-filled by CEIP.

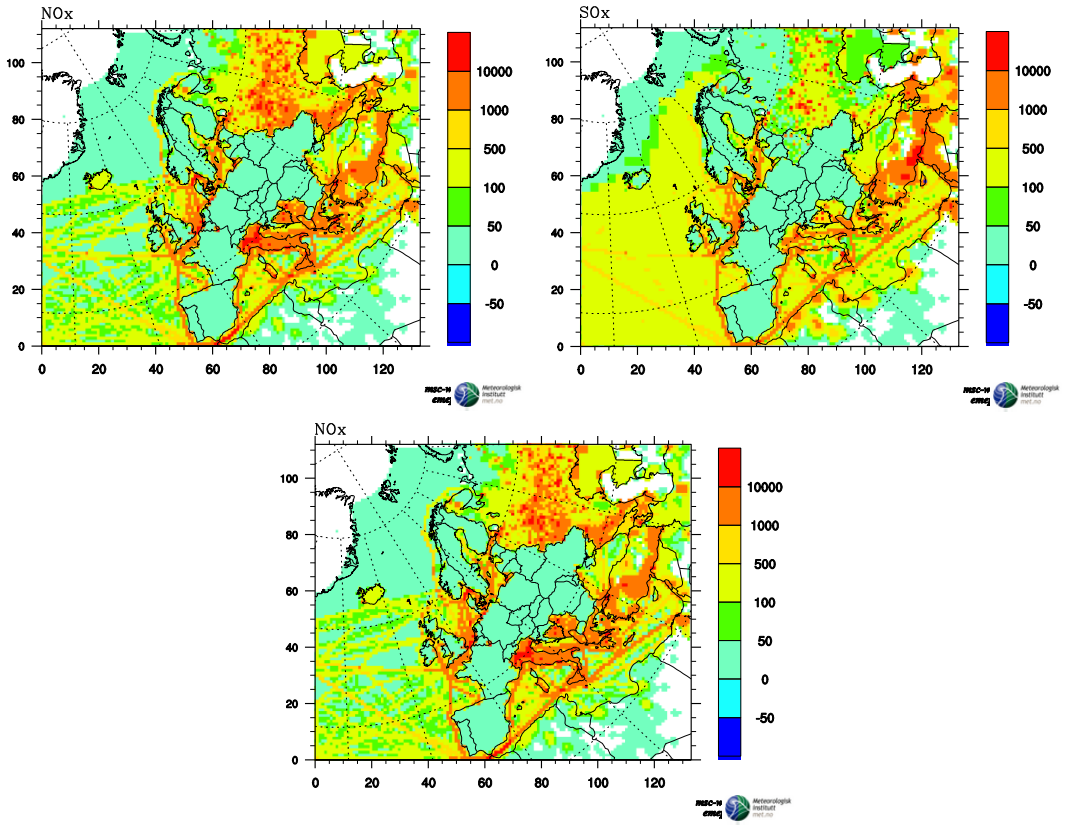

Figure 2.1: Differences between replacements by non-Party estimates and official estimates in 2006 for emissions of precursor gases. Positive values show where the non-Party emissions are higher than the official emissions. Units: Mg.

For all pollutants, the gap-filling leads to over 40% higher emissions over the land areas of the EMEP domain than the officially reported emissions. This is mainly because the Russian Federation, which is a significant emitter country in the EMEP area, is one of the countries where most emission data is gap-filled. The largest relative difference between official emission estimates and non-Party estimates is for primary PM emissions that are more than doubled after the

replacements. The reason for this is that beside the countries which did not submit emission data at all, or sent late submissions, there are several South-Eastern European countries reporting incomplete emissions for primary PM.

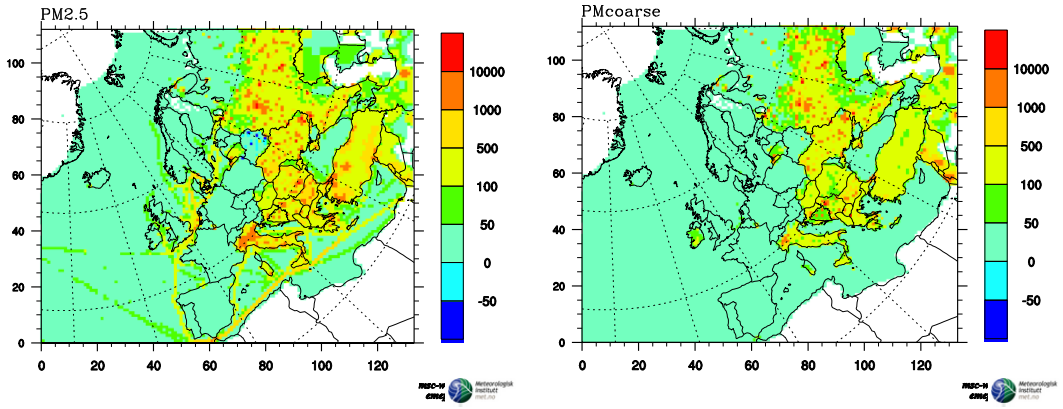

Figure 2.2: Differences between replacements by non-Party estimates and official estimates in 2006 for emissions of primary PM. Positive values show where the non-Party emissions are higher than the official emissions. Units: Mg.

Emissions from ship traffic are not included in the officially reported data but are necessary for modelling. For 2006 shipping data the emissions were linearly interpolated with ENTEC estimates for 2010.

MSC-W assessed and revised the gap-filled expert data prepared by CEIP. SO_x emissions in Cyprus were re-gridded using as basis the national total for SO_x and the spatial distribution in the 2007 reporting round. This changed the sector totals and the spatial distribution within the grid cells in Cyprus. MSC-W also identified that the reported $PM_{2.5}$ and PM_{10} data from Croatia was underestimated, and based on the gap-filling carried out last year we used the same emission estimate for the 2006 model runs as for 2005 runs.

In previous years expert estimates for PM emissions in the Remaining Asian Areas (including Syria, Lebanon, Israel, parts of Uzbekistan, Turkmenistan, Iran, Iraq and Jordan) were not available. In 2008 MSC-W has carried out model calculations with the Unified EMEP model for an extended area covering Kazakhstan, Turkmenistan, Uzbekistan, Tajikistan and Kyrgyzstan. Since the Remaining Asian Areas include parts of Turkmenistan and Uzbekistan and have significant impact on the air concentrations and depositions in the above mentioned five EECCA countries, the importance of this area for this year's model run has risen considerably. Therefore, MSC-W introduced expert estimates for PM emissions in the Asian Areas. A more detailed description of the emissions in the extended EMEP domain can be found in EMEP Status report 1/2008.

2.1.3 Differences between emissions in 2006 and 2005

Changes in the total emissions within the EMEP area from 2005 to 2006 are generally small, with averaged reductions of -1.6% for SO_x, -1.3% for NO_x and -5.9% for NH_3. In the case of particulate matter, there are averaged reductions of

-2.9% for $PM_{2.5}$ and -1% for PM_{coarse} if we consider only those countries and areas where PM emissions were available both in 2006 and 2005. For Asian areas expert estimates of PM emissions were not provided in 2005, while such data are accessible in 2006. Therefore, with the Asian areas included an increase of 0.4% is present for $PM_{2.5}$ over the EMEP area. For PM_{coarse} the increase is 8.1%.

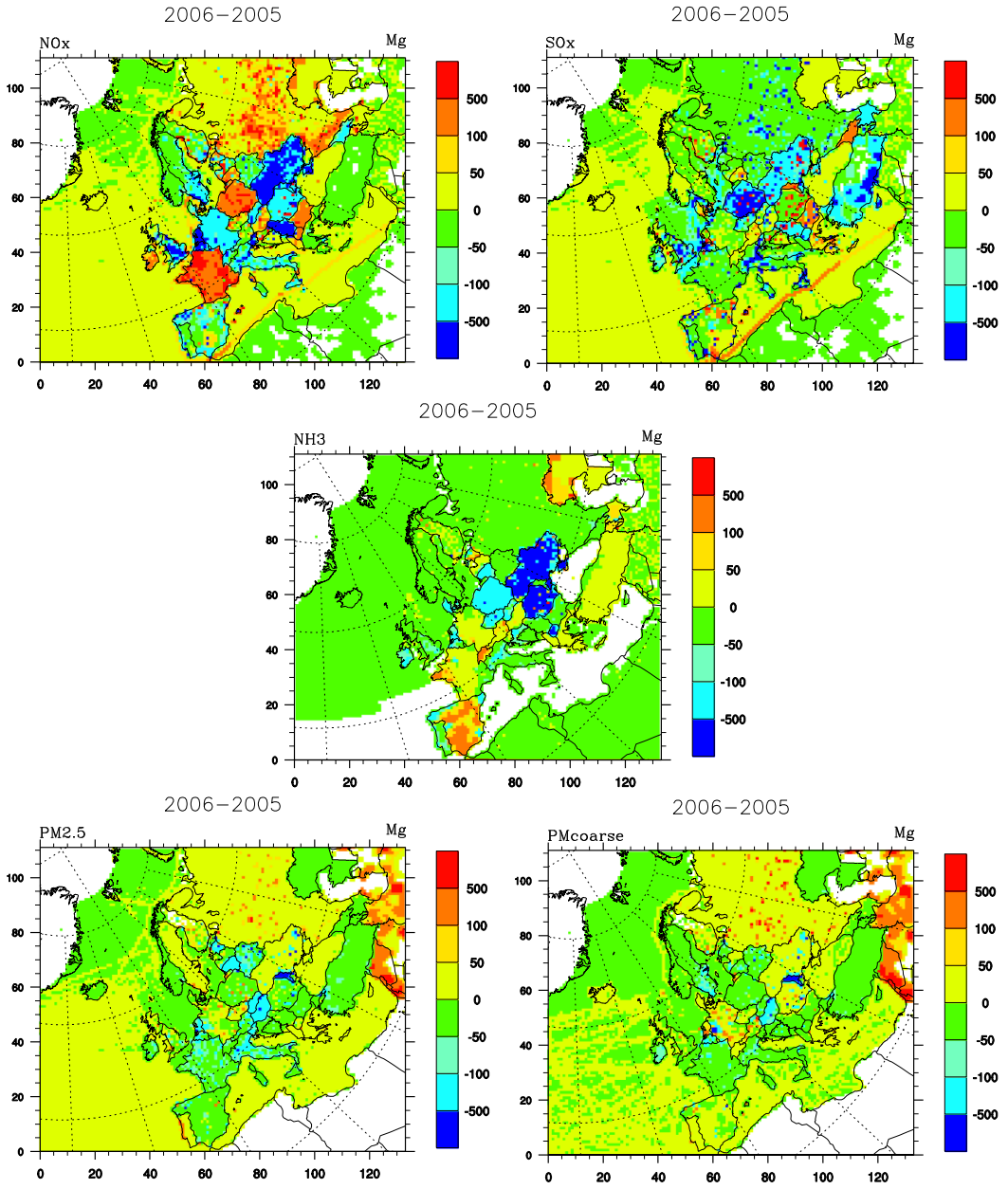

Figure 2.3: Differences in the spatial distribution of emissions between 2006 and 2005. Units: Mg.

The individual country emissions change more significantly from 2005 to 2006. These changes are different from country to country and region to region, as illustrated in Figure 2.3. The figure shows the variability of differences between 2005 and 2006 gridded emissions also within individual countries.

For SO_x, the largest changes in national total emissions have occurred in Finland (23%), Romania (19%), Georgia (179%) and Serbia (36%), Moldova (24%),the Former Yugoslav Republic of Macedonia (-20%) and Slovenia (-57%).

For NO_x, the largest reductions occurred in Sweden(-15%), Ukraine (-49%), Moldova (-20%), Slovenia(-19%), Georgia (-13%) and Serbia (-60%). NO_x emissions increased in France (12%), Poland (10%) and Croatia (15%).

NH_3 emissions decreased most in Poland (-12%), Romania (-25%), Ukraine (-59%), Lithuania (-11%) and the Former Yugoslav Republic of Macedonia (-49%). Increases of 6% and 7% occurred in Spain and Switzerland, respectively.

For $PM_{2.5}$ and PM_{coarse} the largest reductions occurred in Moldova (-71% and -95%, respectively), Slovakia (-17% and -33%), Lithuania (-46% and -41%), Estonia (-23% and -93%), Belarus (-33% and -24%) and Hungary (-26% and -25%).

Common for the above listed pollutant-country pairs for which the largest differences in the national totals from 2005 to 2006 were identified is that in all cases the expert estimates for national totals in 2006 were equal to the reported ones. This implies that the differences are not due to replacements in the 2006 official emissions.

A comparison of the officially reported 2006 and 2005 emission data for these pollutant-country pairs shows that in the case of EU15 countries the same differences occur between the expert emissions for 2006 and 2005 as well. This, however, does not always apply for the EECCA countries and the new EU member states, where the differences between expert estimates for 2006 and 2005 are considerably higher than those between the reported data for the same years. The reason for this deviation is that last year the reported emission data from EECCA and South-Eastern European countries were not only gap-filled, but went through several replacements based on estimates in Cofala et al. (2006) which in many cases led to changes in national totals. These replacements are described in Tarrason et al. (2007).

Ship traffic emissions were also estimated in a different manner than in previous years when MSC-W used ENTEC ship emission data for 2000 with an increase of approximately 2.5% every year for each pollutant (Cofala et al., 2007). This year CEIP applied a linear interpolation with ENTEC estimates for 2010 to derive the 2006 emissions for shipping, which resulted in lower emission values for SO_x in 2006 than in 2005. The total SO_x emissions from shipping decreased by 1.3%. The largest reduction occurred in the Baltic Sea and North Sea (-8% for both), while there is an increase of SO_x in the North-East Atlantic Ocean and Mediterranean Sea (1.5% and 1.3%, respectively). In the Black Sea SO_x emissions increased by only 0.4%. For NO_x the total estimated ship emissions increased by 1.1% and the same was estimated for $PM_{2.5}$ and PM_{coarse}.

2.2 Emissions of Primary Biological Aerosol Particles

2.2.1 General properties of primary biological aerosol particles

An exciting but poorly researched field of atmospheric aerosols concerns primary biological aerosols particles (PBAP). These biological particles derive from living substrate without any chemical transformation. The basic fact that material originating from plants, fungi and – to a lesser extent – also from animals can become airborne is not new. Still almost no information is available on their release process or on atmospheric concentrations.

PBAP in the atmosphere have *i.e.* been described by Jaenicke (2005). They have been observed as viable particles in super-cooled clouds (Sattler et al., 2001), they appear to act as cloud condensation nuclei (Bauer et al., 2003), and may play an important role for the long-range transport of trace elements into and away from specific biomes (Mahowald et al., 2005). Our current knowledge about their contribution to the aerosol mass concentration is rather poor, in particular for size fractions such as PM_{10} and $PM_{2.5}$ for which regulations and limit values exist.

PBAP may be released into the atmosphere as complete structural units or as fractionated material. Structural units have been investigated and identified by electron microscopy (Wittmaack et al., 2005). Important airborne structural units are pollen, spores, bacteria and virus. While airborne breakdown of particles is highly improbable (due to the lack of shear forces that would be needed), such processes might take place on the ground and hence affect structural units such as those described above as well as much larger entities, such as (dry) pieces from plants, animal skin or dried excreta. All this debris, when sufficiently small, may eventually become airborne.

Structural units can easily be distinguished by their size and morphology. Pollen are typically of a size of 30 µm and above, although with some exceptions (e.g. birch pollen can be as small as 10 µm). Fungal spores are frequently below 10 µm and have been estimated to have a mass of 33 pg (see Bauer et al., 2008), bacteria are in the µm size range and their mass is about three orders of magnitude smaller (40 fg C per entity, extrapolated from data presented by Bauer et al., 2002; Sattler et al., 2001). Far smaller mass has been attributed to viruses.

PBAP can be distinguished from other aerosol material based on their chemical composition. Cellulose, sugars and sugar-alcohols can all be used as tracers for various types of PBAP. For example, cellulose is the main constituent of plant cell walls and can be used to trace the total amount of plant debris. PBAP can also be identified and quantified under the microscope, based on their shape or affinity to specific dyes.
Both the traditional microscope based approach and the tracer approach way of quantifying PBAP are labour- and cost intensive. Thus only very limited sets of measurements of atmospheric PBAP concentrations are available to-date.

2.2.2 Quantification of the release of PBAPs

By definition, primary particles are released from the ground and are not formed in the atmosphere. Ideally, information about the release process should be used,

and measurements from this release taken to upscale the emissions for a larger area.

Unfortunately, basically no measured flux of PBAP release can be identified. Even in cases where an active release process is postulated (fungal spores), no useful data for quantification exist. In a recent assessment, Winiwarter et al. (2008) thus applied results from atmospheric measurements of cellulose (Sánchez Ochoa et al., 2007) as a tracer for plant debris (where cellulose is assumed to make up 50% of the cellular material). They also used a few fungal spore counts, which partly had been collected concurrently with the cellulose measurements (Bauer et al., 2008). Pollen contain cellulose (while spores do not) and thus would be accounted for as plant debris if fractionated – intact pollen grains (larger than 10 µm) would not enter the sampling system and are not included in the analysis. In order to quantify emissions, Winiwarter et al. (2008) referred to the concentration and the emissions of a tracer. Assuming that plant debris would follow the same atmospheric dispersion as the tracer compound, we obtain:

$$E_{PD} = E_{tracer} \frac{c_{PD}}{c_{tracer}} \tag{1}$$

where E_{PD} is the emission flux of plant debris, E_{tracer} reflects the emission flux of a tracer compounds, and c_{PD} and c_{tracer} refer to the respective atmospheric concentrations.

No single compound was identified to reproduce the temporal and spatial emission pattern of plant debris. Moreover, emission data are available only for very specific compounds. So any attempt to apply this indirect approach will have to rely on compounds for which both concentration data and emissions are available concurrently to cellulose (plant debris) measurements.

The above-mentioned cellulose measurements (Sánchez-Ochoa et al., 2007) have been collected as part of the CARBOSOL project from six sites along a west-east transect of Europe (but two remote sites had to be excluded). Simultaneous aerosol measurements have been reported by Pio et al. (2007), which include the compounds Black Carbon (BC), Organic Carbon (OC) and $PM_{2.5}$ mass (1 site only). Furthermore, measurements of levoglucosan have been performed (Puxbaum et al., 2007). Levoglucosan is a tracer for biomass burning..

Emission inventory data have been taken from IIASA's GAINS model (wood smoke as PM_{10} emissions from wood combustion in domestic sources, PM_{10} – OS1 – DOM, as well as total $PM_{2.5}$ according to IIASA, 2005; BC and OC according to Kupiainen and Klimont, 2004). Emissions are only available as annual mean values and as country data, thus comparisons to atmospheric concentrations were limited to the same scales.

The results of an evaluation according to Equation (1) have been normalized by relevant area (only barren land and water were considered not to be a possible source area for plant debris) in order to move from a country-specific number to an emission factor that is generally applicable. Winiwarter et al. (2008) provide a detailed discussion on the range (roughly 4 – 170 kg km^{-2} yr^{-1}, applying all tracers

individually for the respective sites) and the reasons why to select a best estimate of 6 kg km^{-2} yr^{-1}. It is obvious that this number provides an estimate only, even if the upper end of the range can be dismissed quite clearly (these figures derive from mountain sites using BC and wood smoke as tracers, which in the specific case may point towards pollution events rather than being representative for atmospheric dispersion in general).

For fungal spores, Winiwarter et al. (2008) used the ratio between spore mass and plant debris mass in the atmosphere (roughly a factor 3 on an annual average, from a limited set of measurements in the Vienna area: Bauer et al., 2008) to arrive at an emission factor of 18 kg km^{-2} yr^{-1} for fungal spores. Measured spore counts were converted to mass applying the above-mentioned factor of 33 pg per spore by Bauer et al. (2008).

Consequently, the overall emission factor for PBAP's was estimated at 24 kg km^{-2} yr^{-1}. Using assumptions consistent to those chosen to derive the emission factors, we conclude that virtually all structural units (fungal spores) are larger than 2.5 µm diameter, but smaller than 10 µm. The only available information (Puxbaum and Tenze-Kunit, 2003) on size distribution of plant debris reports an unexpectedly high fraction of small aerosol (more than 40% smaller than 1.5 µm). Overall we suggest a size distribution of plant debris and spores where 15% are smaller than 2.5 µm and 85 % range between 2.5 and 10 µm. It should be noted though that this distribution is being indicative and based on a few datasets only. By assuming that PBAP mainly consists of carbohydrates, we obtain a stoichiometric carbon content of 40 %, hence we may imply an emission factor of 10 kg/km^2 OC from PBAP. Fig. 1 compares – by European country – the contribution of OC associated with PBAP to the total emission of primary OC (from Kupiainen and Klimont, 2004). Large contributions of PBAP are expected for countries with a low population density, i.e. when anthropogenic emissions per area are small. Measurement data from a Norwegian site (Yttri et al., 2007a) coincide with the figure of 30% presented here for Norway.

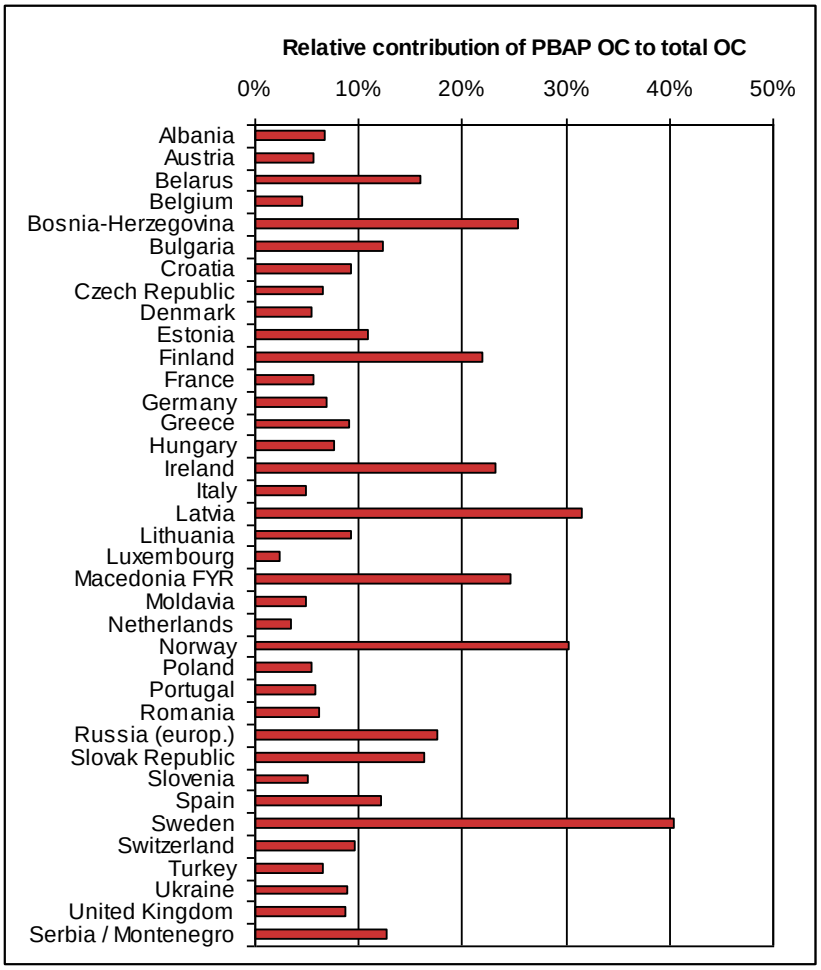

Figure 2.4: Estimated contribution of OC associated with PBAP emissions to total OC emissions in different European countries.

2.2.3 Emissions in Europe and worldwide

The most important sources of atmospheric PBAPs have been identified as plant debris and fungal spores. Annual emissions of 233 Gg (as PM_{10}) have been derived for Europe (Winiwarter et al., 2008), using an emission factor based on comparing atmospheric concentrations of PBAPs to other atmospheric compounds. Scaling European emissions by land area provides an indication for a global figure. Europe covers about 7% of global land mass, estimated emissions thus are in the range of a few Tg. Available estimates for global emissions of PBAP range from 56 Tg annually (Penner et al., 2001), to a value as high as 1000 Tg (Jaenicke, 2005). Even considering the large uncertainty involved and the potential of higher activity of the tropical biosphere, this assessment tends to support the lower of the literature values available, if at all, and rather suggests even considerably lower estimates.

Considerable progress in estimating PBAP emissions is still to be made. More specific tracers, as sugars and sugar alcohols already mentioned, may contribute to obtain more precise emission factors. This can ultimately lead to an understanding where PBAP actually derive from, a prerequisite to investigate the release mechanism and to develop a source term of emissions.

3 Model assessment of Particulate Matter in Europe: Status in 2006

By Svetlana Tsyro

3.1 Introduction

In this chapter, the main results of assessment of the transboundary air pollution in Europe with respect to particulate matter are presented for the year 2006. The assessment has been done based on both model calculation results and observations from the EMEP monitoring network. The contribution from different type of sources to the regional background PM has been calculated with the EMEP model and the results are provided here. Included are also the calculated exceedances of the EU standards and WHO guideline values by the regional background PM_{10} and $PM_{2.5}$.

The description of the Unified EMEP model can be found in EMEP (2003), EMEP (2004) and EMEP (2005). The calculations presented here have been performed with an extended version of the model, which allows for description of the chemical composition of primary PM and which also includes natural mineral dust (EMEP, 2003; EMEP, 2005; EMEP, 2006a; Tsyro, 2005). The meteorological data for 2006 used to drive model simulations was produced with the HIRLAM-PS Weather prediction model. The national emissions of SO_x, NO_x, NH_3, PM_{10} and $PM_{2.5}$ for the year 2006 were prepared by EMEP/CEIP and gridded at MSC-W. The PM_{10} and $PM_{2.5}$ emissions of elemental carbon (EC), primary organic carbon (POC) and dust is presently based on the estimates of BC/OC emissions in 2000 in Europe by Kupiainen and Klimont (2006).

The results of the evaluation of the model performance with respect to PM_{10}, $PM_{2.5}$ and the main aerosol components with EMEP observations in 2006 are provided.

3.2 PM_{10} and $PM_{2.5}$ in 2006

Annual mean concentration fields of PM_{10} and $PM_{2.5}$ in 2006 presented in Figure 3.1 have been obtained by combining EMEP model calculation results and EMEP measurements. Calculated PM_{10} and $PM_{2.5}$ include primary PM and secondary inorganic aerosols (SIA) from anthropogenic emissions, natural aerosols of sea-salt and wind blown dust and particle water. Particle water has been included in the calculated PM concentrations in order to account for the water in PM mass measured with gravimetric methods according to the CEN standard (Tsyro, 2005). Still, secondary organic aerosols (SOA) have not been incorporated in the standard model.

Annual mean concentrations of regional background PM_{10} ranged from 5 to 20 μg m^{-3}, whereas the corresponding range for $PM_{2.5}$ was from 2 to 15 μg m^{-3} in 2006 over most of Europe. The regions characterized by the enhanced PM_{10} and $PM_{2.5}$ pollution, with concentrations exceeding 20 μg m^{-3} and 15 μg m^{-3} respectively, were the Benelux countries, central and northern Italy, south of Spain, central Europe (the Czech Republic, Slovakia, Hungary) and the southern part of the Russian Federation.

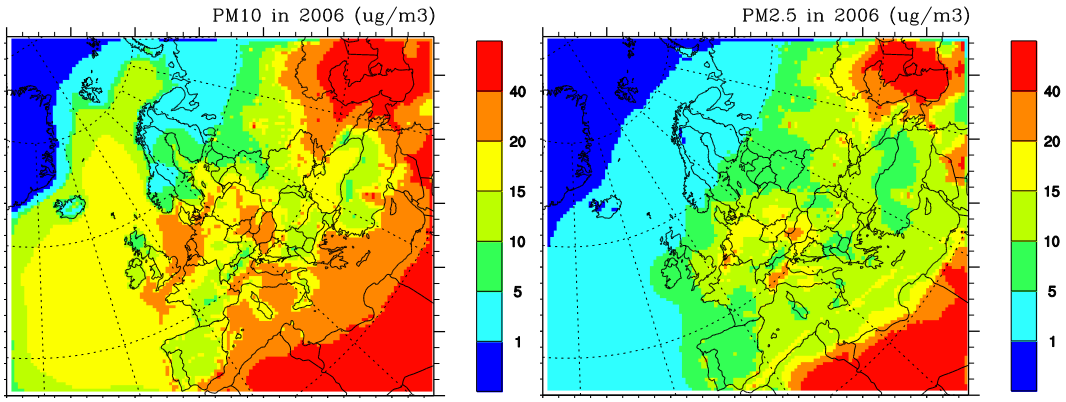

Figure 3.1: Annual mean concentrations of PM_{10} and $PM_{2.5}$ in 2006, derived from the EMEP model calculation results and EMEP observations.

Annual mean concentration maps of PM constituents, namely SO_4^{2-}, NO_3^-, NH_4^+, primary $PM_{2.5}$, coarse PM and natural particles (sea salt and mineral dust) are provided in Figure 3.2. Model results show that SO_4^{2-} is the main SIA component, which contribution to PM_{10} varies from 10-15% in western Europe to 25-30% in southern European countries and Russia. The contribution of NO_3^- to PM_{10} is 15–25% in central and western Europe, exceeding 30% in the Benelux countries and Germany, and varies between 5 and 15% in the rest of Europe. The contribution of NH_4^+ to PM_{10} is fairly flat, lying around 10-14% over central and eastern Europe, while it goes down to 5-10% in northern Europe, Spain and Russia.

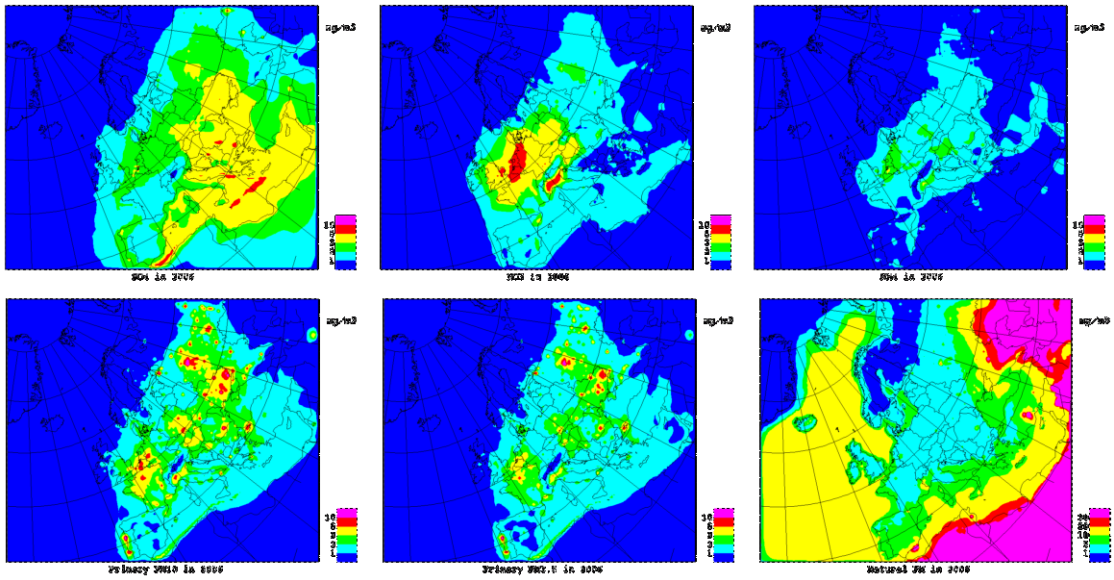

Figure 3.2: Calculated annual mean concentrations of aerosols: (a) sulphate, (b) nitrate, (c) ammonium, (d) primary coarse PM, (e) primary $PM_{2.5}$, (f) sea salt and mineral dust in 2006.

Figure 3.3 shows model calculated ratios of primary PM_{10} concentration to SIA concentrations for 2006. In most of Europe air pollution due to SIA is larger than that of primary PM_{10}. The concentrations of primary PM_{10} exceed SIA concentrations in areas surrounding large sources of PPM, in particular close to large cities and industrial areas.

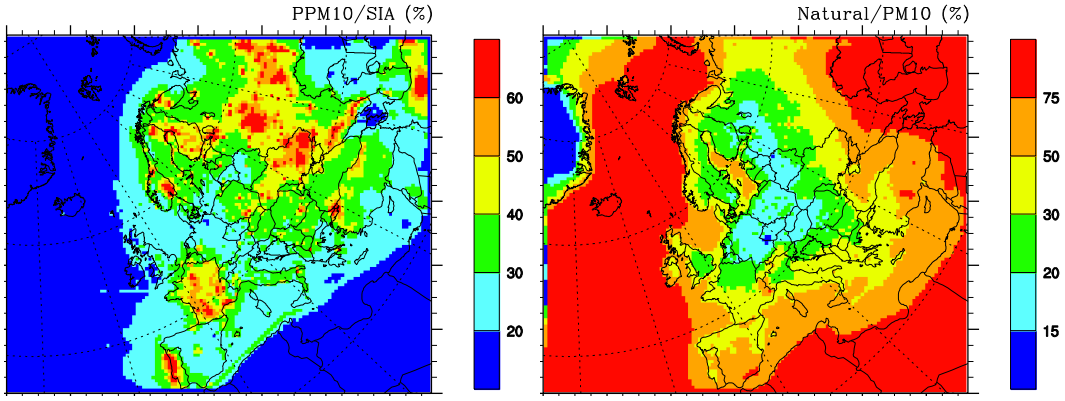

Figure 3.3: Calculated concentration ratios of primary PM_{10} to SIA (left panel) and the contribution of natural particles in PM_{10} (right panel) for 2006.

3.2.1 Differences between PM concentrations in 2006 and 2005

Changes in pollutant concentrations are driven by emission changes and by meteorological variability. Maps in the left column in Figure 3.4 shows the relative differences in calculated concentrations for 2006 compared to those for 2005 for $PM_{2.5}$, PM_{10}, SIA, primary $PM_{2.5}$ and coarse PM. To study separately the effect of emission and meteorology on PM concentrations changes two additional model simulations have been performed: the first one is for meteorological conditions in 2006, but using 2005 emissions and the second one is for the meteorological conditions in 2005 using 2006 emissions. The differences between the base run (both emissions and meteorology for 2006) and each of those test runs are visualized in the second and third columns of Figure 3.4. At the first glance one can note opposite effects of emission and meteorology changes on the concentrations changes from 2006 to 2005. That is, the increase/decrease in PM concentrations due to meteorological variability is lessened by the counteracting effect of emissions decrease/increase in the respective areas.

The concentrations of PM_{10} and $PM_{2.5}$ are lower by 5 to 20% in the Alps, in Finland, in the Russian Federation and in several EECCA countries, especially Ukraine and Moldova, in the year 2006 compared to 2005. Elsewhere, PM_{10} and $PM_{2.5}$ concentrations are higher by 5 to 15% in 2006 than in 2005 over the rest of EMEP area.

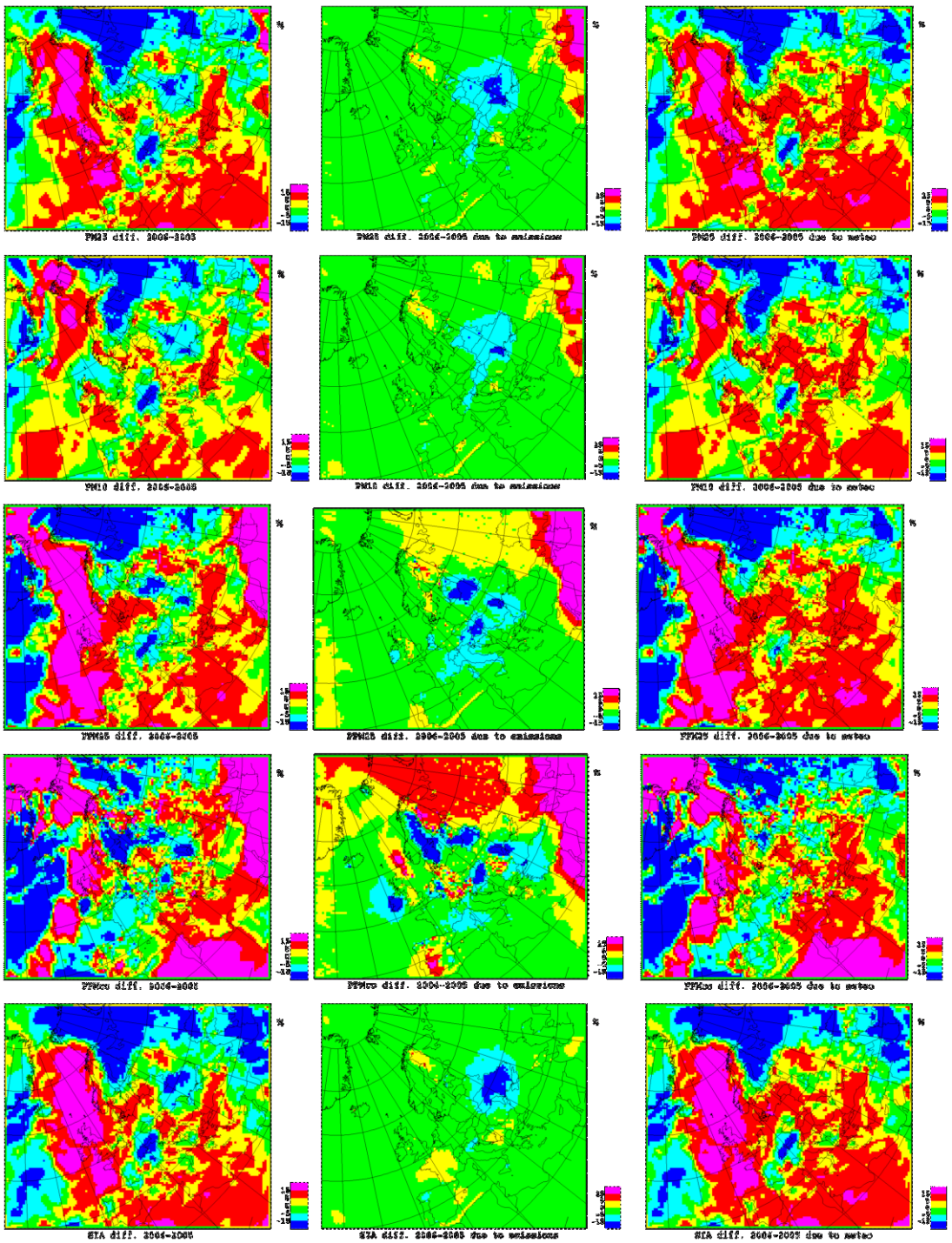

Figure 3.4: Relative differences between annual mean concentrations of PM_{10}, $PM_{2.5}$, primary $PM_{2.5}$ and coarse PM SIA in 2006 compared to 2005: left column – total changes, middle column – changes due to emissions, and right column – changes due to meteorological variability.

3.2.2 Differences due to emissions

The main differences between emissions in 2005 and 2006 are documented in Chapter 2 of this EMEP Status Report 4/2008. One of the major differences in primary PM emissions for the model runs this year is that expert estimated emissions in Turkmenistan and Uzbekistan in 2006 were taken into account. Among the most significant changes in PM emissions from 2005 to 2006 are the reductions in $PM_{2.5}$ emissions in Moldova by 72%, Belarus by 32%, Estonia and Hungary by 25%, Slovakia by 15%, Austria by 12% and Italy by 9%. There is some smaller $PM_{2.5}$ emission decrease in France, Lithuania, the Netherlands, Norway, Romania, Turkey and Ukraine, and $PM_{2.5}$ emission increase in Portugal, the Russian Federation and Sweden in 2006 compared to 2005. The largest changes in the emissions of coarse PM from 2005-2006 are the reduction in Moldova by 90%, in Sweden by 76% and in Slovakia by 15%, whilst the increase in Hungary by 27%, in Austria by 11% and in the Russian Federation by 8%. The corresponding changes in model calculated annual mean concentrations of $PPM_{2.5}$ and coarse PPM between 2006 and 2005 are quite pronounced in the maps in Figure 3.4 (middle pictures in the 3rd and 4th rows). The relative changes in primary $PM_{2.5}$ vary from below -40% in Belarus and Moldova (and in Sweden for primary coarse PM) to 15% southern Kazakhstan (and in Spain for coarse PPM).

The overall levels of SIA concentrations are lower in 2006 than in 2005 due to the minor decreases in total emissions of SO_x, NO_x and NH_3 by 1.6, 1.1 and 5.9 % respectively. The most pronounced decrease in SIA concentrations by 15-20% are found in Ukraine, which is due to much smaller NO_x (by 49%) and NH_3 (by 41%) emissions and despite lower by 4% SO_x emissions in 2006 compared to 2005. SIA concentrations are about 2 to 5% higher in Finland and France as a result of larger SO_x and NO_x emissions in 2006 than in 2005.

3.2.3 Differences due to meteorological variability

Meteorological conditions determine the formation of secondary aerosols, the atmospheric dispersion of pollutants and their removal from the atmosphere. For aerosol particles, wet scavenging is the main removal process. The characterization of the mean meteorological conditions in 2006 with respect to the average for the period from 1995 to 2002 was given in the EMEP Status Report 1/2007. The map of deviation of annual mean temperature at 2 m height from the 9-year average values are shown on the left panel in Figure 3.5, while the right panel presents a map of the differences between annual accumulated precipitation in 2006 and 2005. Lower temperatures and larger precipitation amounts were associated with a low pressure system centred over Russia in 2006. Another low, centred over the North Atlantic, was responsible for more precipitation in 2006 than in 2005 in Spain and France. This precipitation efficiently cleaned the atmosphere from PM pollution. On the other hand, high pressure and thus more stable conditions resulted in considerably less precipitation in 2006 than in 2005 over southern and eastern Europe. Thus, in these regions, we expect slower wet and dry depositions and a suppressed dispersion of pollutants.

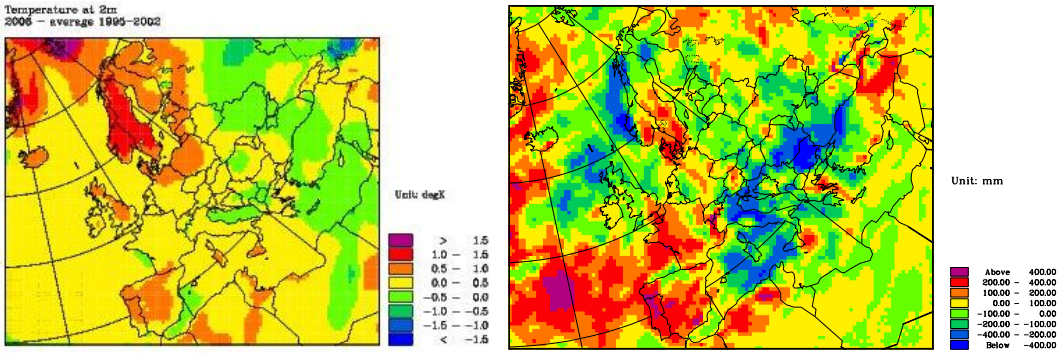

Figure 3.5: Deviations of annual mean 2m temperature in 2006 from the average for the period 1995-2002 (left) and differences in annual accumulated precipitation amount between 2006 and 2005 (right).

The differences in model calculated concentrations shown in the right column of Figure 3.4 are only due to meteorological variability between 2005 and 2006. A general pattern of concentrations changes from 2005 to 2006 are very similar for PM_{10}, $PM_{2.5}$, primary PM and SIA, although the ranges can somewhat differ. It can be noted that the general pattern of annual precipitation differences is particularly well reflected in the map of concentrations differences of coarse PM in 2005 and 2006. This is because these particles are relatively short lived so that the effect of wet scavenging of coarse PM has a more local character.

The meteorological variability explains somewhat 10-30% lower annual mean concentrations of $PM_{2.5}$ and PM_{10} (and individually primary PM and SIA) over Russia and 5 to 15% higher concentrations in the countries of southern and eastern Europe for 2006 compared to 2005. The largest decrease in PM concentrations is in the Alps and Finland (by 20-30%), on the Russian-Kazakhstan boarder (35-45%) and the north of Russia due to much more rainfall in 2006 than in 2005 in those areas. The greatest increase of 20-25% in PM concentrations is found in the north of England and Scotland due to the drier weather there in 2006 compared to 2005. Somewhat higher PM concentrations over southern Scandinavia and Denmark despite more precipitation there in 2006 are probably because of the transport of pollution from the UK. Finally, higher PM concentrations over Spain and Italy are also due to the higher concentrations of wind blown dust in 2006 than in 2005, as predicted by the model.

3.2.4 Evaluation of model performance for 2006

In this section we present the evaluation results of the model performance with EMEP observation data for the year 2006. Note that the model evaluation results presented here may differ from those presented in the EMEP Status Report 1/2008, which is due to different model versions used. In the EMEP Report 1/2008, the most updated version of the EMEP Unified model was used (rv3.1), whereas the extended model version used for this report is the same as last year (rv2.7.10).

The scatter-plots of calculated versus observed annual mean concentrations of PM_{10} and $PM_{2.5}$ at EMEP stations for 2006 are given in Figure 3.6, while

Figure 3.7 shows scatter-plots for secondary inorganic components (SO_4^{2-}, NO_3^-, NH_4^+) and their sum (SIA), and also Na^+. The summary of annual and seasonal comparison statistics between calculated and measured concentrations of PM_{10}, $PM_{2.5}$, SIA, SO_4^{2-}, NO_3^-, NH_4^+ and Na^+ for 2006 is provided in Table 3.1. Only sites which satisfied requirements for the data coverage were included in the comparison with model calculations. The data coverage requirements adopted here were 75% days with data for SIA components and 50% days with data for PM_{10}, $PM_{2.5}$ and Na^+. Due to this requirement the number of sites included in calculations of annual mean and daily mean statistics for PM_{10} and $PM_{2.5}$ are different (Table 3.1).

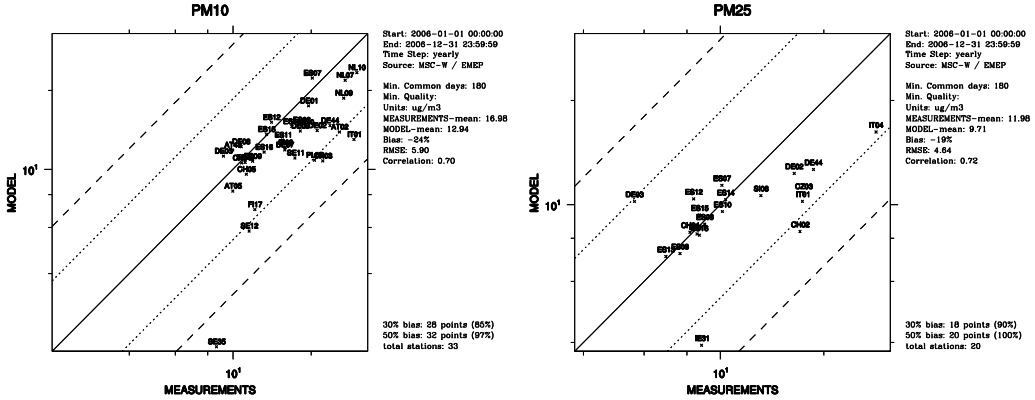

Figure 3.6: Scatter-plots of calculated versus observed annual mean concentrations of PM_{10} and $PM_{2.5}$ at EMEP stations for 2006

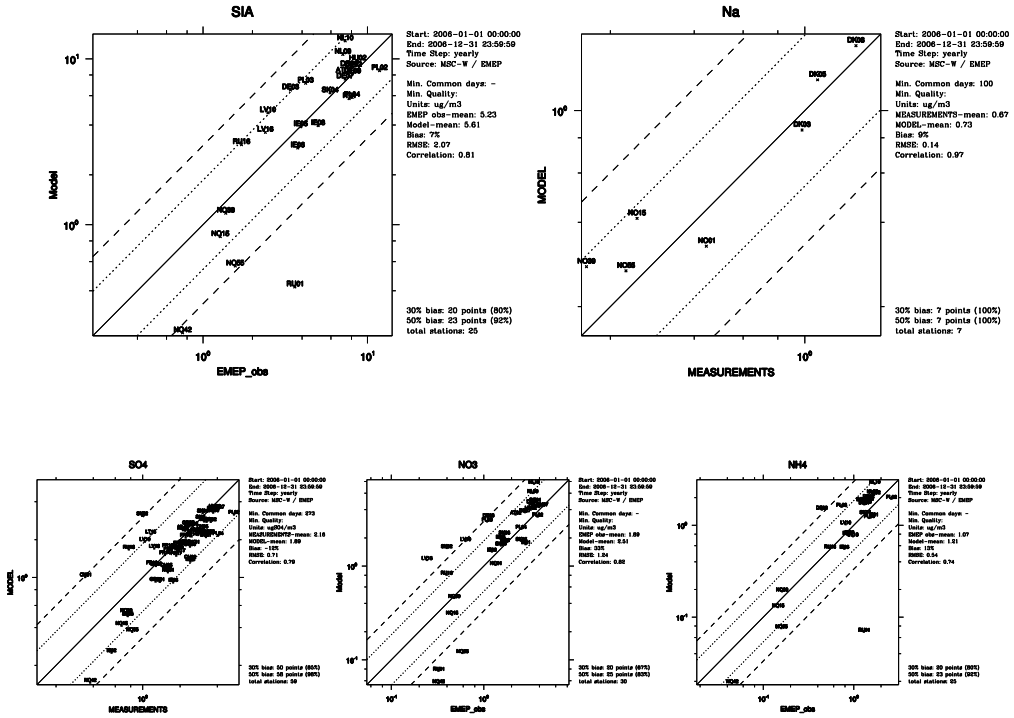

Figure 3.7: Scatter-plots of calculated versus observed annual mean concentrations of secondary inorganic aerosols and Na^+ at EMEP stations for 2006

Table 3.1: Annual and seasonal comparison statistics between EMEP model calculated and EMEP measured concentrations of PM_{10}, $PM_{2.5}$, SIA, SO_4^{2-}, NO_3^-, NH_4^+ and Na^+ for 2006

Period	N sites	Obs (ug/m^3)	Mod (ug/m^3)	Bias	RMSE	R
PM_{10}						
Yearly mean	33	16.98	12.94	-24	5.9	0.70
Daily mean	39	17.04	12.91	-24	12.76	0.51
JanFeb	35	20.35	17.12	-16	16.35	0.52
spring	36	16.35	11.95	-27	11.57	0.51
summer	39	17.13	10.92	-36	12.75	0.49
autumn	34	16.52	12.98	-21	11.21	0.56
$PM_{2.5}$						
Yearly mean	20	11.98	9.71	-19	4.64	0.72
Daily mean	28	11.71	9.51	-19	10.7	0.45
JanFeb	23	16.53	13.09	-21	17.36	0.43
spring	24	10.95	8.76	-20	8.33	0.56
summer	27	11.02	8.41	-24	8.24	0.38
autumn	22	10.28	8.89	-14	9.21	0.47
SIA						
Yearly mean	25	5.23	5.61	7	2.07	0.81
Daily mean	25	5.26	5.68	8	5.35	0.65
JanFeb	24	7.91	9.64	22	7.82	0.63
spring	25	5.59	5.14	-8	4.68	0.64
summer	25	4.00	3.62	-9	3.07	0.63
autumn	25	4.79	5.38	12	4.98	0.67
SO_4^{2-}						
Yearly mean	59	2.16	1.89	-12	0.71	0.79
Daily mean	63	2.17	1.88	-13	1.96	0.57
JanFeb	61	2.96	2.82	-5	3.28	0.45
spring	63	2.13	1.59	-25	1.69	0.62
summer	63	2.04	1.98	-3	1.53	0.59
autumn	63	1.97	1.61	-18	1.52	0.69
NO_3^-						
Yearly mean	30	1.89	2.51	33	1.24	0.82
Daily mean	30	1.91	2.54	33	3.22	0.61
JanFeb	29	3.01	4.52	50	4.75	0.6
spring	30	2.17	2.41	11	2.54	0.63
summer	30	1.21	0.92	-24	1.35	0.54
autumn	30	1.71	2.55	49	3.1	0.67
NH_4^+						
Yearly mean	25	1.07	1.21	13	0.54	0.74
Daily mean	25	1.06	1.22	15	1.32	0.58
JanFeb	24	1.67	2.07	24	1.71	0.65
spring	25	1.13	1.15	2	1.16	0.58
summer	25	0.78	0.77	-1	0.71	0.59
autumn	25	0.96	1.15	20	1.48	0.5
Na^+						
Yearly mean	7	0.67	0.73	9	0.14	0.97
Daily mean	7	0.67	0.73	9	0.61	0.8
JanFeb	7	0.53	0.74	40	0.7	0.62
spring	7	0.6	0.67	10	0.5	0.82
summer	7	0.5	0.42	-15	0.42	0.75
autumn	7	0.82	0.86	5	0.6	0.86

Here, Ns – the number of stations, Obs – the measured mean, Mod – the calculated mean, Bias is calculated as Σ(Mod-Obs)/Obs x 100%, RMSE – the Root mean Square Error= $[1/Ns\Sigma(Mod\text{-}Obs)^2]^{1/2}$, R – the tempo-spatial correlation coefficient between modelled and measured daily concentrations and spatial correlation for seasonal mean concentrations.

The model underestimates annual mean PM_{10} concentrations by 28% and $PM_{2.5}$ concentrations by 23% compared to the observed values in 2006. The spatial correlations between calculated and measured concentrations, which characterise model ability of reproducing mean regional gradients, are 0.70 for PM_{10} and 0.72 for $PM_{2.5}$.

Model calculated the annual mean concentrations of the individual PM components lie mostly within 15% of the measured values; however, bias for NO_3^- is larger, being 33%. The coefficients of spatial correlation between calculated and observed concentrations of PM components vary between 0.74 and 0.97 on the annual basis. The comparison statistics between calculated and measured concentrations of all components and for all sites on a daily basis are shown in rows titled "Daily mean". Note that the correlation in this case is an annual mean of daily spatial correlations and, thus, characterises the model ability to reproduce the spatial distribution of daily concentrations for the whole year.

In the following Table 3.2-Table 3.4, the comparison statistics between calculated and observed daily concentrations of PM_{10}, $PM_{2.5}$ and SIA for EMEP are provided for the year 2006.

Table 3.2: Comparison of EMEP model calculated and measured concentrations of $PM_{2.5}$ for EMEP stations for 2006.

Code	Station	Obs	Mod	Bias	R	RSME
AT02	Illmitz	14.86	8.10	-46	0.41	8.67
CH02	Payerne	17.08	8.44	-51	0.58	15.91
CH04	Chaumont	8.17	8.40	3	0.45	6.89
DE02	Langenbruegge/Waldhof	16.43	12.39	-25	0.54	11.62
DE03	Schauinsland	5.63	10.30	83	0.23	10.03
DE07	Neuglobsow	8.03	6.12	-24	0.58	4.19
DE44	Melpitz	18.68	12.74	-32	0.67	10.67
ES07	Viznar	10.11	11.51	14	0.47	10.37
ES08	Niembro	9.02	9.00	0	0.53	5.78
ES09	Campisabalos	7.63	7.35	-4	0.36	6.46
ES10	Cabo de Creus	10.11	9.64	-5	0.5	6.36
ES11	Barcarrota	8.55	8.65	1	0.48	6.13
ES12	Zarra	8.37	10.49	25	0.56	6.78
ES13	Penausende	6.95	7.46	7	0.54	5.01
ES14	Els Torms	10.32	10.44	1	0.61	6.23
ES15	Risco Llano	8.72	9.53	9	0.32	8.27
ES16	O Savinao	8.71	9.29	7	0.45	7.92
IE31	Mace Head	8.82	3.94	-55	0.49	6.28
IT01	Montelibretti	17.25	10.30	-40	0.5	11.06
IT04	Ispra	28.33	16.35	-42	0.29	29.63
NO01	Birkenes	5.41	4.05	-25	0.63	4.68
SE11	Vavihill	13.00	10.65	-18	0.47	9.76
SE12	Aspvreten	8.09	3.77	-53	0.6	6.4
SI08	Iskrba	13.12	10.71	-18	0.57	8.89

Here, Obs – the measured mean, Mod – the calculated mean, Bias is calculated as Σ(Mod-Obs)/Obs x 100%, R– the temporal correlation coefficient and RMSE – the Root mean Square Error= $[1/Ns\Sigma(Mod\text{-}Obs)^2]^{1/2}$.

Table 3.3: Comparison of EMEP model calculated and measured concentrations of PM_{10} for EMEP stations for 2006.

Code	Station	Obs	Mod	Bias	R	RSME
AT02	Illmitz	25.55	13.99	-45	0.56	19.05
AT05	Vorhegg	10.01	8.35	-17	0.51	8.05
AT48	Zoebelboden	9.99	11.94	20	0.41	9.52
CH01	Jungfraujoch	3.44	7.23	110	0.22	10.06
CH02	Payerne	23.14	10.70	-54	0.62	20.31
CH03	Taenikon	22.16	10.86	-51	0.49	19.67
CH04	Chaumont	10.82	10.64	-2	0.38	9.46
CH05	Rigi	11.27	9.65	-14	0.54	9.51
DE01	Westerland/Wenningsted	19.50	17.51	-10	0.64	8.84
DE02	Langenbruegge/Waldhof	21.11	14.14	-33	0.52	13.55
DE03	Schauinsland	9.21	11.31	23	0.15	11.62
DE07	Neuglobsow	15.86	11.94	-25	0.6	10.95
DE08	Schmuecke	10.77	12.27	14	0.24	10.56
DE09	Zingst	18.16	14.07	-23	0.63	9.91
DE44	Melpitz	23.63	14.78	-37	0.61	13.56
ES07	Viznar	20.16	22.43	11	0.47	21.5
ES08	Niembro	18.38	14.96	-19	0.38	10.25
ES09	Campisabalos	11.91	10.86	-9	0.37	12.33
ES10	Cabo de Creus	18.92	14.55	-23	0.48	9.66
ES11	Barcarrota	15.53	13.33	-14	0.38	11.67
ES12	Zarra	14.09	15.20	8	0.5	12.35
ES13	Penausende	11.16	10.99	-2	0.5	9.14
ES14	Els Torms	16.83	14.67	-13	0.57	10.35
ES15	Risco Llano	13.49	13.76	2	0.29	14.46
ES16	O Savinao	13.18	12.72	-4	0.38	11.41
IT01	Montelibretti	29.13	13.06	-55	0.56	19.44
NL07	Eibergen	26.99	21.93	-19	0.7	11.75
NL09	Kollumerwaard	26.66	18.75	-30	0.66	12.44
NL10	Vreedepeel	29.98	23.50	-22	0.49	17.69
NO01	Birkenes	8.53	5.24	-39	0.62	6.39
PL05	Diabla Gora	20.62	11.06	-46	0.56	14.83
SE11	Vavihill	17.31	11.12	-36	0.35	11.57
SE12	Aspvreten	11.54	5.92	-49	0.5	8.68
SE35	Vindeln	8.66	2.28	-74	0.45	7.95
SI08	Iskrba	15.91	12.18	-24	0.53	10.07

Here, Obs – the measured mean, Mod – the calculated mean, Bias is calculated as Σ(Mod-Obs)/Obs x 100%, R– the temporal correlation coefficient and RMSE – the Root mean Square Error= $[1/Ns\Sigma(Mod-Obs)^2]^{1/2}$.

Table 3.4: Comparison of EMEP model calculated and measured concentrations of SIA for EMEP stations for 2006.

Code	Station	Obs	Mod	Bias	R	RSME
AT02	Illmitz	7.20	8.22	14	0.53	7.00
DE01	Westerland/Wenningsted	7.58	8.89	17	0.76	5.44
DE02	Langenbruegge/Waldhof	8.25	8.90	8	0.67	5.87
DE03	Schauinsland	3.41	6.50	91	0.35	6.55
DE07	Neuglobsow	7.29	7.55	4	0.69	4.90
DE09	Zingst	8.13	8.13	0	0.73	4.74
HU02	K-puszta	8.73	9.70	11	0.75	6.00
LV16	Zoseni	2.46	3.61	47	0.45	3.94
NL09	Kollumerwaard	7.13	10.67	50	0.72	7.78
NL10	Vreedepeel	7.36	12.87	75	0.59	10.12
NO15	Tustervatn	1.28	0.85	-34	0.52	1.58
NO39	Kaarvatn	1.38	1.17	-15	0.50	1.77
NO42	Spitzbergen, Zeppelin	0.75	0.22	-70	0.28	0.92
NO55	Karasjok	1.58	0.56	-64	0.40	1.95
PL02	Jarczew	11.88	8.50	-29	0.68	6.32
PL03	Sniezka	4.21	7.16	70	-0.12	6.83
PL04	Leba	8.09	5.86	-28	0.66	4.62
RU01	Janiskoski	3.62	0.42	-89	0.02	7.29
RU16	Shepeljovo	1.72	3.04	77	0.49	3.76

Here, Obs – the measured mean, Mod – the calculated mean, Bias is calculated as Σ(Mod-Obs)/Obs x 100%, R– the temporal correlation coefficient and RMSE – the Root mean Square Error= $[1/Ns\Sigma(Mod-Obs)^2]^{1/2}$.

3.3 PM exceedances of EU standards and WHO AQGs in 2006

Model estimated exceedances of the EU limit values and the WHO Air Quality Guidelines (AQGs) by regional background PM_{10} and $PM_{2.5}$ concentrations in 2006 are presented in this section.

The Council Directive 1999/30/EC requires annual mean PM_{10} concentrations not to exceed a limit value of 40 µg m^{-3} and daily PM_{10} concentrations not to exceed 50 µg m^{-3} more than 35 times per calendar year. The WHO AQGs (WHO, 2005) are:

for PM_{10}: 20 µg m^{-3} annual, 50 µg m^{-3} 24-hour (99^{th} percentile or 3 days per year)
for $PM_{2.5}$: 10 µg m^{-3} annual, 25 µg m^{-3} 24-hour (99^{th} percentile or 3 days per year).

3.3.1 Annual mean exceedances in 2006

Model calculations show that the regional background PM_{10} concentrations were below the EU annual limit value of 40 µg m^{-3} in all of Europe in 2006, with the exception of the outmost southern areas of the model domain. In addition, the annual mean PM_{10} exceeded the WHO AQG of 20 µg m^{-3} in some parts of the Benelux countries and in the Po Valley in northern Italy. These exceedances were mainly due to anthropogenic emissions, whereas in the south of Spain and the Russian Federation, eastern parts of Ukraine, Kazakhstan and in the Caucasus, PM exceedances were also due to a large influence of windblown dust.

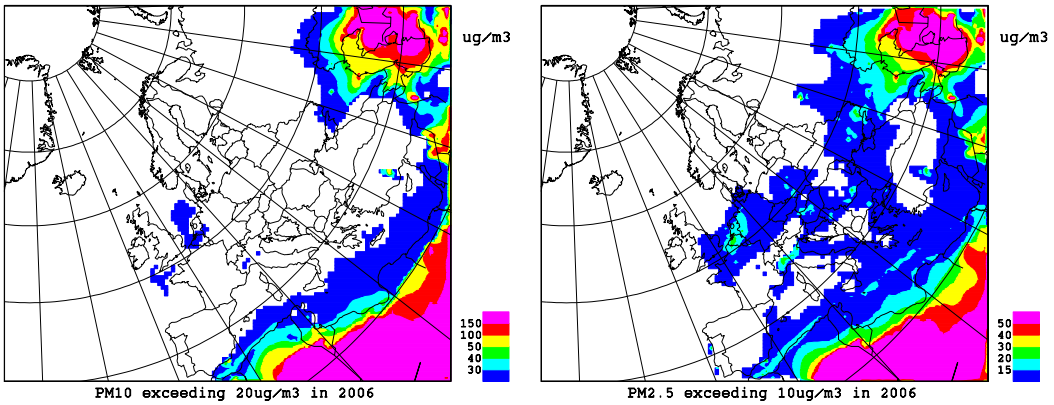

Figure 3.8: Calculated annual mean background PM_{10} and $PM_{2.5}$ concentrations in excess of the WHO annual AQGs of 20 µg m^{-3} and 10 µg m^{-3} respectively for 2006.

The calculated annual mean background concentrations of $PM_{2.5}$ exceeding 10 µg m^{-3} were found in most of central and eastern Europe, the Po Valley, the south of the Russian Federation and the EECCA (eastern Europe, Caucasus, central Asia) countries. In most of these areas, with the exception of the most southern ones, the exceedances were found already for anthropogenic $PM_{2.5}$. Also, $PM_{2.5}$ exceeded 10 µg m^{-3} along the main ship routs in the Mediterranean Sea. In the southern regions of the modelled domain, windblown dust contributed considerably to the $PM_{2.5}$ exceedances in 2006.

3.3.2 Daily exceedances

The calculated maps showing the number of days when regional background PM_{10} and $PM_{2.5}$ concentrations exceeded the 24-hourly EU limits and WHO AQGs in 2006 in Europe are provided in Figure 3.9 and Figure 3.10. The maps on the left panels show the limit exceedances due to the total PM concentrations and the maps on the right panels show the limit exceedances solely due to the anthropogenic PM concentrations.

Model results show that in 2006, there were several places in Europe where the EU daily limit value of 50 µg m^{-3} was exceeded by regional background PM_{10} more than 35 days. Those are the Milan region, the Moscow region, in Belgium, in eastern Ukraine and southern parts of the Russian Federation and EECCA countries (Figure 3.9 left panel). Figure 3.9, right panel indicates that only exceedances in the cities of Milan and Moscow and in one grid cell in Belgium were due to anthropogenic emissions, while the exceedances in the southern parts of the EMEP area are due to the windblown dust episodes.

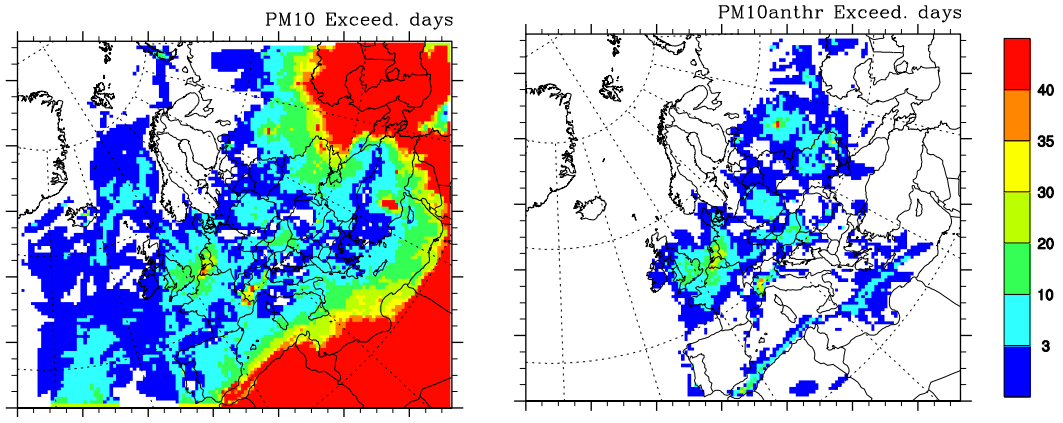

Figure 3.9: Calculated number of days with background PM_{10} concentrations exceeding 50 µg m^{-3} in 2006: left panel – for total PM_{10}, right panel – for anthropogenic PM_{10}. EU standard requires not more than 35 exceedance days, WHO AQG – not more than 3 exceedance days.

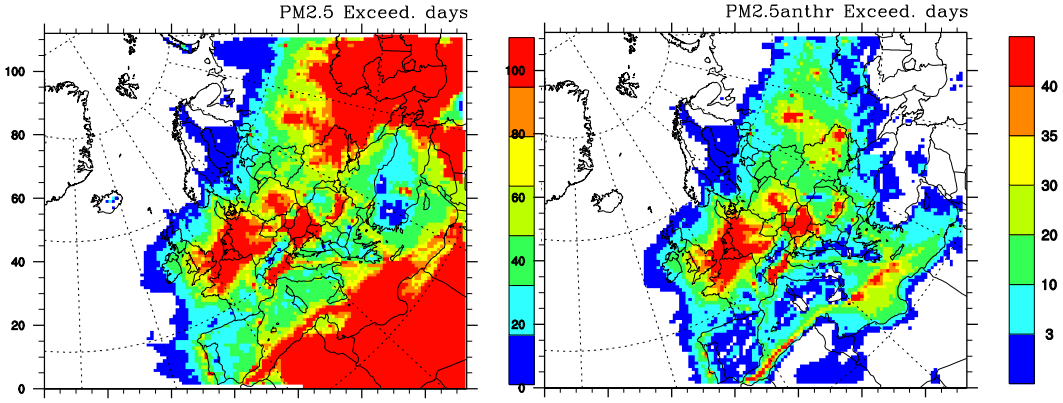

Figure 3.10: Calculated number of days with background $PM_{2.5}$ concentrations exceeding the 25 µg m^{-3} in 2006: left panel – for total $PM_{2.5}$, right panel – for anthropogenic $PM_{2.5}$. EU standard requires not more than 35 exceedance days, WHO AQG – not more than 3 exceedance days.

According to the WHO AQGs, daily concentrations of 50 µg m^{-3} for PM_{10} and 25 µg m^{-3} for $PM_{2.5}$ should not be exceeded more than 3 days in a calendar year. In 2006, the daily AQGs for PM_{10} were exceeded in 4 and more days in the Benelux countries, in the Po Valley, in parts of Germany and the UK, in the south of Spain, in eastern Europe, the Russian Federation and EECCA countries (Figure 3.10 left panel). Calculated daily mean $PM_{2.5}$ exceeded AQGs for 4 and more days almost all over Europe, except for Scandinavia, north of the Russian Federation and central Spain. Model calculations suggest that the emissions from anthropogenic sources were responsible to a large degree for the exceedances of the WHO AQGs for PM_{10} and especially for $PM_{2.5}$ in most parts of central and eastern Europe (Figure 3.10 right panel), whereas natural dust pollution is responsible for the impairment the air quality in the south of Europe and especially in the southern parts of Russia and EECCA countries.

Overall, the exceedances of the EU limit values and WHO AQGs remained approximately at the same level in 2006 as in 2005.

3.4 Changes in PM_{10} and $PM_{2.5}$ levels from 2001 to 2006

The changes in the annual mean levels of PM_{10} and $PM_{2.5}$ concentrations from 2001 to 2006 calculated with the EMEP model are visualised in Figure 3.11. Shown separately are PM_{10} and $PM_{2.5}$ concentrations averaged over all countries members of the LRTAP Convention (EMC) and the average for the EU27 countries. In both cases, the year with the highest mean PM_{10} and $PM_{2.5}$ levels is 2003. This is particularly pronounced for $PM_{2.5}$ in the EU27 countries, where the heat wave was the most pronounced in the summer of 2003. From 2003 to 2005, the mean concentration levels of PM_{10} and $PM_{2.5}$ decreased, and remained practically unchanged in 2006 (there was a 1-2% increase compared to 2005).

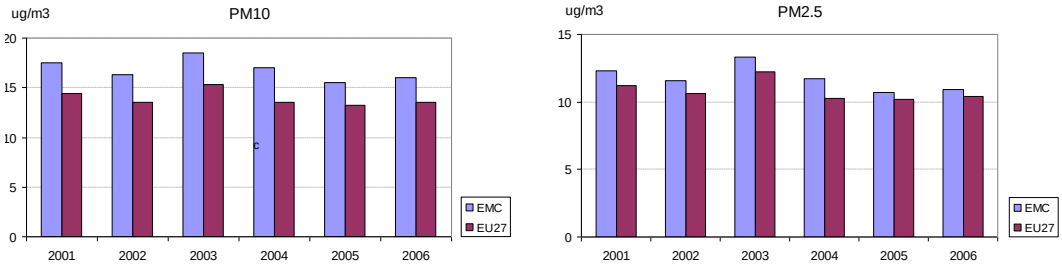

Figure 3.11: Calculated changes in the annual mean concentrations of PM_{10} and $PM_{2.5}$ from 2001 to 2006, averaged over all countries within the EMEP area (EMC) and over the EU27 countries.

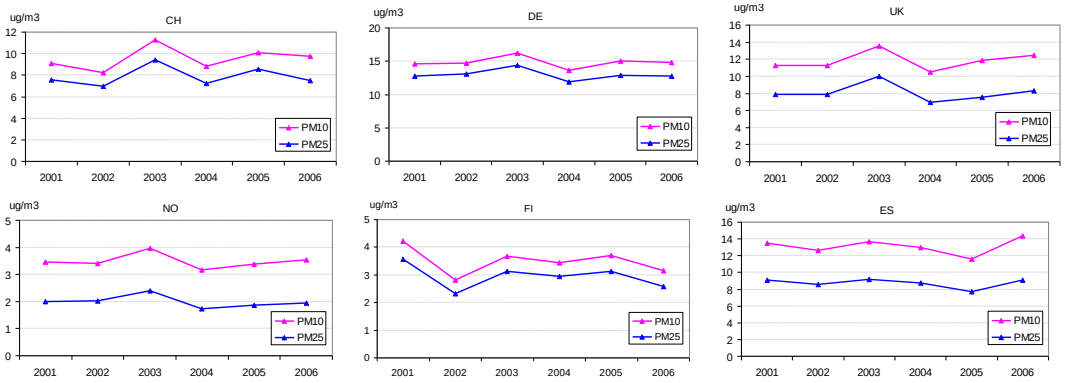

Figure 3.12: Calculated changes in the annual mean concentrations of PM_{10} and $PM_{2.5}$ from 2001 to 2006 for Switzerland, Germany, the UK, Norway, Finland and Spain.

Figure 3.12 shows some examples of calculated changes in the mean national concentration levels of PM_{10} and $PM_{2.5}$ from 2001 to 2006 for selected countries. In all of these countries, the highest annual mean PM_{10} and $PM_{2.5}$ concentrations were in 2003, except for Finland where the concentrations were highest in 2001. Mean PM_{10} and $PM_{2.5}$ concentrations decreased in Switzerland, Germany and Finland, whereas they increased in the UK, Norway and Spain from 2005 to 2006. Among these countries, PM_{10} and $PM_{2.5}$ levels decreased in 2006 relative to their

levels in 2001 in Finland, while they increased in the UK, Switzerland and Spain. In Norway and Germany, the 2006 levels of PM_{10} and $PM_{2.5}$ were about the same as in 2001.

4 Agricultural fires in spring 2006

By Karl Espen Yttri and Svetlana Tsyro

4.1 Introduction

PM emissions from wild fires and their impact on ambient air quality on the European regional scale has been discussed in EMEP report 4/2006 (EMEP, 2006b). With traditional anthropogenic emissions of PM and PM precursors likely to decline further in Europe in the foreseeable future, e.g. as a result of the Gothenburg protocol, other sources will become relatively more important. Emission from wild fires is a source which may increase not only on the relative basis, but also in absolute concentration. A dryer environment for large parts of Europe caused by less rainfall and increased warming, following from climate change predictions, could potentially lead to an increased frequency of wild fires in Europe and in adjacent regions. Of particular importance in this matter is the widespread boreal forest.

Forest fires are not always initiated naturally, i.e. by lightening. Human activity starting fire events either deliberately or by accident should be regarded equally important. E.g. burning of agricultural waste is common practice in large parts of the world. Besides emitting large amounts of PM pr. se, agricultural waste burning often spread to and ignites the natural vegetation. Thus, emissions from what initially was a minor event could escalate substantially.

In spring 2006, large parts of Europe experienced reduced air quality for a prolonged period of time caused by emissions from agricultural waste burning in eastern Europe; i.e. the Baltic States, western Russia, Belarus, and the Ukraine. Of particular interest was that this episode also affected the European Arctic. This episode has been extensively reported in a handful of pr. reviewed papers: Myhre et al. (2007), Stohl et al., (2007) and Treffeisen et al. (2007) reported on observations made in the Arctic environment, whereas Saarikoski et al. (2007) and Withman and Manning (2007) presented results from the urban environment. Here we summarize some of the major findings from these studies as well as presenting results from the EMEP-monitoring network, illustrating that this source affected the air quality severely in both the urban, rural and remote environment.

4.2 Initiation of fire event

The episode was initiated by the late onset of spring in eastern Europe, forcing the farmers to await burning of agricultural waste until the snow was melted in late April. These initially prescribed fires, which spread to the natural vegetation, lead to concurrent fires over a large area and caused huge PM and gaseous emissions to the atmosphere. In total it is estimated that 2 million hectare burnt during the 12 days period from 25 April to the 6 May 2006 (Stohl et al., 2007).

4.3 The remote environment - the European Arctic

The unusual warm Arctic spring in 2006 and (un-)favorable meteorological conditions augmented transport of eastern European air masses towards the European Arctic. At Ny-Ålesund at the western coast of the Svalbard archipelago the mean monthly temperature for the period January - May 2006 was 10.7, 3.8,

1.4, 10.3 and 4.2°C above the corresponding values averaged over the period since 1969 (Meteorological Institute, 2006). The monthly means reported for January, April and May were the highest ever recorded at Ny-Ålesund. Stohl et al. (2007) argued that the high temperatures in the Arctic allowed for isentropic transport from eastern Europe, as the temperature-based transport barrier generated by the polar dome was overcome. A detailed description of the meteorological conditions experienced during the episode can be found in Stohl et al. (2007).

During this event record high levels of several pollutants were recorded in the European Arctic (see Stohl et al., 2007). E.g. the hourly O_3 concentration reached 166 µg m^{-3} at the Zeppelin observatory, whereas at Storhofdi (Iceland) an hourly concentration of 176 µg m^{-3} was observed. At Zeppelin, the previous highest level of O_3 recorded was 122 µg m^{-3} (1989), whereas for Storhofdi the O_3 concentration has passed 140 µg m^{-3} only three times before. Also the AOD (500 nm) levels (0.5 - 0.6) observed during the episode were the highest ever recorded at Zeppelin, being approximately 5 times higher than the long term means for the months April and May. PM concentrations were not measured directly at the Zeppelin observatory during the event, but could be estimated from the DMPS measurements. Given a density of the aerosols of 1.5 g cm^{-3} and that the upper cut-off size of the DMPS is 0.7 µm, the highest 24 hour mass concentration of aerosols < 0.7 µm was estimated to be 29 µg m^{-3}. This corresponds to more than one order of magnitude higher than before and after the episode. It should be noted that 29 µg m^{-3} is a conservative estimate of the PM loading experienced during the episode, which most likely contained aerosols larger than 0.7 µm. The aerosol chemistry at the Zeppelin observatory changed substantially during the episode and was dominated by carbonaceous material, whereas secondary inorganic constituents and sea salts typically are the major contributors during normal conditions (Figure 4.1). The hourly concentrations of ECB (Equivalent Black Carbon), reached a record high concentration of 0.85 µg m^{-3} during the episode. The concentrations of OC during the week covering the main episode, i.e. 30 April – 7 May, was 3.5 µg m^{-3}, whereas the corresponding value for ECB was 0.28 µg m^{-3}.

The highly absorbing feature of the aerosols in the plume perturbed the radiation transmission in the Arctic atmosphere. When calculating the radiative forcing of this extreme smoke episode in the Arctic, Lund Myhre et al. (2007) found that the aerosols had a strong cooling effect above the ocean, and a weak heating effect above the ice and snow covered area. In total the scattering and thus the atmospheric cooling was found to be the dominating process. The future climate effect of aerosols in the Arctic region is however particularly sensitive to changed in the surface albedo, i.e. changes in the snow and ice cover and deposition of absorbing aerosols on ice and snow surfaces.

If the warming of the Arctic continues to proceed more quickly than that of the middle latitudes, new areas may be recruited as source regions, which consequently could contribute to an even more polluted Arctic environment. Thus, the spring 2006 episode might serve as an early warning of a potential future scenario.

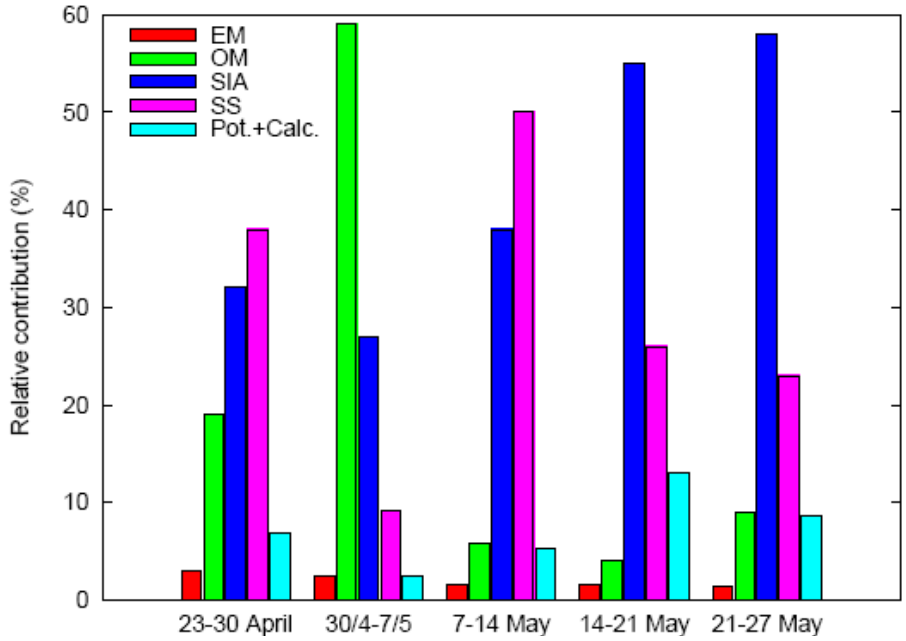

Figure 4.1: Relative contribution of various chemical compounds and compound classes to the total speciated aerosol mass at the Zeppelin observatory for the weeks 17 – 21, 2006. Abbreviations: EM (Elemental Matter), OM (Organic Matter), SIA (Secondary Inorganic Aerosol constituents), SS (Sea Salts), Pot. + Calc. (Potassium and Calcium). The Figure is from Stohl et al. (2007), Figure 22, page 528.

4.4 The urban enviroment

The agricultural waste burning episode's influence on the urban air quality has been described in Saarikoski et al. (2007) and in Witham and Manning (2007). Witham and Manning examined PM_{10} concentrations at urban sites of various sub categories (kerbside, urban background, urban industrial) in the UK of Great Britain and northern Ireland, Scotland and Wales, during the period, i.e. 6 – 11 of May, when the filament of the agricultural waste burning plume past the north-western part of Europe.

Their findings show that the 24 hour mean concentration of PM_{10} was within the range 65 – 96 µg m^{-3}, corresponding to the *moderate* level or above in the UK Air Quality Standards and Objectives for a prolonged period of time during the event for all 19 sites addressed. Further, the EU daily limit value of PM_{10} (50 µg m^{-3} not to be exceeded more than 35 times per year) was violated on multiple days at most of the sites. Witham and Manning (2007) also made references to non published measurements from Denmark, Germany and Norway showing elevated levels of PM_{10}, when affected by the agricultural waste burning emissions.

Saarikoski et al. (2007) added a wide range of chemical analysis, partly with high time resolution, to the PM measurements performed at an urban background site in Helsinki when the agricultural waste burning plume affected Finland. Saarikoski et al. (2007) reported two episodes of elevated PM concentrations during the period 25 April to 5 May. During the first period (24 – 29 April) the

maximum $PM_{2.5}$ concentration observed was 52.9 µg m^{-3}, whereas it was 68.8 µg m^{-3} for the second period (1 – 5 May). The average concentration of PM_{10} during the two periods was 68 ± 13 µg m^{-3} (period 1) and 81 ± 19 µg m^{-3} (period 2). Interestingly, the coarse fraction of PM_{10} ($PM_{10-2.5}$) increased equally to that of $PM_{2.5}$ when comparing the concentrations observed during the two episodes with that of the reference period (24 March–24 April). This demonstrates that pyro-convection could advect a substantial fraction of $PM_{10-2.5}$ to such altitudes that it acquires a long range transport potential. Levels of various carbonaceous sub-fractions (WSOC, WISOC, EC, and OC) and organic (levo-glucosan and Oxalate) and inorganic (water soluble potassium) tracers of biomass burning was considerably elevated during the episode as compared to the reference period before the impact. For the tracers, levels between 0.2 and 0.4 µg m^{-3} were observed. For the inorganic aerosol constituents, Ca^{2+}, Cl^-, NO_3^-, Mg^{2+}, Na^+, NH_4^+ and SO_4^{2-}, no such increase was observed except for SO_4^{2-} during episode 2. When attempting mass closure of $PM_{2.5}$ based on chemical speciation of PM_1, particulate organic matter (OM = OC x 1.6) dominated the mass concentration accounting for 52 ± 4.5% of $PM_{2.5}$ during episode 1 and 39 ± 9.0% during episode 2. As expected, the majority of the carbonaceous fraction could be attributed to the water soluble part (WSOC) during the episodes, however, the difference was not significantly different from that of the reference period.

4.5 The rural environment

So far no study has examined the effect of the spring 2006 agricultural waste burning emissions on the PM level in the European rural background environment. However, such data could be obtained from the EMEP monitoring network. Here we present PM data for sites affected by the plume according to the predictions made by the FLEXPART particle dispersion model.

Predictions made by the FLEPART biomass burning CO tracer for the lowest model layer (height 50 m agrl) (see Figure 4.2), show that large parts of Europe was influenced by air masses from the area subject to the massive agricultural fires, although to a various extent. From the 24 April the plume caused high PM levels in eastern Europe, Scandinavia, and the European Arctic. From the 4 May the plume also affected the air quality in continental Europe, in particular the northern parts and the UK; even Iceland was affected. A filament of the plume also affected the Balkans.

The 24 hour maximum PM_{10} concentration observed when the plume affected the various sites are presented in Table 4.1 along with the annual mean concentration of PM_{10} for 2006. Similar data is also presented for water soluble potassium (ws K^+), which can be used as a tracer for biomass burning emissions (Table 4.2). There is a very good agreement with the overpass of the polluted air masses and the observed maximum concentrations of PM and ws K^+ at the selected sites. This provides confidence in using such models as a tool for studying emission from wild and prescribed fires in the future. Time series of PM_{10} for selected sites based on 24 hours measurements are presented in Figure 4.3. The figure nicely shows the influence of the episode relative to the general background level of PM_{10} at the various sites.

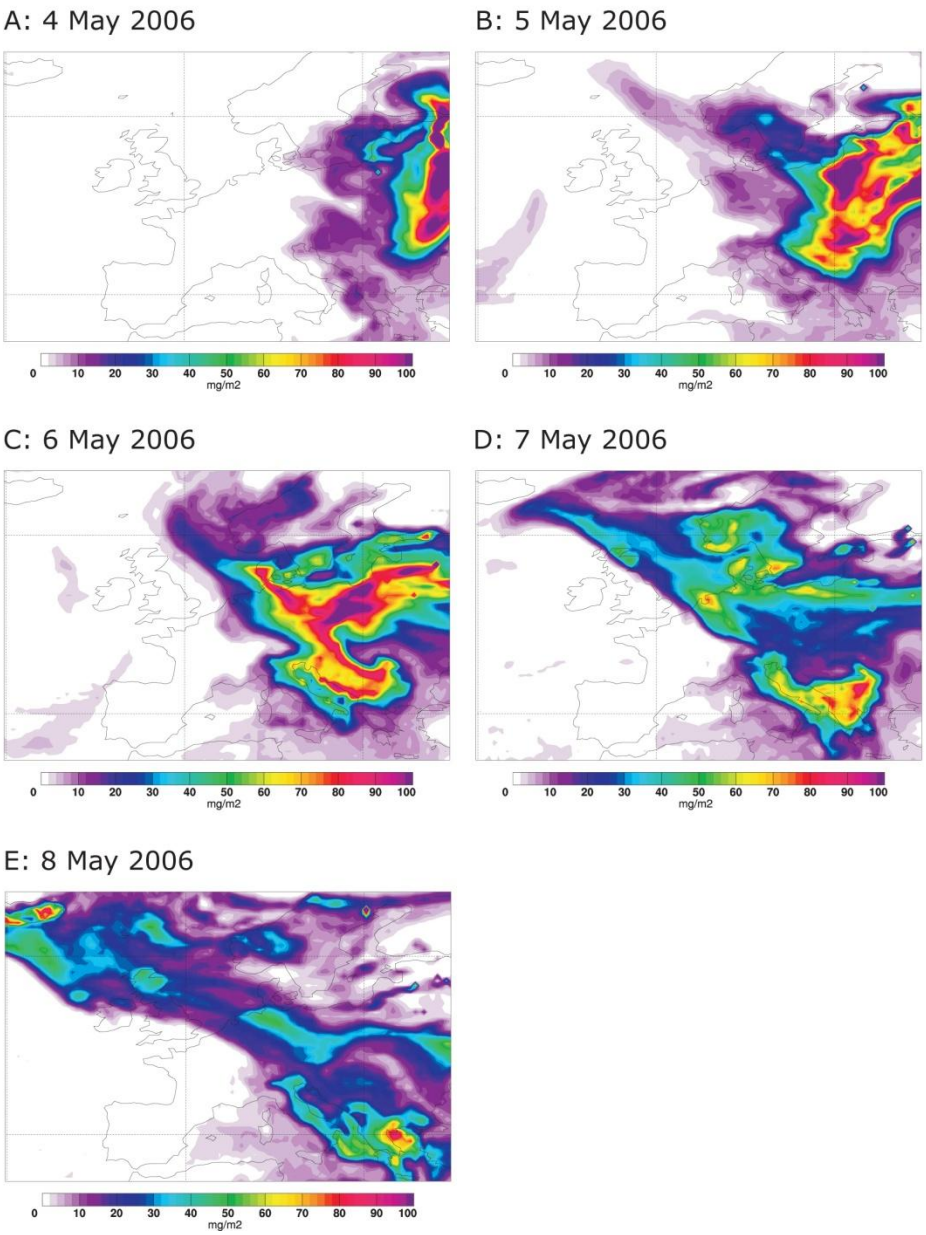

Figure 4.2: Surface layer (50 m agl) of the FLEXPART biomass burning CO tracer for the days (A) 4 May, (B) 5 May, (C) 6 May, (D) 7 May, (E) 8 May 2006; i.e. the second part of the period during which the plume affected the air quality in continental Europe.

Table 4.1: Maximum and annual mean concentrations of PM_{10} at the time of the agricultural waste burning plume overpass, as well as number of exceedances of the PM_{10} daily limit value during the actual period.

Site	Date	Max. 24 hour concentration (µg m^{-3})	Annual mean (2006) (µg m^{-3})	No. of days > 50 µg m^{-3} during plume overpass
AT02	6-7 May	43.1	25.6	0 / 37
AT05	5-6 May	23.3	10	0 / 0
AT48	6-7 May	35.3	10	0 / 0
CZ01	5-6 May	52.0	23.6	1 / 2
CZ03	5-6 May	39.0	19.7	0 / 3
DE01	6-7 May	53.5	19.6	1 / 3
DE02	6-7 May	60.0	20.7	2 / 15
DE03	5-6 May	22.4	8.3	0 / 0
DE07	6-7 May	49.9	15.6	0 / 11
DE08	6-7 May	44.0	10.5	0 / 1
DE09	5-6 May	49.5	18.4	0 / 10
DE44	6-7 May	54.1	23.6	1 / 11
DK05	6-7 May	52.9	24.6	2 / 9
GB06	8 - 9 May	37.2	11.5	0 / 0
GB36	10-11 May	38.5	21.7	0 / 3
GB43	12-13 May	38.0	17.6	0 / 11
NL07	8-9 May	43.1	27	0 / 19
NL09	7-8 May	54.0	26.8	1 / 18
NL10	8-9 May	45.8	26.5	0 / 17
PL05	5-6 May	54.1	20.6	2 / 12
SE11	5-6 May	46.6	17.3	0 / 0
SE12	1-2 May	55.2	11.6	1 / 1
SE35	2-3 May	44.7	8.6	0 / 0

The maximum concentrations of PM_{10} ranged from 22.4 µg m^{-3} at the Schauinsland site in southern Germany to 60 µg m^{-3} at Langenbrügge in northern Germany. In general, the maximum concentrations observed at the various sites did not differ much, thus the largest difference (factor of 4 - 5) compared to the annual mean was observed for the sites reporting the lowest annual mean concentrations, i.e. the Swedish sites SE12 and SE35, the German site DE02 and the Austrian site AT48. Somewhat lower maximum concentrations were observed for sites in the western parts of Germany and in Austria, being the border of the plume to the south-west.

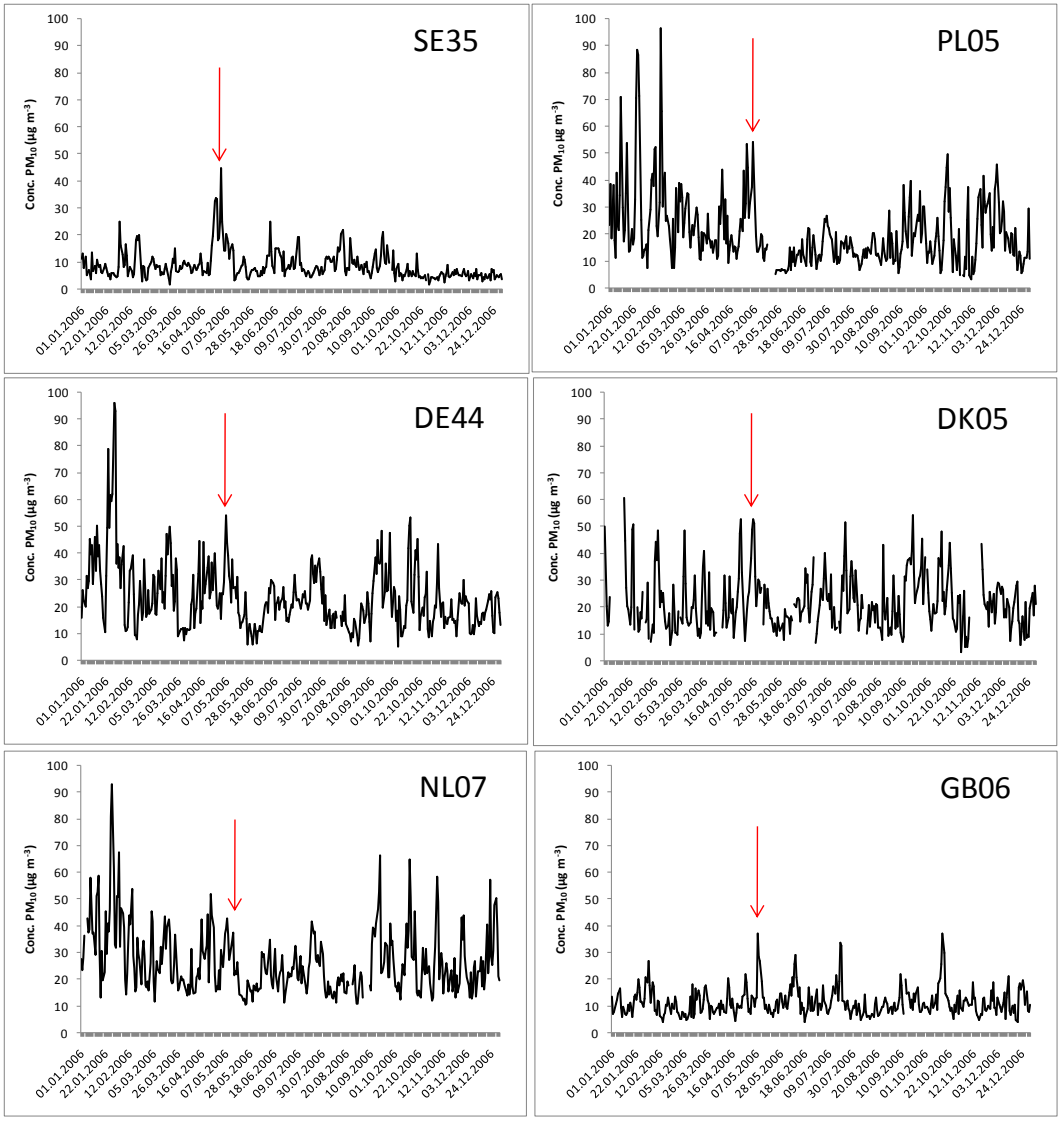

Figure 4.3: Time series of PM_{10} at selected rural background sites affected by the agricultural waste burning plume as it passed over Europe.

For the sites CZ01, GB06, SE12 and SE35, the maximum 24 hour PM_{10} concentration in 2006 was reported during the overpass of the plume. For the two Swedish sites the margin to the second highest concentration (also observed during the plume) was substantial; i.e. 11 µg m^{-3} higher for SE12 and 9 µg m^{-3} for SE35. Further, the five highest 24 hour concentrations reported for SE35 was all observed during the actual period. It should be noted that the data capture for the CZ01 site is rather poor (~ 40%). For all but six of the 23 sites examined, the maximum 24 hour concentrations seen during the plume were found within the 3% highest concentrations observed during 2006. The PM_{10} daily limit value, i.e. 50 µg m^{-3} not to be exceeded by more than 35 times per year, was exceeded at 35% of the sites for one or two days during the overpass of the plume.

Table 4.2: Annual mean and 24 hour maximum concentration of water soluble potassium (ws K^+) in 2006, as well as 24 hour maximum concentration of ws K^+ at the time of the agricultural waste burning plume overpass.

Site	ws K^+ (Annual mean 2006) (µg m^{-3})	ws K^+ (Max 2006) (µg m^{-3})	ws K^+ (Episode) (µg m^{-3})
AT02	0.221	1.31	0.438
DK05	0.155	1.04	0.565
DE01	0.167	0.6	0.44
DE02	0.206	1.08	0.49
DE07	0.195	0.96	0.43
DE09	0.214	0.83	0.44
DE44	0.172	1.02	0.403
NO01	0.049	0.30	0.28
NO42	0.017	0.26	0.26
SI08	0.135	1.16	0.261
SK04	0.173	0.893	0.43

Concentrations of water soluble potassium (ws K^+) were found to be elevated during the overpass of the plume, as seen for PM_{10} (see Table 4.2). The maximum ws K^+ concentration during the plume was observed at the Danish site DK05, being 0.565 µg m^{-3}. For the sites in central and eastern Europe the maximum concentrations were remarkably consistent (mean ws $K^+_{max\ plume}$ = 0.45 ± 0.05 µg m^{-3}). This level is in accordance with the mean concentration of ws K^+ reported by Saarikoski et al. (2007) for an urban background site in Helsinki. For the two Norwegian sites (NO01 and NO42) the maximum concentrations were rather similar as well, even though one of the sites (NO42) is situated in the European Arctic. The maximum concentrations observed during the plume were typically 2 - 2.5 times higher than that of the annual mean for the sites situated in continental Europe, while it was 4, 6 and 15 times higher for the DK05, NO01 and NO42 sites. Only the NO42 site reported the annual maximum concentration during the plume.

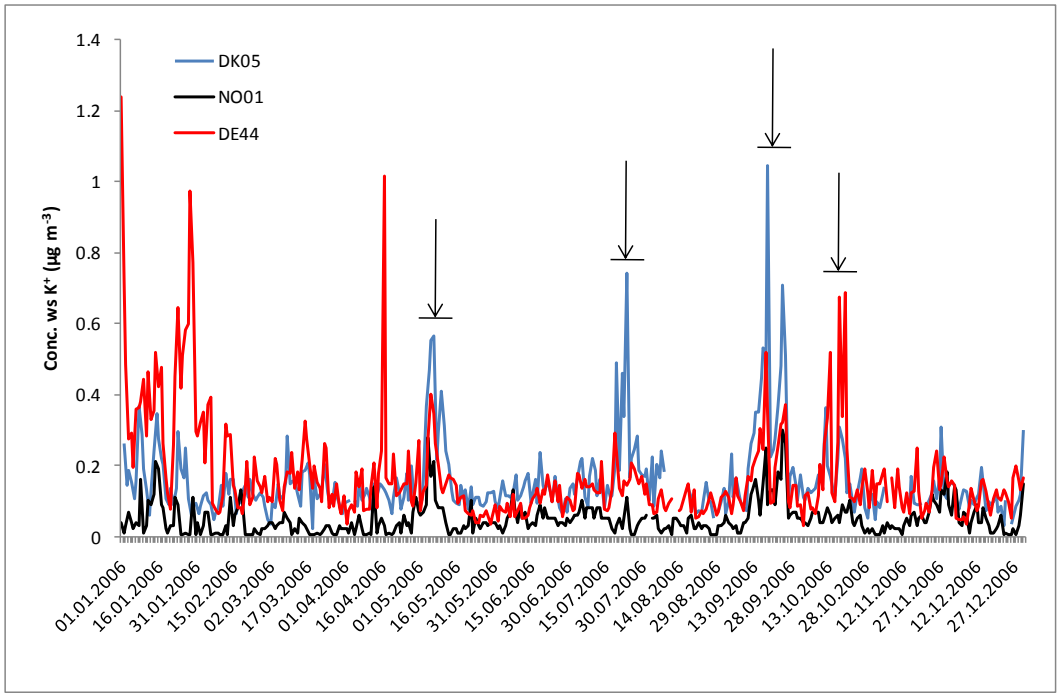

Figure 4.4: Time series of water-soluble potassium (ws K^+) at the Danish site Keldsnor (DK05), the Norwegian site Birkenes (NO01) and the German site Melpitz (DE44). Elevated ws K^+-concentrations are observed for extended time periods at several occations during summer and early fall, suggesting influence by biomass burning emissions.

Maximum ws K^+ concentrations exceeding 1 µg m^{-3} was observed for almost half of the sites when examining the whole year. One would typically expect the maximum concentrations to occur in winter, reflecting intrusions of emissions from residential wood burning, however this was not observed for more than half of the sites, suggesting influence by wild and prescribed fires in summer. Interestingly, three more events of elevated ws K^+ concentrations was observed during summer and fall at the Danish site DK05, and for the episode occurring in October the concentration was twice of that reported during the agricultural waste burning episode in May. Indications that some of these are events of regional character can be seen in Figure 4.4, as concurrent peaks are observed for other sites as well, as illustrated for the German site DE44 and the Norwegian site NO01. It is worth noting that the events of elevated ws K^+ levels are prolonged; e.g. 14 days for the NO01 site in September.

Combustion of biomass gives PM emissions with a high Carbon content. Unfortunately, only two of the sites affected by the agricultural waste burning plume reported such measurements. The increase in the relative contribution of elemental matter (EM) and organic matter (OM) to the speciated mass concentration for these two sites, Birkenes (NO01) and Melpitz (DE44), is shown in Figure 4.5. A similar increase is observed for the episode in September (both sites) and in October (DE44).

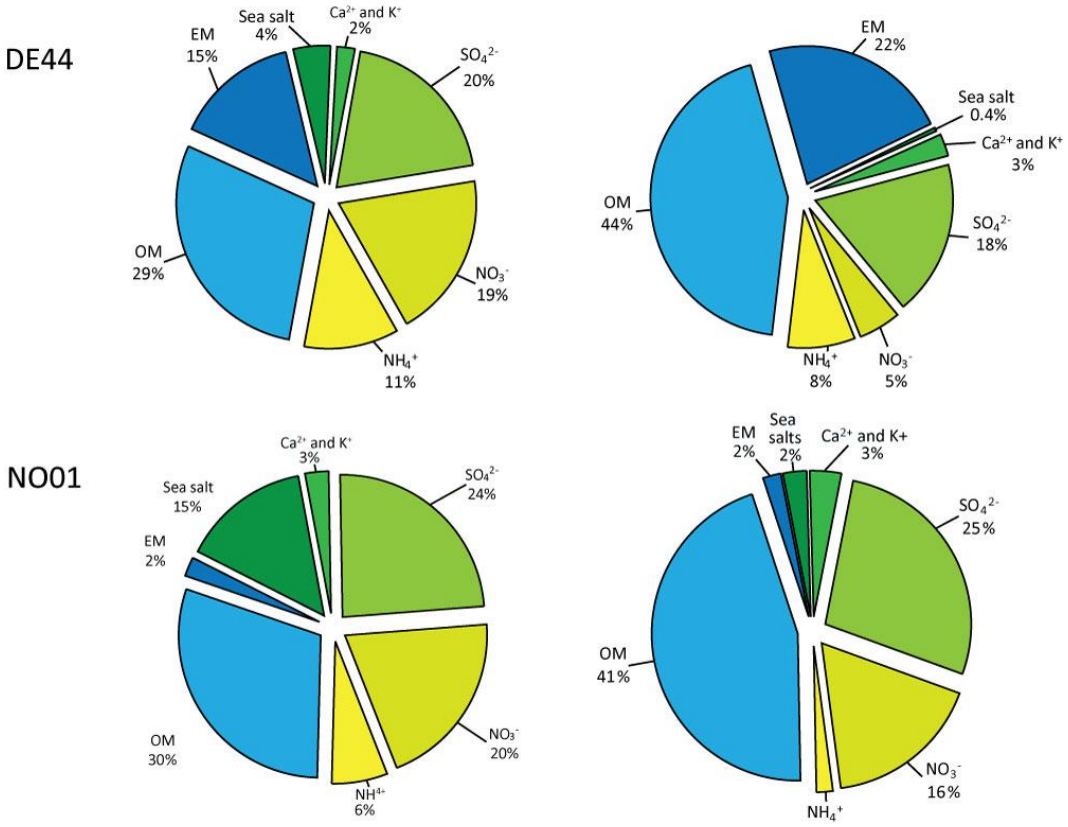

Figure 4.5: Relative chemical composition of the speciated particulate mass during the agricultural waste burning event (right) and for the year 2006 (left) for Melpitz (DE44) (top) and Birkenes (NO01) (bottom).

4.6 EMEP model calculations of fire pollution episode

The EMEP model has been used to simulate the episode of enhanced particulate matter pollution, which originated from agricultural and forest fires in eastern Europe and western Russia in spring 2006. Emissions of $PM_{2.5}$ from fires are available from the Global Fire Emission Database version 2 (GFED2) as monthly averages (Figure 4.6). Two test runs have been performed using different temporal distributions of the fire emissions. In these tests we assumed that virtually all fires occurred in the period between 15 April and 10 May 2006. In the first run, the emissions were evenly distributed in time, i.e. April emissions were distributed over the period 15 to 30 April and May emissions over the period 1 to 10 May. In the second run, the fire emissions were distributed over the same period based on the information about the number of fires from Stohl et al. (2007). As shown in the study by Stohl et al. (2007) and based on MODIS fire detection data, the daily number of detected fires in the region north of 40°N and between 20 and 60°E increased significantly in this period, with more than 300 fires per day being detected from 25 April to 6 May 2006.

The emissions from fires were distributed between the eight lowest model layers, which corresponds to an injection height up to about 2000 m. According to sensitivity tests performed by Withan and Manning (2007), the best fit between

model calculated and measured PM_{10} during the overpass of fire plume in the UK (7-9 May 2006) was obtained using a maximum fire emission height of 2000 m.

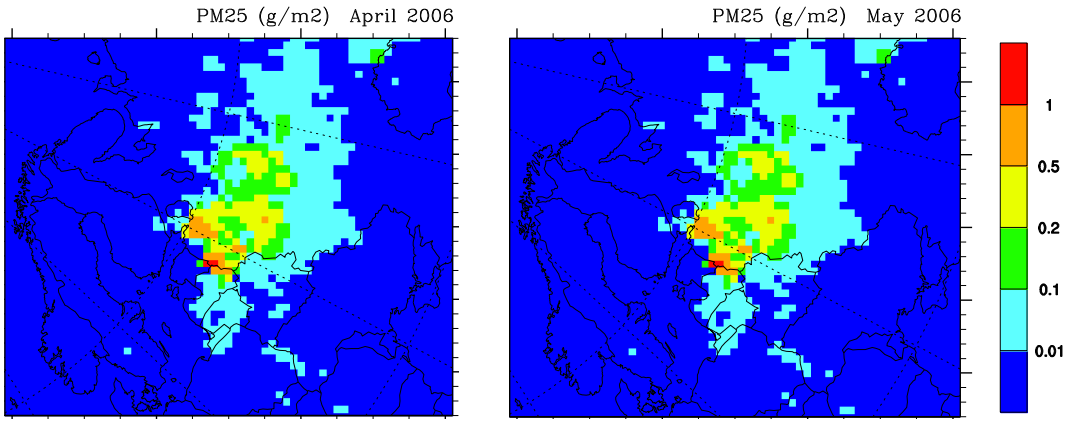

Figure 4.6: Monthly emissions of $PM_{2.5}$ from agricultural and forest fires in western Russia and eastern Europe in April and May 2006 (Data source: GFED2 database).

Figure 4.7 illustrates the spreading of $PM_{2.5}$ from the agricultural and forest fires in western Russia and eastern Europe for the period from 24 April to 13 May calculated with the EMEP model. In the beginning of the considered period, the plume was transported to the north, affecting firstly Finland and northern parts of Sweden and Norway on 25 to 27 April and then the whole of Scandinavia between 28 April and 2 May. From 5 May, the main transport direction of the fire plume was westward. Between 5 and 8 May the fire plume affected central Europe, in particular Poland, Germany and Denmark, northern England and Scotland, and even Iceland. Also south-eastern European countries was influenced by the plume, in particular on 5, 6, 11 and 12 May.

The evolution of the fire plume as predicted by the EMEP model corresponds quite well with the predictions made with other models. For example, the filament of the fire plume, which passed over Finland and reached Spitsbergen on 27 April (see Figure 4.7), agrees well with the results from the Finnish emergency and air quality modelling system SILAM (Saarikoski et al., 2007) and from the FLEXPART model (Stohl et al., 2007). There is also a fairly good match between the pattern of fire plume for 9 May 2006 as predicted by the EMEP model and the NAME model (Withan and Manning, 2007). The results from both models show how the plume moved across central Europe, over the North Sea, the UK and reached Iceland, which was also pronounced in the Meteosat image for 9 May 2006 (Withan and Manning, 2007).

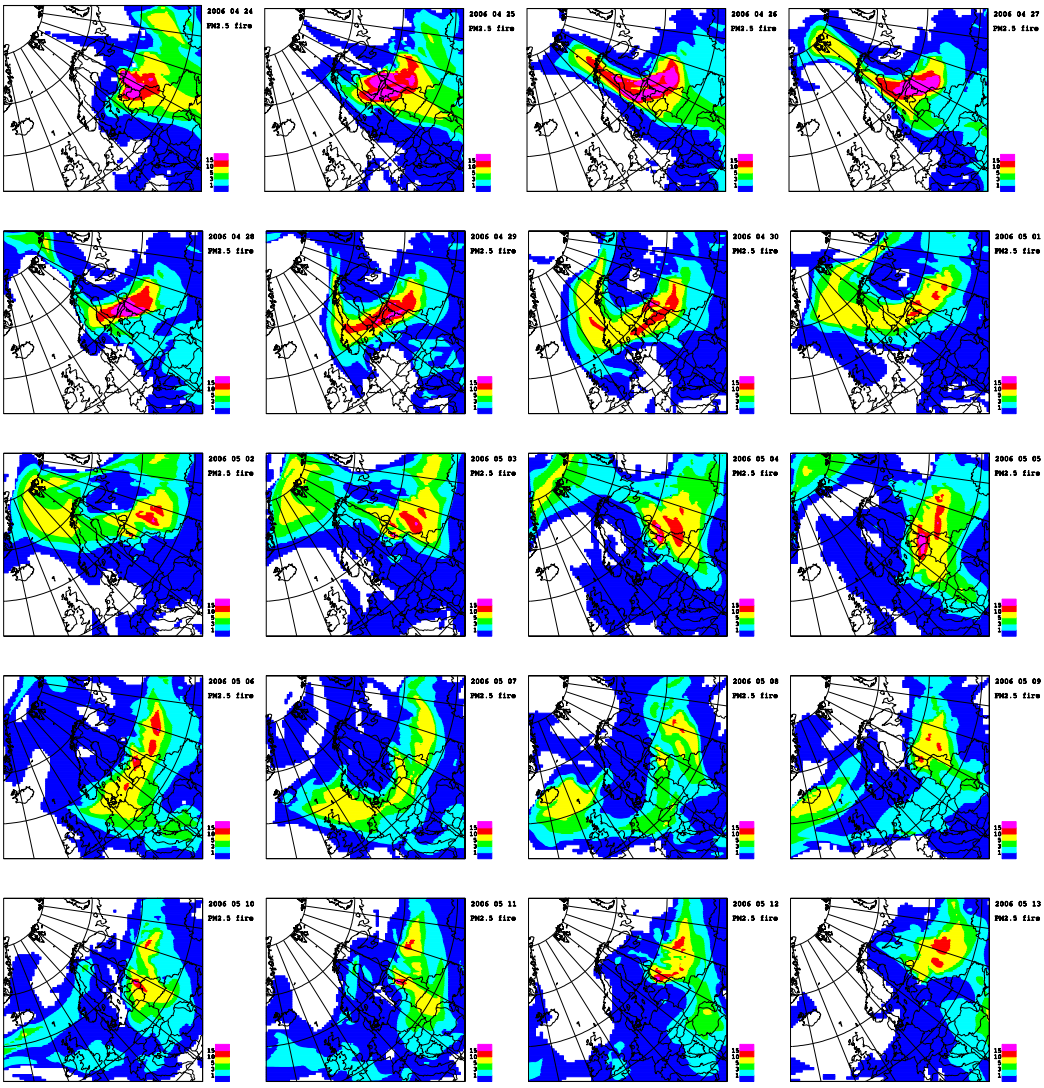

Figure 4.7: Evolution of agricultural waste burning plume ($PM_{2.5}$ concentrations) calculated with the EMEP model for the period from 24 April to 13 May. Emission data source: GFED2.

Time series of calculated PM_{10} and $PM_{2.5}$ concentrations, with and without contribution from the fire smoke, are compared with measured values for selected sites for the period 15 April to 15 May 2006 (shown in Figure 4.8). For all stations (also not included in the report), accounting for the emissions from the fire event improved the agreement between calculations and measurements, especially with respect to correlation. The model manages to predict the fire smoke episode on 25-28 April at the Finnish site Virolahti and the episode between 1 and 5 May at Virolahti and Aspvreten located in the south-east of Sweden.

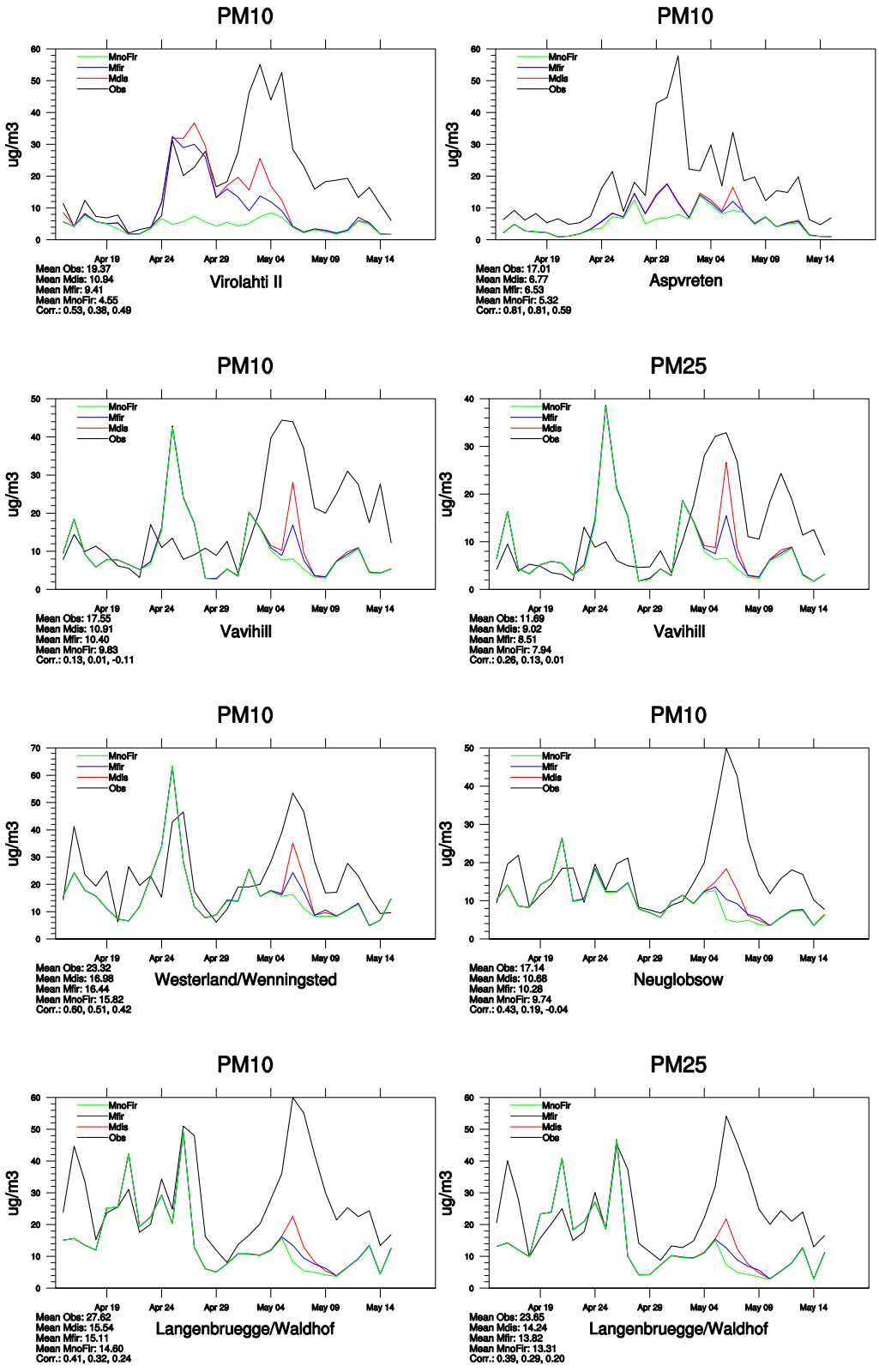

Figure 4.8: Daily time series of observed and calculated concentrations of PM_{10} and $PM_{2.5}$ from 15 April to 15 May 2006. Model calculated curves: green (MnoFir) – without fire emissions, blue (Mfir) – constant fire emissions for April and May periods, and red (Mdis) – fire emissions are temporarily distributed loosely based on the information about the number of fires in Stohl et al. (2007).

The occurrence of the second episode, 1 to 5 May, is also captured by the model, but the PM concentration levels are considerably underestimated. A few reasons for that can be pointed out. Firstly, there are uncertainties in the fire emission data and also in the way they have been distributed in time and between the model layers. Another aspect to be considered is related to the atmospheric transport calculations. In the EMEP model advection is calculated using wind fields from the HIRLAM weather prediction model. As can be seen in Figure 4.7, the modelled transport pattern changes after 1 May. Between 3 and 5 May the fire plume was transported northward, thus southern Scandinavia experienced lower concentrations outside of the plume core. It is interesting to note that the same episode was missed by the SILAM model as well when calculating the $PM_{2.5}$ concentrations for Helsinki (Saarikoski et al., 2007). Fire emission input for SILAM is based on MODIS information of active fires. The authors Saarikoski et al. (2007) argue that the most probable reason for missing this episode was that the fire was not detected by MODIS due to the occurrence of dense clouds in the beginning of May. However, they also point out that the particles measured during that episode may have originated from some other burning region. It is worth pointing out that SILAM calculations also used HIRLAM meteorology, as the EMEP model did.

The EMEP model manages to predict the occurrence of the observed episode of fire pollution on 5-8 May at German, Dutch and Austrian sites, but predicted PM_{10} and $PM_{2.5}$ concentrations are lower than the measured values. This also indicates a possible underestimation of fire emissions from the GFED database.

In summary, the EMEP model has managed to reproduce rather well the main features of the smoke transport and the pollution episodes associated with the agricultural and forest fires in western Russia and eastern Europe in spring 2006. Accounting for the biomass burning emissions improves considerably the correlation between modelled and measured PM concentrations, but calculated values are lower than observations in most of the cases.

5 Comparison of model results with data from the EMEP intensive measurements

By Svetlana Tsyro and Wenche Aas

5.1 Introduction

In the EMEP Monitoring Strategy (EB.AIR/GE.1/2004/5) it is stated that full chemical speciation should be conducted at EMEP super sites (level 2). Currently it is, however, not realistic to get a complete year of speciation measurements at many sites due to labour intensive and costly methods. The Task Force of Measurement and Modelling (TFMM) therefore recommend to conduct co-ordinated intensive measurements between the level 2 sites, and the first two sampling periods were set for June 2006 and January 2007.

A comparison is made between EMEP model calculated and measured PM_{10} and $PM_{2.5}$ mass concentration and the particulate chemical composition. The measurements of aerosol component concentrations in PM_{10} and $PM_{2.5}$ available for the comparison are summarized in Table 5.1. In this section we discuss the seasonal differences in model performance, i.e. in June 2006 (summer) and in January 2007 (winter), and look at the models ability to reproduce the aerosol mass distribution between the fine and the coarse mode. In the following text we will not use much space to discuss uncertainties in the measurements and on the comparability of measured and modelled data, but rather leave this to future reports and publications. Some discussion concerning artefacts in NO_3^- and NH_4^+ measurements can be found in Chapter 6 of the EMEP Status Report 1/2008.

Table 5.1: Overview of measurement data used for comparison with model calculations

		$PM_{10}/PM_{2.5}$	SO_4^{2-}	NO_3^-	NH_4^+	EC	OC	Na^+	Cl^-	Miner.
Birkenes	NO01	x/x	x	x	x	x	x	x	x	(x)
Melpitz	DE44	x/x	x	x	x	x	x	x	x	(x)
Montelibretti	IT01	x/x	x	x	x	x	x	x	x	x
Ispra	IT04	-/x	x	x	x	x	x	x	x	(x^{**})
Montseny	ES17	x/-	x	x	x			x	x	x
Virolahti	FI17	x/x	x	x	x			x	x	(x)
Payerne	CH02	x/-	x	x	x			x	x	(x)
Illmitz	AT02	x/x	x^*	x^*	x^*	x^h				
Košetice	CZ03					x				

x^* - total concentrations, x^{**} - in PM_{10}, x^h - hourly

5.2 Chemical speciation

Figure 5.1 compares observed and model calculated chemical composition of PM_{10} and $PM_{2.5}$ averaged over each of the measurement periods for the sites participating with such measurements. Each bar-diagram contains four columns: the first two columns show results for June 2006 (June06), whereas the two last columns show results for January 2007 (January07). Figure 5.2 is similar to Figure 5.1, except that measured and calculated concentrations of organic carbon are converted to organic matter, using a conversion factor of 1.7 for all sites. It should be noted that: (1) only primary anthropogenic OC is included in the model results, (2) for Montelibretti (IT01) OC concentrations for January 2007 are corrected for positive artefacts using the correction factors for June 2006, (3) PM_{10} and $PM_{2.5}$ concentration data were not made available for neither of the Italian sites (IT01 and IT04) for January 2007 period, therefore the not-determined fraction ND is not present at the correspondent bars.

The summaries of comparison of statistics between calculated and measured concentrations of PM_{10} and $PM_{2.5}$ and their components are provided in Table 5.2 and Table 5.3. Additionally, Figure 5.3 and Figure 5.4 visualise the seasonal differences in model bias for PM_{10}, $PM_{2.5}$ and their components as compared to measurements. It is important to note that the temporal coverage of measurement data varies from site to site, as can also be seen in time-series in Appendix A. A very few days with observations are available for the following sites: Birkenes for NO_3 in $PM_{2.5}$, Melpitz for EC in $PM_{2.5}$ in June06, Montseny for all PM_{10} and especially $PM_{2.5}$ components, and Virolahti for $PM_{2.5}$ components in June06.

The results of model performance for various components compared to intensive measurement data are rather mixed for the various stations. The main findings are outlined below:

- In general, the model manages to reproduce the main features of the observed chemical composition of PM_{10} and $PM_{2.5}$ for the actual sites
- The model underestimates PM_{10} and $PM_{2.5}$ in both summer and winter for all sites, except Montseny (ES17)
- For most of the sites, except Illmitz (AT02), the model underestimation of PM_{10} and $PM_{2.5}$ is larger for the summer month June06 compared to the winter month January07
- Although to a various degree, the model underestimates PM_{10} and $PM_{2.5}$ components for both months, only with a few exceptions: NO_3^- and NH_4^+ are overestimated for some sites in January07 and for Montseny for both months, and EC is overestimated for Birkenes for June06
- A larger underestimation of carbonaceous aerosols (elemental and organic carbon) in summer appears to be the main reason for model PM underestimation at the three sites with EC/OC measurements (Birkenes, Melpitz and Montelibretti). The OC underestimation is most likely due to not accounting for secondary OC and primary natural OC in the model. The underestimation was particularly pronounced in northern and central Europe (NO01 and DE44)

- There is still a considerable part of the measured PM mass concentration that is unidentified, even at the sites where all main PM components were determined. The undetermined PM mass decreases when OC is converted to organic matter. The largest discrepancies between speciated and measured mass concentration for PM_{10} and $PM_{2.5}$, was observed for Melpitz and Birkenes. The undetermined PM fraction is thought to include water present on the particles at 20ºC and 50% relative humidity (equilibration conditions of PM samples). Particle water is accounted for in the model calculations (also denoted by ND), but the calculated water concentrations are smaller than undetermined PM mass for most of the cases. Large uncertainties are also associated with the conversion factors used to convert OC to OM.

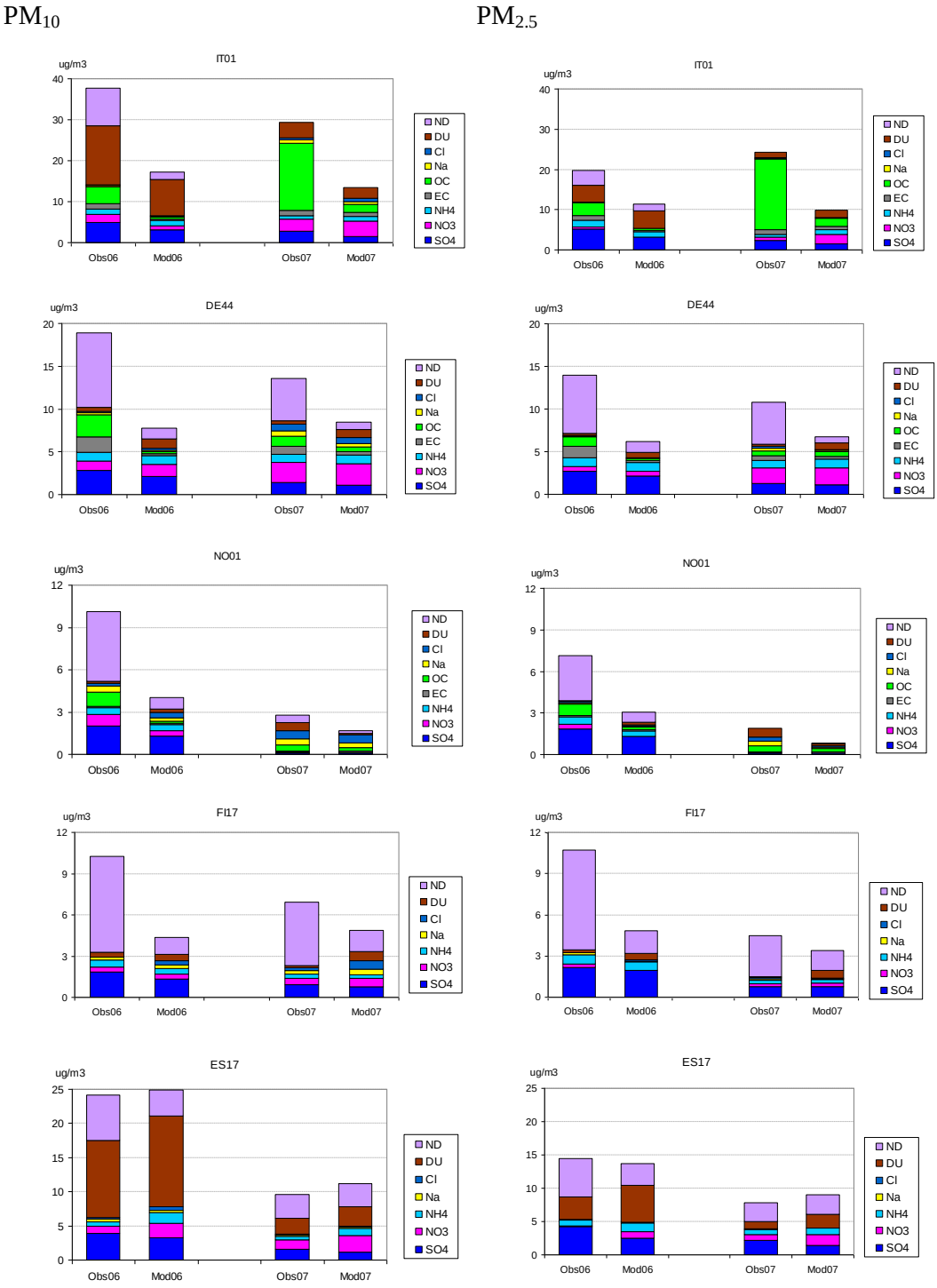

Figure 5.1: Observed and modelled chemical composition of PM_{10} (left panels) and $PM_{2.5}$ (right panels). In each bar-diagram, the first two columns are for June 2006, whereas the two last columns are for January 2007. Here, ND denotes not determined PM mass in measurements and particle water in calculations. Note that only primary anthropogenic OC is included in the model.

PM_{10} $PM_{2.5}$

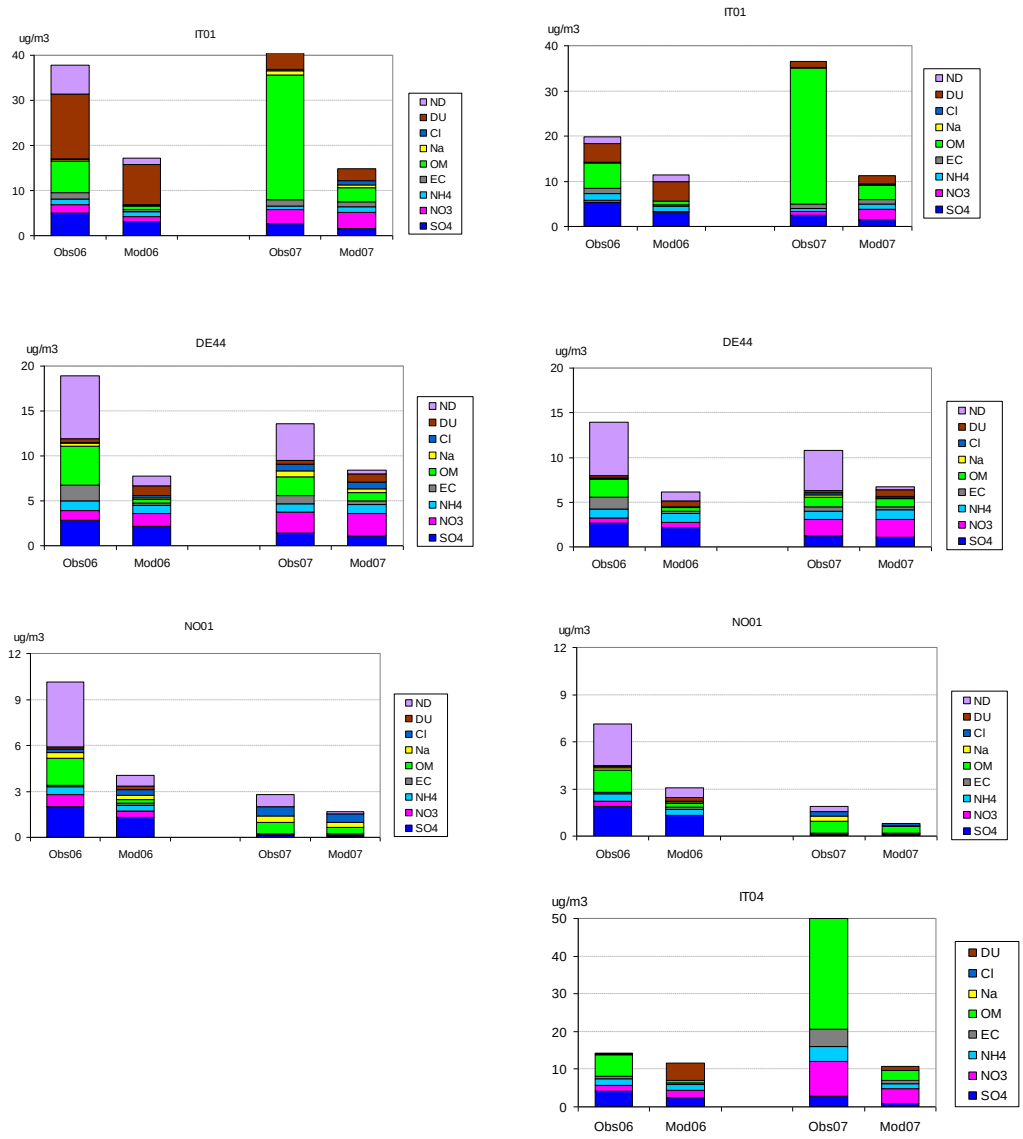

Figure 5.2: Observed and modelled chemical composition of PM_{10} (left panels) and $PM_{2.5}$ (right panels) for sites with OC measurements. In each bar diagram OC is converted to organic matter (OM). Here, ND denotes Not Determined PM mass in measurements and particle water in calculations. Note that only primary anthropogenic OC is included in the model.

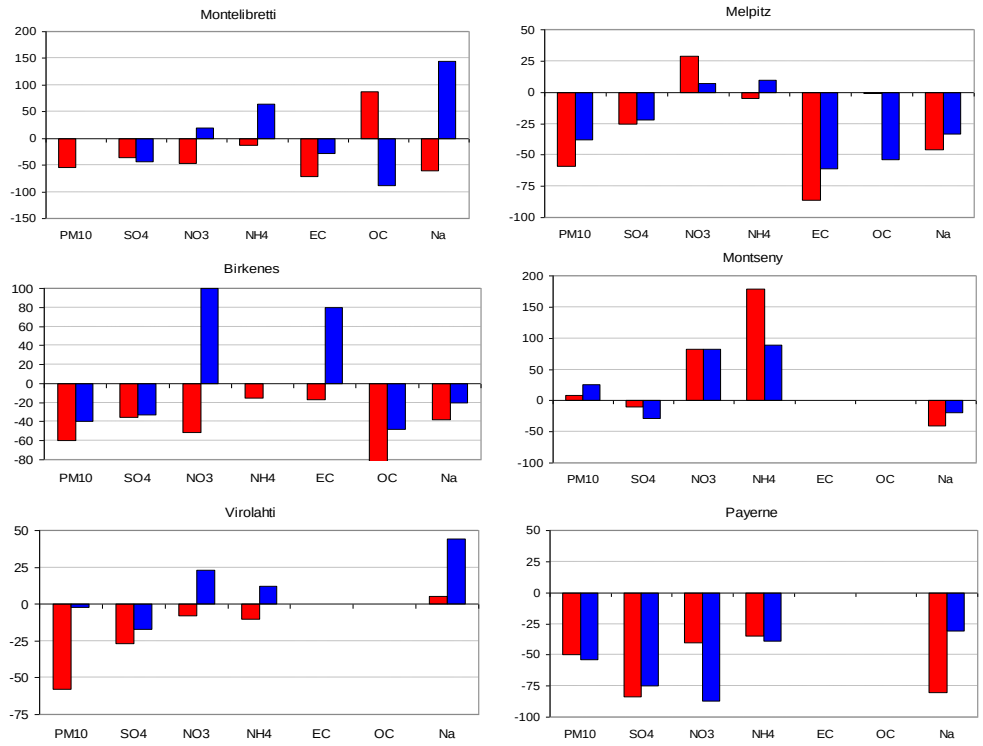

Figure 5.3: Relative model biases (%) for PM_{10} and chemical components of PM_{10} compared to observations in June 2006 (red) and January 2007 (blue). Note that only primary anthropogenic OC is included in the model.

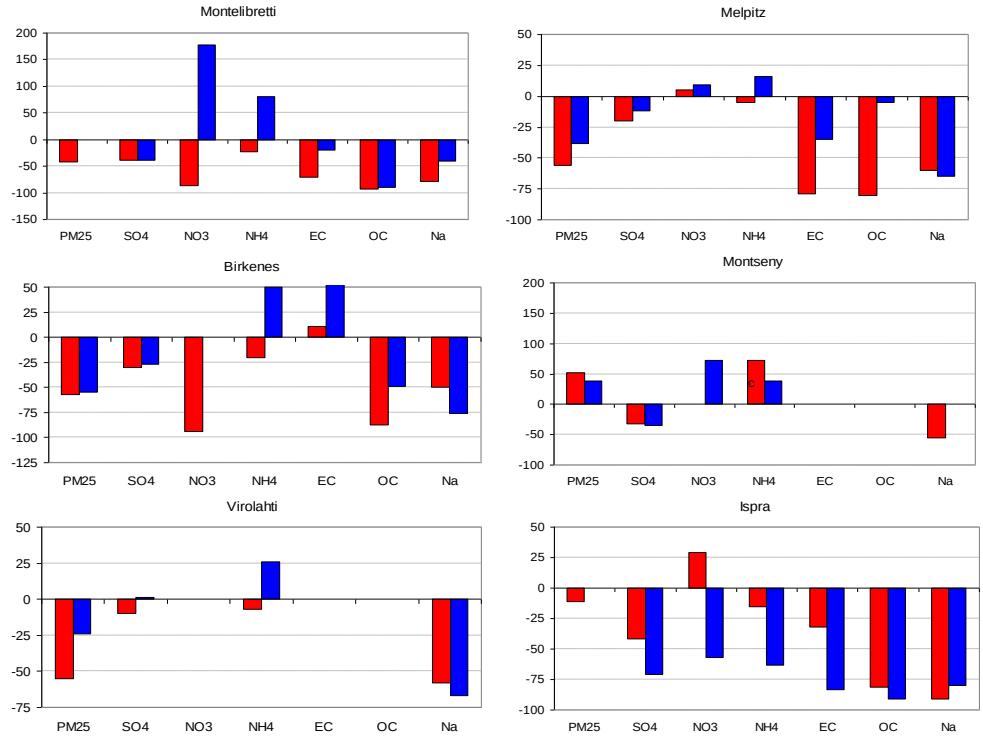

Figure 5.4: Relative model biases (%) for $PM_{2.5}$ and chemical components of $PM_{2.5}$ compared to observations in June 2006 (red) and January 2007 (blue). Note that only primary anthropogenic OC is included in the model.

Table 5.2: Comparison statistics between model calculations and observations for PM_{10} and PM_{10} constituents.

			PM_{10}	SO_4^{2-}	NO_3^-	NH_4^+	EC	OC	Na^+	Cl^-	Miner.
IT01	2006	Bias	**-54**	**-36**	**-47**	**-13**	**-72**	**-88**	**-61**		**4**
		R	**0.85**	**0.2**	**0.12**	**0.19**	**0.83**	**0.75**	**-0.25**		**0.87**
	2007	Bias		**-43**	**19**	**65**	**-28**	**-88**	**-33**	**144**	**43**
		R		**0.14**	**-0.01**	**0.07**	**0.46**	**0.45**	**0.53**	**0.44**	**0.07**
DE44	2006	Bias	**-59**	**-25**	**29**	**-5**	**-86**	**-91**	**-46**	**118**	no Si
		R	**0.37**	**0.56**	**0.21**	**0.37**	**0.66**	**0.55**	**0.88**	**0.79**	no Si
	2007	Bias	**-38**	**-22**	**7**	**10**	**-61**	**-54**	**-33**	**-15**	
		R	**0.44**	**0.58**	**0.50**	**0.59**	**0.62**	**0.44**	**0.66**	**0.61**	
NO01	2006	Bias	**-60**	**-35**	**-51**	**-15**	**-17**	**-84**	**-38**	**81**	
		R	**0.85**	**0.84**	**0.63**	**0.81**	**0.86**	**0.61**	**0.69**	**0.69**	
	2007	Bias	**-40**	**-33**	**100**	**0**	**80**	**-48**	**-20**	**-2**	
		R	**0.4**	**0.42**	**0.15**	**-0.13**	**0.63**	**0.33**	**0.32**	**0.25**	
ES17	2006	Bias	9	-10	83	179			-40	52	45
		R	0.18	0.15	-0.15	0.58			0.53	0.79	-0.05
	2007	Bias	25	-28	82	89			-20	12	103
		R	0.20	0.55	0.26	0.49			0.08	0.40	-0.09
FI17	2006	Bias	**-58**	**-27**	**-8**	**-10**			**5**		
		R	**0.46**	**0.78**	**0.54**	**0.87**			**0.32**		
	2007	Bias	**-29**	**-17**	**23**	**12**			**44**	**170**	
		R	**0.34**	**0.63**	**0.12**	**0.79**			**0.80**	**0.85**	
CH02	2006	Bias	**-50**	**-84**	**-40**	**-35**			**-80**		
		R	**0.67**	**0.25**	**-0.47**	**0.2**			**0.08**		
	2007	Bias	**-54**	**-75**	**-87**	**-39**			**-31**		
		R	**0.43**	**0.41**	**0.64**	**0.56**			**0.78**		
AT02	2006	Bias	**-49**	**-11**	**34**	**38**					
		R	**0.42**	**0.44**	**0.19**	**0.47**					
	2007	Bias	**-70**	**-32**	**65**	**31**					
		R	**-0.11**	**-0.11**	**-0.14**	**0.08**					
CZ03	2006	Bias					-39	-92			
		R					0.17	0.06			
	2007	Bias	-18				-81	103			
		R	0.73				0.63	0.69			

Temporal data coverage: bold font - 90-100% coverage, normal font – more than 30% coverage, shaded – less than 30% coverage.

Table 5.3: Comparison statistics between model calculations and observations for $PM_{2.5}$ and $PM_{2.5}$ constituents.

			$PM_{2.5}$	SO_4^{2-}	NO_3^-	NH_4^+	EC	OC	Na^+	Cl^-	Miner.
IT01	2006	Bias	**-42**	**-39**	**-86**	**-22**	**-70**	**-93**	**-79**		**-39**
		R	**0.75**	**0.26**	**-0.32**	**0.25**	**0.79**	**0.81**	**0.08**		**0.87**
	2007	Bias		**-38**	**177**	**81**	**-19**	**-89**	**-41**	**129**	**-33**
		R		**0.22**	**0.04**	**-0.03**	**0.45**	**0.48**	**0.15**	**0.1**	**0.04**
DE44	2006	Bias	**-56**	**-20**	**5**	**-5**	-79	**-80**	**-60**	**100**	no Si
		R	**0.43**	**0.58**	**0.21**	**0.36**	0.96	**0.29**	**0.78**	**0.50**	no Si
	2007	Bias	**-38**	**-12**	**9**	**16**	**-35**	**-5**	**-65**	**-44**	no Si
		R	**0.39**	**0.62**	**0.54**	**0.60**	**0.67**	**0.49**	**0.61**	**0.44**	no Si
NO01	2006	Bias	**-57**	**-30**	**-94**	**-20**	**11**	**-87**	**-50**	**81**	no Si
		R	**0.85**	**0.87**	**0.06**	**0.85**	**0.87**	**0.73**	**0.41**	**0.69**	no Si
	2007	Bias	**-55**	**-27**	0	**50**	**80**	**-49**	**-76**	**-54**	no Si
		R	**0.11**	**0.47**	-0.16	**0.50**	**0.1**	**0.1**	**0.47**	**0.66**	no Si
ES17	2006	Bias	52	-32	977	72			-55	167	46
		R	0.30	0.12	0.43	0.30			0.13	-0.12	-0.05
	2007	Bias	39	-35	73	38				12	39
		R	0.23	0.98	-0.28	0.11				0.40	0.23
FI17	2006	Bias	-55	-10	100	-7			-58	700	no Si
		R	0.49	0.84	mod=0	0.90			0.83	-0.06	no Si
	2007	Bias	**-24**	**1**	**0**	**26**			**-67**	**-12**	no Si
		R	**0.37**	**0.71**	**-0.01**	**0.79**			**0.82**	**0.83**	no Si
IT04	2006	Bias	-11	**-42**	**29**	**-15**	-32	-81	**-91**	**-85**	no Si
		R	0.30	**0.36**	**0.57**	**0.39**	0.58	0.58	**0.09**	**-0.07**	no Si
	2007	Bias		**-71**	**-57**	**-63**	**-83**	**-91**	**-80**	**-91**	no Si
		R		**0.35**	**0.18**	**-0.32**	**-0.1**	**0.04**	**-0.06**	**0.0**	no Si

Temporal data coverage: bold font - 90-100% coverage, normal font – more than 30% coverage, shaded – less than 30% coverage, dark grey – only 3 days with measurements.

5.3 PM_{10} and $PM_{2.5}$ chemical components

Figure 5.5 and Figure 5.6 summarise the results obtained when comparing model calculations and observations by the individual chemical components of PM_{10} and $PM_{2.5}$, respectively. Model biases for summer (June06) are shown as red bars and those for winter (January07) are shown as blue bars for each of the measurement sites.

- PM_{10} is underestimated by the model by 50-60% in June06 and by 40-70% in January07 for all sites except Montseny, where it is overestimated by 10-25%. No particular seasonal pattern in the model bias can be found.

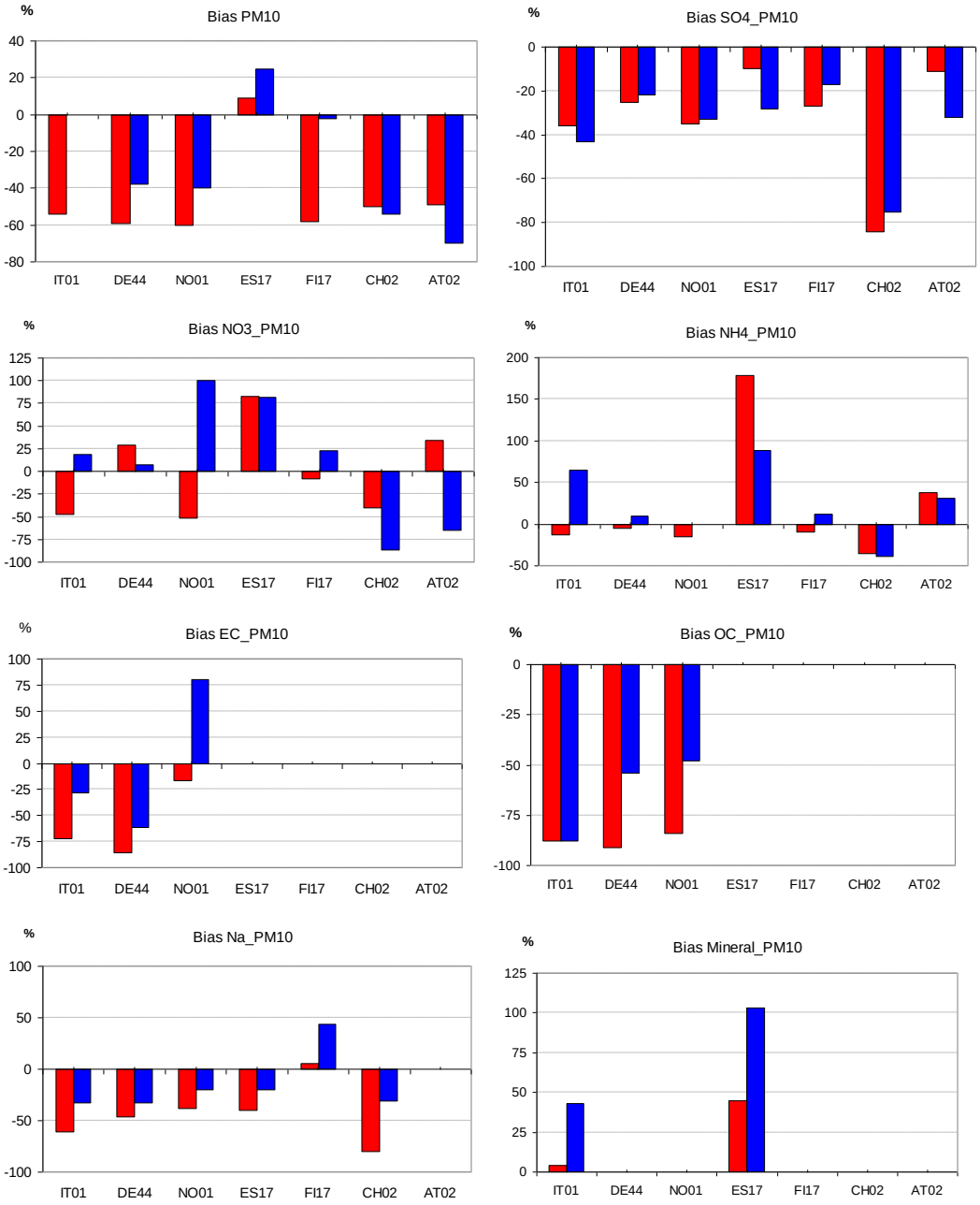

Figure 5.5: Relative model biases (%) for PM_{10} and chemical components of PM_{10} compared to observations in June 2006 (red) and January 2007 (blue). Note that only primary anthropogenic OC is included in the model.

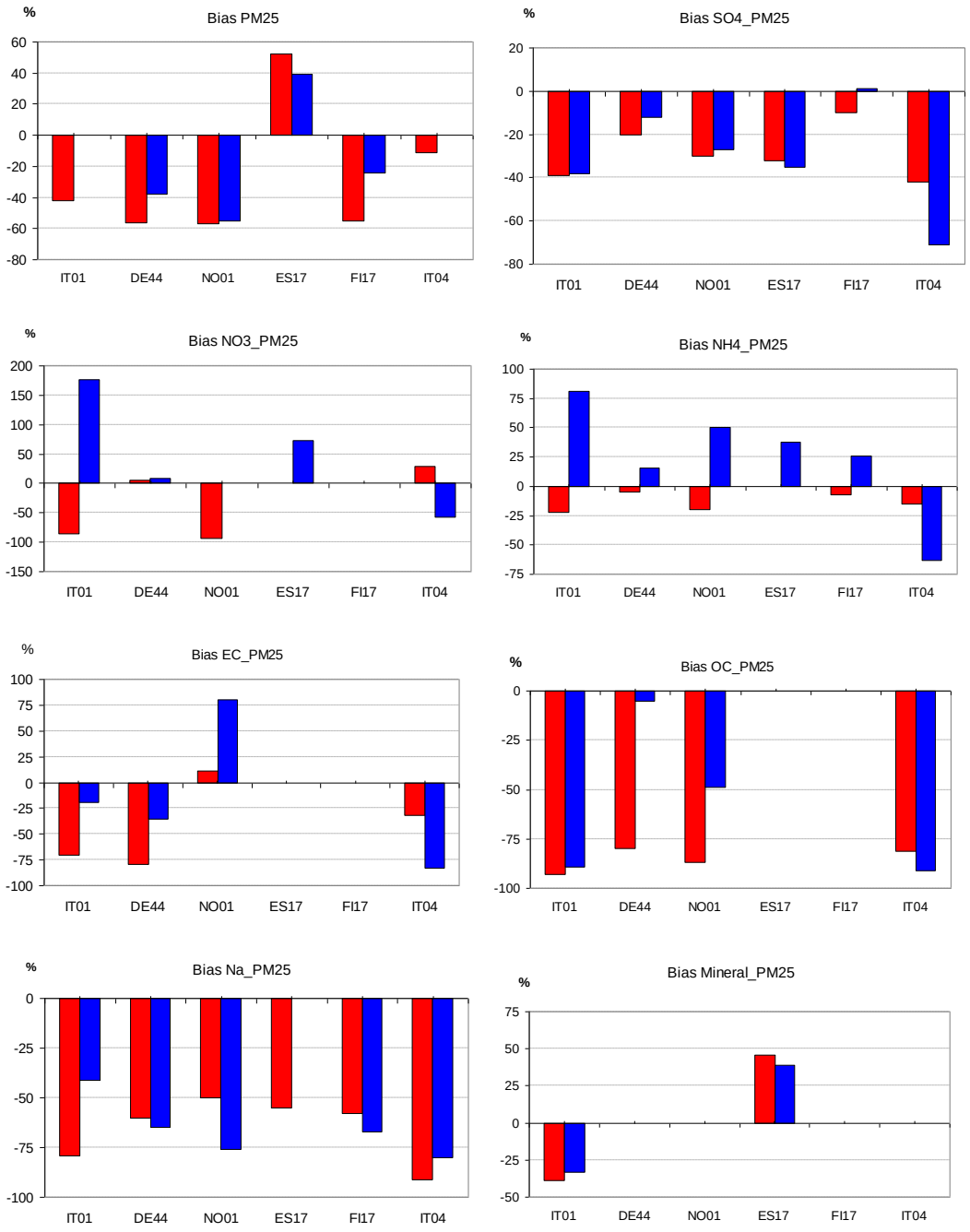

Figure 5.6: Relative model biases (%) for $PM_{2.5}$ and chemical components of $PM_{2.5}$ compared to observations in June 2006 (red) and January 2007 (blue). Note that only primary anthropogenic OC is included in the model.

- $PM_{2.5}$ is underestimated by 10-58 % in June06 and by 20-57% in January07 for all sites except Montseny, where it is overestimated by 40-50%. The model underestimates $PM_{2.5}$ somewhat more in June 2006 compared to January07.

- Sulphate (SO_4^{2-}) concentrations in both PM_{10} and $PM_{2.5}$ are underestimated by 20-40% on average (by 70-80% at Payerne), and the underestimation is somewhat greater in summer than in winter (except for Illmitz and Ispra).

- Comparison results for nitrate (NO_3^-) and ammonium (NH_4^+) concentrations for the considered sites are rather inconclusive. The levels are both underestimated and overestimated, in summer as well as in winter. The bias is mostly within 50% (Montelibretti, Melpitz, Virolahti and Illmitz). The largest model overestimation of NO_3^- and NH_4^+ in PM_{10} for both seasons is found for Montseny (from 75 to 175%), but rather little data is available for this site. For Birkenes, the model underestimates NO_3^- in PM_{10} in summer by 50%, but overestimates it greatly in winter (by 100%). The latter is probably due to evaporation during filter conditioning, this is confirmed by much higher nitrate concentration in the parallel filterpack measurements. The model bias for NH_4^+ is zero for January07, but this is solely due to a huge peak in observation data on 26 January, which probably is due to filter contamination (see time series in Appendix XX). Otherwise model calculated NH_4^+ is considerably higher than the measured data. As to fine NO_3^- and NH_4^+, the model tend to underestimate NO_3^- and NH_4^+ concentrations in $PM_{2.5}$ for summer (June06), while overestimations occur more often for winter (January07) for all sites, with the exception of Ispra. For further discussion on measurement artefacts for NO_3^- and NH_4^+ see Chapter 6 in EMEP Status Report 1/2008.

- The model seems to have trouble to reproduce the formation of fine NO_3^- for the relatively clean atmosphere in northern Europe in summer. E.g., calculated concentrations of NO_3^- in $PM_{2.5}$ are zero for Birkenes and Virolahti in June06.

- Measurements of EC and OC concentrations are only available at three sites for PM_{10} and four sites for $PM_{2.5}$. Apart from EC for Birkenes, the model underestimates concentrations of EC and OC more in summer than in winter.

- EC is underestimated by the model for Montelibretti and Melpitz for both Jun06 and Jan07, whereas for NO01 EC model prediction is fairly good for Jun06, but greatly overestimated for Jan07. These results support the geographical differences in the model performance based on the EMEP EC/OC campaign data reported by Tsyro et al. (2007). In that study, the model was found to considerably underestimate EC in central and southern Europe, especially in summer, while it overestimated EC in northern Europe in winter.

- The main reason for model underestimation of OC is that the model does not account for secondary OC nor primary natural OC. Therefore, the underestimation is larger in summer than for winter for Birkenes and Melpitz. This is consistent with the seasonal variation of the intensity of biogenic emissions of VOCs and primary biological aerosol particles. In Figure 5.1 it is shown that 30% of the total OC emissions in Norway could be attributed to PBAP..

- Sodium (Na^+) from the marine aerosol is underestimated by the model for all sites, except Virolahti, and the underestimation is in general somewhat greater in summer. Na^+ in PM_{10} is underestimated by 40-60% (by 80% for Payerne) in

June06 and 20-40% in January07, whereas fine Na^+ is underestimated by 50-90% for June06 and 40-80% for January07.

- Concentrations of mineral dust were derived from measurement data, using the formula suggested by Chan et al. (1997), i.e. $(1.89 \cdot Al + 2.14 \cdot Si + 1.4 \cdot Ca + 1.2 \cdot K + 1.36 \cdot Fe) \cdot 1.12$ for the two sites Montelibretti and Montseny.

- For Montseny, the model overestimates mineral dust in $PM_{2.5}$ by 46% for June06 and 39% for January07, and it overestimates mineral dust PM_{10} by 45% in June06, while mineral dust in PM_{10} is overestimated by 103% in January07. For Montelibretti, dust is overestimated by the model for June06 and underestimated for January07, with the bias being within 40%. Calculations of mineral dust are associated with rather large uncertainties in the model due to the uncertainties in anthropogenic dust emissions and in the parameterisation of windblown dust generation.

5.4 Temporal correlation

The correlation coefficients between calculated and measured concentrations of PM components are provided in Table 5.2 and Table 5.3 and visualised in Figure 5.7. The correlation coefficient varies over wide range, from negative to as high as 0.87 for different components and sites.

Overall, the best model performance with respect to temporal correlation is for Birkenes for June 2006 and for Melpitz, in particular for January 2007. For Birkenes, correlation coefficients for PM_{10} and $PM_{2.5}$ components lie mostly between 0.6 and 0.85 for June06. However for January07, the correlation goes down to as low as 0.1, ranging between 0.1 and 0.6. The poorest correlation is found for NO_3^- in $PM_{2.5}$, but these results are rather uncertain, as for June06 the model does not produce any fine NO_3^-, while for January07 most of the measurements are set to the detection limit value. For Melpitz, the correlation coefficients are mostly in the range of 0.4 to 0.6 for January07 and somewhat lower for June06, particularly for NO_3^-.

Quite good correlation (between 0.4 and 0.9) is found for SIA components and sea salt for Virolahti (carbonaceous concentrations were not determined at this site). The exception is a poor correlation for NO_3^- in winter and fine NO_3^- in summer. For Montelibretti, model calculated PM_{10} and $PM_{2.5}$ concentrations correlate fairly well with observed concentrations in June06, with correlation coefficients being 0.85 and 0.75, despite rather poor correlation for all SIA components. Closer analysis shows that the good correlation obtained for PM_{10} and $PM_{2.5}$ is to a large degree due to a good model performance for mineral dust, as the model manages to capture two dust episodes in June 2006.

For Montseny, the correlation for PM_{10} is 0.2 for both months. These relatively low correlations are probably caused by low correlation between calculated and measured concentrations of mineral dust, which contributes significantly to PM mass in Spain. Correlation between calculated and observed SIA components is better for January07 than for June06.

None of the individual components can be pointed out, for which model results correlate with measurements equally well for both months and for all of the sites.

In particular, the correlation results are quite varying for NO_3^- concentrations. In some cases, the correlation for NO_3^- in PM_{10} and NO_3^- in $PM_{2.5}$ is negative even though calculated SO_4^{2-} and NH_4^+ are positively correlated with observations (as at Montelibretti, Virolahti, Payerne and Montseny). This occurs most often in June06, but is also observed for January07. At Ispra, a negative correlation is found for NH_4^+ in $PM_{2.5}$ for January07, while the correlation coefficients for both SO_4^{2-} in$PM_{2.5}$ and NO_3^- in $PM_{2.5}$ are positive. Such cases cannot be explained by the advection alone, but are probably due to the in-situ chemistry not captured by the model or due to inconsistencies (artefacts) in the measurements.

It is worth pointing out the fairly good correlations between modelled and observed EC and OC concentrations. Particularly for the winter month January07, the correlation coefficients for EC and OC often exceeded those for the SIA components.

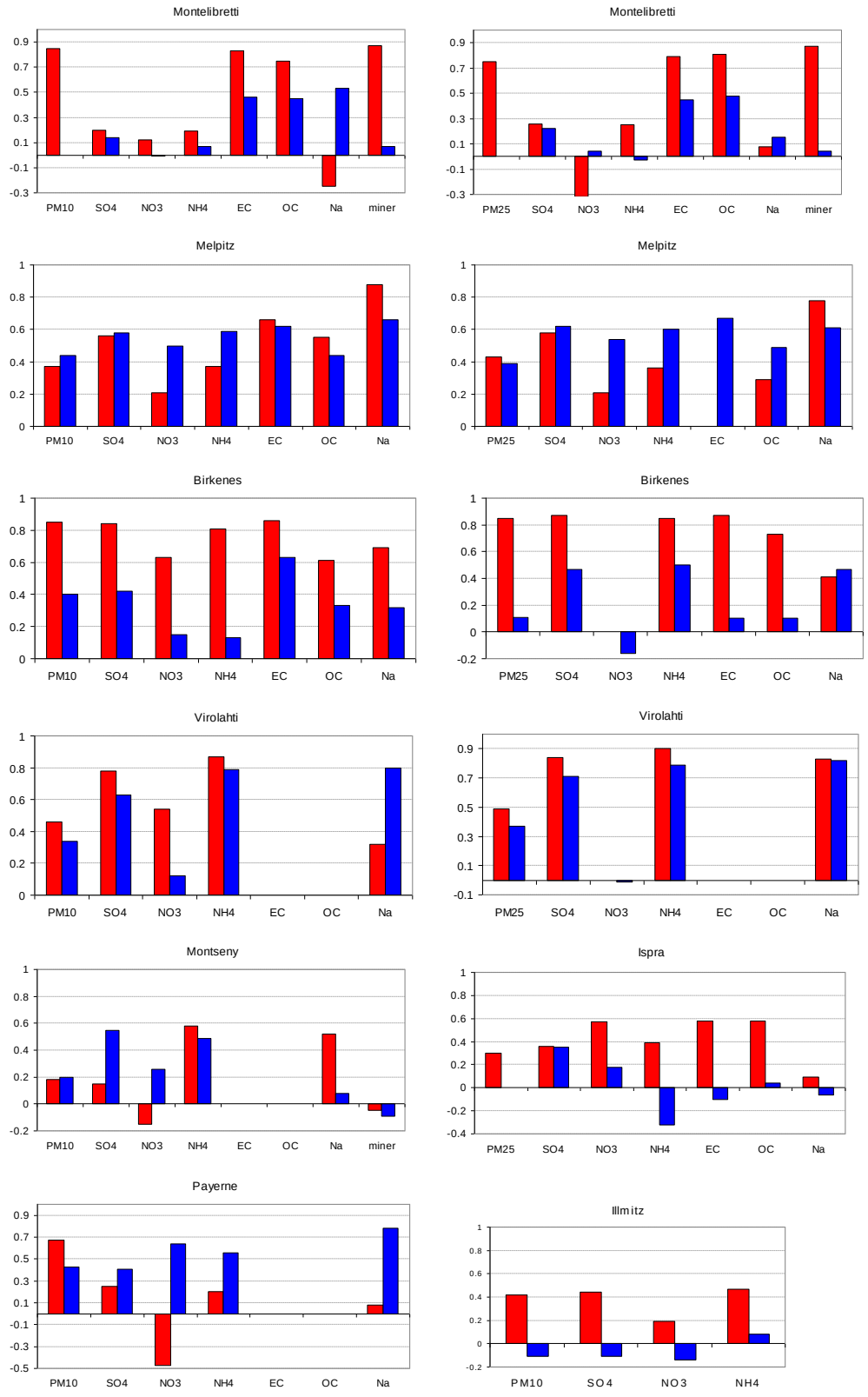

Figure 5.7: Correlation coefficients (R) between calculated and measured PM_{10} (left hand side) and $PM_{2.5}$ (right hand side) and their chemical components for June 2006 (red) and for January 2007 (blue).

5.5 Particle size distribution

In the EMEP model the coarse PM fraction consists of nitrate, elemental carbon, sea salt and mineral dust. Figure 5.8 compares calculated distribution of NO_3^- between fine and coarse aerosols with that observed. There is a quite good agreement between model and observations for Virolahti (FI17) in January07 and for Melpitz (DE44) for June06. For Montseny (ES17), the model predicts much more NO_3^- in the fine fraction compared to the measurements both during summer and winter. For the Nordic sites Birkenes and Virolahti, the model does not produce any fine NO_3^- at all for June06.

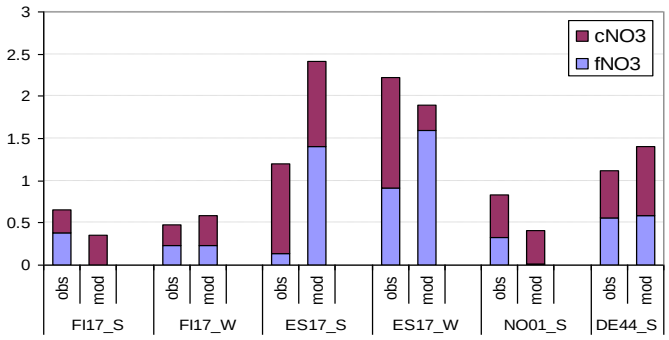

Figure 5.8: Observed and calculated distribution of nitrate between fine and coarse particles for several sites in June 2006 (denoted by S) and in January 2007 (denoted by W).

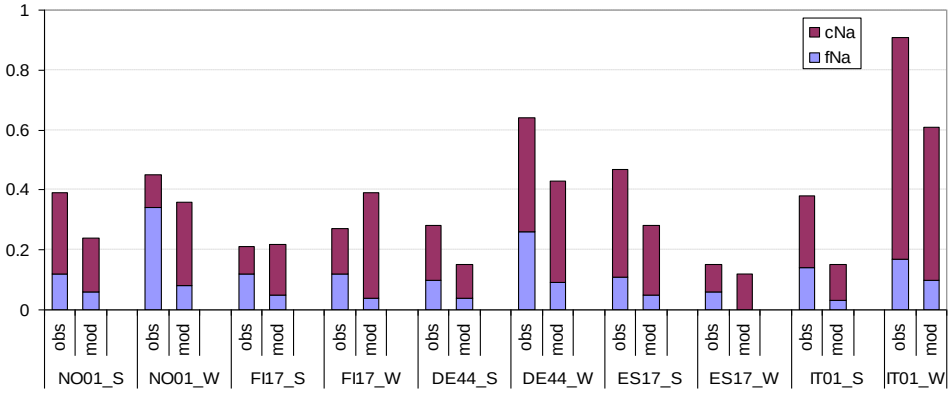

Figure 5.9: Observed and calculated distribution of sodium between fine and coarse particles for several sites in June 2006 (denoted by S) and in January 2007 (denoted by W).

For the sea salt aerosol, the model tends to underestimate Na^+ in the fine fraction. It predicts the contribution from fine Na^+ to Na^+ in PM_{10} to be between 10 and 25% for different sites, while the measured contributions vary mostly between 20 and 60%.

Time series for coarse NO_3^- (calculated as NO_3^- in PM_{10} - NO_3^- in $PM_{2.5}$) and Na^+ (calculated as Na^+ in PM_{10} - Na^+ in $PM_{2.5}$) are included in the Appendix A.

For coarse NO_3^-, model performance appears to be better for June06 (based on observations available from Virolahti and Birkenes) than for January07 (based on observations available from Virolahti and Montelibretti). The results for Montseny are rather poor for both months, but there are rather few days with NO_3^- measurements at this site.

The model seems to calculate coarse Na^+ better for January07 than for June06 for most of the sites, while the results are better for June06 for Birkenes and Melpitz. In fact, Melpitz is the only site for which the model manages to reproduce coarse Na^+ concentrations for both months June06 and January07 quite well and the correlation is as high as 0.87 and 0.67 respectively.

5.6 Conclusions

Preliminary results have been presented where we analyse whether the model is able of reproducing PM_{10} and $PM_{2.5}$ chemical composition measured during the two EMEP intensive periods in June 2006 and January 2007. The datasets collected during those two intensive measurement periods represent a very valuable material for model evaluation with respect to different PM components and to distribution of such constituents between the fine and the coarse mode. The comparison between calculated and measured concentrations of PM_{10} and $PM_{2.5}$ components has shown rather mixed results for different stations.

- In general, the model manages to reproduce the main characteristics of chemical composition of PM_{10} and $PM_{2.5.}$

- The model underestimates PM_{10} and $PM_{2.5}$ for almost all sites, and the underestimation tends to be larger for the summer month (June 2006) compared to the winter month (January 2007).

- With a few exceptions, the model underestimates PM_{10} and $PM_{2.5}$ components, though to a various degree, for both months.

- Underestimation of the carbonaceous (elemental and organic carbon fraction of the aerosol), and in particular OC, appears to be the main reason for model PM underestimation in summer. Interestingly, the correlation coefficients between calculated and measured concentrations for EC and OC are among the highest.

- Among the individual aerosol components nitrate, in particular NO_3^- in the fine fraction, appears to be the least robust component in model results compared with measurements at different sites.

Further analysis of model versus intensive measurements is necessary with particular attention to the uncertainties in measurement data due to measurements artefacts and to the comparability of data collected at different stations.

6 Remote sensing

By Svetlana Tsyro, Kerstin Stebel, A.M. Fjæraa, M. Johnsrud, A. Fahre Vik, T. Holzer-Popp and M. Schroedter-Homscheidt

6.1 Introduction

Air pollution by aerosols has become a global issue with the recognition of inter-continental transport as a significant source to the background levels of polluted air, especially in Europe and North-America. While current regional monitoring networks are suitable for monitoring air pollution from regional sources, new measurement techniques and platforms are required to quantify the hemispheric transport and its contribution to regional background levels of aerosols. Utilizing satellite observations for the detection of the aerosol load is an interesting approach, as it offers data coverage over large areas, including the oceans, and is able to provide "images" of the spatial air pollution distribution.

Satellite remote sensing could provide information on PM concentrations in regions which have a poorly developed surface monitoring network (e.g. eastern Europe). At present, data from satellites alone cannot fulfil the requirements for protocol monitoring, but in the future, remote sensing from satellites could become an integral part of a network where ground-based stations and remote sensing complement each other. In particular, the combined use of remote sensing observations (from satellites) and in-situ observations with modelling through data assimilation ("integrated monitoring") might become best practice. In the future, we expect improved Earth Observation data retrieval and products, sensors/satellites (e.g. ESA's EarthCARE (Earth Clouds, Aerosols and Radiation Explorer), and the so-called Sentinel -4 and Sentinel -5 for Atmospheric chemistry, space-based systems operating from geostationary (GEO) and low Earth orbit (LEO) respectively, to be better suited for Air Quality purposes. In addition, the possibility of adapting the legislation to utilize the potential of remote sensing, e.g. trough the introduction of new indicators is a topic for discussion.

EMEP-CCC and MSC-W are currently seeking to incorporate space borne Earth Observation data in operational routines for assessment of air quality levels in Europe. An assessment of the accuracy and applicability of these data sources are therefore needed in order to make this possible. AOD calculated with the EMEP-model is compared with AOD retrieved from Moderate resolution Imaging Spectrometer (MODIS) onboard the NASA polar-orbiting earth observation satellites Aqua and Terra. Following the work described in the EMEP/CCC-Report 3/2006 (EMEP, 2006a), the SYNAER data product (SYNergetic Aerosol Retrieval product), provided through the ESA-GSE project PROMOTE, is chosen as a state-of-the-art satellite aerosol data set and is compared to EMEP's regular aerosol monitoring program.

6.2 Implementation of AOD calculations in the EMEP model

Aerosol optical depth (AOD) describes the extinction of light beam traversing an atmospheric layer containing aerosol particles. Light extinction by aerosols occurs

by attenuation of the incident light due to scattering and absorption. AOD within the atmospheric layer between z_1 and z_2 (τ_{ext}) is calculated as

$$\tau_{ext} = \int_{z1}^{z2}\int_{r1}^{r2} \pi \cdot r^2 \cdot Q_{ext}(\lambda, r) \cdot N \, dr \, dz \qquad (6)$$

where r is the aerosol radius, N is the aerosol number density, r_1 and r_2 are the lower and upper radii of the particle size distribution, Q_{ext} is the aerosol extinction efficiency, which is a function of the particle size and the light wavelength (λ).

The absorption and scattering of light by spherical particles is described by Mie theory. The key parameters that govern the scattering and absorption of light by a particle are (1) the wavelength of the incident radiation, (2) the size of the particle, which are combined in a dimensionless size parameter $\alpha=2\pi r/\lambda$, and (3) the complex refractive index of the particle relative to the surrounding air: $m= n+ik$, where n and k denote the non-absorbing (scattering) and absorbing parts. Complex refractive index is a specific material's property, and it is believed to apply down to the material's smallest particle. Based on the value of particle size parameter, three main domains of light scattering can be identified: Rayleigh scattering ($\alpha << 1$), Mie scattering ($\alpha \cong 1$), and geometrical scattering ($\alpha >> 1$).

In the EMEP aerosol model the extinction efficiency is calculated using the Mie scattering mathematical formalism and based on an effective complex refractive index for each of the four size fractions. The particles are assumed to be spherical and internally mixed. As a first approximation, the effective complex refractive index is calculated as the sum of volume weighted complex refractive indices of all aerosol components, including aerosol water, as

$$m_{eff} = \Sigma (v_i \cdot n_i) + i \, \Sigma (v_i \cdot k_i)$$

where v_i is the volume fraction of a component i to the total volume in the size bin. This approach gives a reasonable estimate for effective refractive index in many cases. However, some results indicate that the plain volume mixing approach may slightly exaggerate the absorption under certain circumstances. To overcome this Maxwell Garnett mixing rule for elemental carbon is planned to be applied in the future (Chýlek et al., 1998; Kirkevåg et al., 2005).

It should be noted that the effect of aerosol water is explicitly accounted for in the model. The scattering is a complex function of both refractive index and particle size. Increase in ambient relative humidity leads to a larger water uptake by aerosols, which causes aerosol growth, while both the real and imaginary parts of their refractive index tend to decrease. In fact, decrease in refractive index as relative humidity increases is not large enough to counteract the increase of the particles' cross-section due to size increase. Thus, aerosol water uptake with increase in relative humidity will lead to an increase in aerosol scattering. The real and imaginary parts of complex refractive index for aerosol components adopted in the present work are provided in Table 6.1.

For Mie scattering calculations a code developed by Mishchenko (Mishchenko et al., 2002 and 2008) have been employed. A lookup table have been made, which allows to find extinction efficiency (Q_{ext}) and extinction cross-section (C_{ext}) at the wavelength of 0.55 μm for a given particle radius and a complex refractive index (m_{eff}) both for monodisperse particle distribution and for log-normal particle distribution within each size fraction. Using the effective extinction efficiency from the lookup table, AOD is calculated in the model as

$$\tau = \sum_{k=1}^{ktop} (\pi r_i^2 N_i \cdot Q_{ext,i}) \, \Delta z_k \ ,$$

where N_i, r_i, and $Q_{ext,\ i}$ are the number density, the radius, and the extinction efficiency for particles in size fraction *i*. AOD is calculated at every advection time step based on calculated concentrations of aerosol components and particle number densities for the four size modes.

Table 6.1: Real (n) and imaginary (k) parts of the complex refractive index (m = n + ik) for different aerosol components adopted in the EMEP model calculations.

	SO_4^{2-} 1)	NO_3^- 1)	NH_4^+ 1)	OC 1)	EC 2)	Min. dust 3)	Sea salt 2)	Water 4)
n	1.43	1.43	1.43	1.53	1.95	1.5	1.56	1.333
k	10^{-8}	10^{-8}	10^{-8}	0.006	0.79	10^{-8}	0.0025	0.0

The sources are: 1) Köpke et al. (2006), 2) Bond and Bergstrom (2006), 3) Sokolik and Toon (1999), 4) Hale and Querry (1973)

A series of sensitivity tests have been carried out using two different representations of aerosol distribution in calculations of Mie scattering efficiencies. In general, model calculations using log-normal aerosol distribution yield higher AOD values than those using monodisperse aerosols and agree better with MODIS data. Below are presented model calculation results using the log-normal aerosol distribution.

6.3 MODIS data

The Moderate resolution Imaging Spectrometer (MODIS) onboard the NASA polar-orbiting earth observation satellites Aqua and Terra detects radiances in the visible and infrared spectrum region at least once daily. The aerosol retrieval algorithm uses data in the visible spectrum region, so only daytime data are considered for retrieval. A concise description of the aerosol retrieval algorithms can be found in Remer et al. (2006). The measured reflectance is corrected for extinction by the water vapour, ozone, and carbon dioxide based on climatology data. Observations over land and ocean are processed with two separate algorithms.

In the over-ocean algorithm, cloud, sun glint and underwater sediment masks are applied to the data and the contaminated pixels are identified and discarded. The inversion part of the algorithm is based on a look-up table approach with pre-

computed spectral reflectances for a set of aerosol and surface parameters. The climatology used for the look-up table is mainly based on measurements by sun/sky photometers (AERONET; Holben et al., 1998). It is assumed that a properly weighted combination of one fine and one coarse log-normal aerosol mode (called "aerosol model") can represent the ambient optical and physical aerosol properties over the target. The algorithm makes use of four fine and five coarse pre-defined aerosol modes.

The over-land retrieval algorithm discards pixels with clouds, in-land water bodies and snow/ice. As in over-ocean retrievals, this algorithm also applies an inversion procedure for aerosol optical properties retrieval, but using a different look-up table. The land retrieval algorithm uses a priori assigned fine aerosol types ("aerosol models"), depending on the geographical location and the season. Three types of fine aerosol models are defined, namely non-absorbing (urban/industrial), absorbing (savanna/grass smoke) and neutral (forest smoke), which are assumed to be spherical. In addition, one type of spheroid aerosol represents coarse dust particles. It is assumed that one fine-dominated aerosol model and one coarse-dominated aerosols model can be combined with proper weightings to represent the ambient aerosol properties.

6.3.1 MODIS data used in this work

The data from "Collection 5" have been used in this work. For the initial tests we selected data sets representing different seasons and years: July-August 2003, November-December 2003, March-April 2004 and July-August 2004. Data obtained with MODIS instruments from both Terra and Aqua satellites have been used. The MODIS data, provided by the Goddard Space Flight Center (NASA), are stored as one granule per file, with each granule consisting of 203x135 of $10x10km^2$ boxes following the satellite track. From these data hourly and daily averaged AOD maps aggregated in the EMEP grid were created.

6.3.2 Uncertainties and limitations of AOD data

In the present work, we have used the MODIS product called "Optical Depth Land And Ocean", which contains data for AOD at 0.55 μm. This MODIS product was chosen for the present work because it: (1) relies on primary retrieved data only, (2) has most stringent quality control, and (3) is a joint product covering both land and ocean.

The reported in Remer et al. (2006) error-bars of retrieved AOD are $\Delta\tau = \pm 0.03 \pm 0.05\tau$ over ocean and $\Delta\tau = \pm 0.05 \pm 0.15\tau$ over land. The main data uncertainties over ocean are due to the effect of non-spherical dust and cloud contamination, particularly low altitude ice clouds at high latitudes. The main uncertainties over land are due to cloud contamination, and surfaces with sub-pixel snow, ice or surface water (coastal regions, marshes, etc.). Furthermore, pre-assigned aerosol optical models for over-land retrieval lead to either positive or negative bias for large AOD in many regions. Choosing optimal refractive indices for the different chemical components is not a straightforward task, and is another source of uncertainties.

The representativeness of MODIS data may vary from one cell to another cell of the EMEP grid. This may happen because the MODIS algorithm checks and discards pixels in order to avoid different types of contamination as described above. The algorithm requires that minimum 2.5% of the pixels remain to produce an AOD value for a 10x10 km^2 box. For the purpose of comparison with EMEP model calculations MODIS AOD values are aggregated to 50x50 km^2 EMEP grid cells. Thus, the mean AOD values for different grid cells may be calculated based on different amount of MODIS data.

6.4 Preliminary model AOD results and comparison with MODIS data

6.4.1 AOD distribution over Europe

The EMEP aerosol model has been used to calculate AOD at 0.55 μm wavelength for the years 2003 and 2004. An example of daily mean AOD calculated with the model and from MODIS retrieval for 1 April 2004 is given in Figure 6.1, showing quite a good match between calculated AOD and MODIS AOD. For this day, the model nicely reproduces the retrieved AOD pattern, in particular the belt of enhanced AOD over the North Atlantic and the North Sea due to sea salt particles, stretching across Germany and the Czech Republic eastwards, and also in the Po Valley.

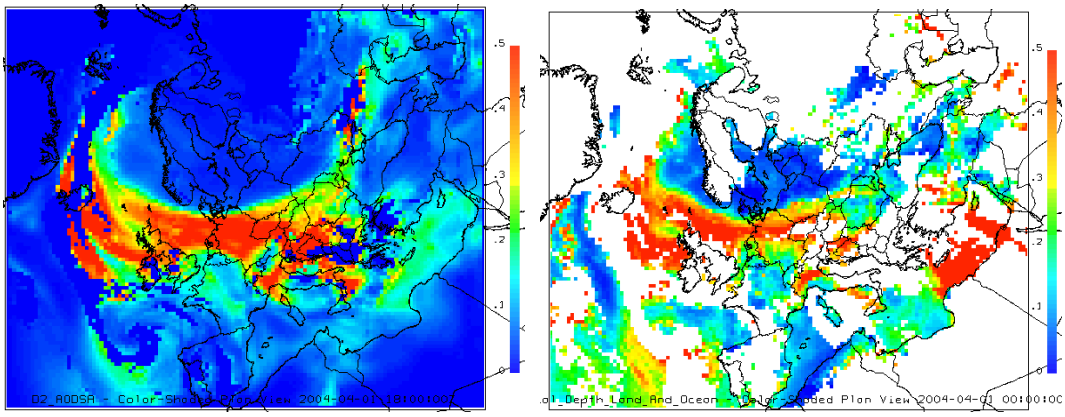

Figure 6.1: Daily mean calculated AOD (left panel) and MODIS AOD (right panel) and at 0.55 μm wavelength for 1 April 2004. The scale goes from 0.0 (blue) to 0.5 (red) in both maps.

6.4.2 Forest fire episodes

In summer 2003, severe wildfires occurred in Portugal. In particular, two critical fire periods were recorded between 27 July and 4 August and between 7 and 12 August, as documented in the report of the European Forest Fire Information System (EC JRC, 2004). Emission data for model simulations of black and organic carbon from wildfires have been taken from the Global Fire Emission Database (GFED2). The emissions were available as monthly values, which we have flatly distributed over the month.

In Figure 6.2 we show a series of maps of MODIS retrieved and model calculated AOD for the period 8 to 11 August 2003. Apparently the model is able of reproducing the main features of AOD distribution retrieved from MODIS

measurements. Model calculated AOD values due to the wildfires in Portugal are lower than those from MODIS data, which is partly due to the flat temporal distribution of fire emissions used in the calculations.

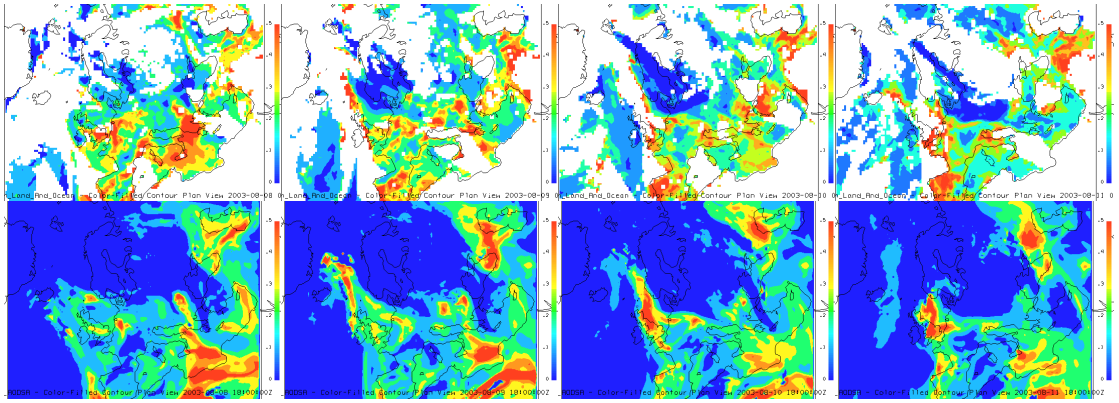

Figure 6.2: Daily mean model calculated AOD (bottom panels) and MODIS AOD data (upper panels) at 0.55 μm for days with intensive forest fires in Portugal: 8, 9, 10 and 11 August 2003.

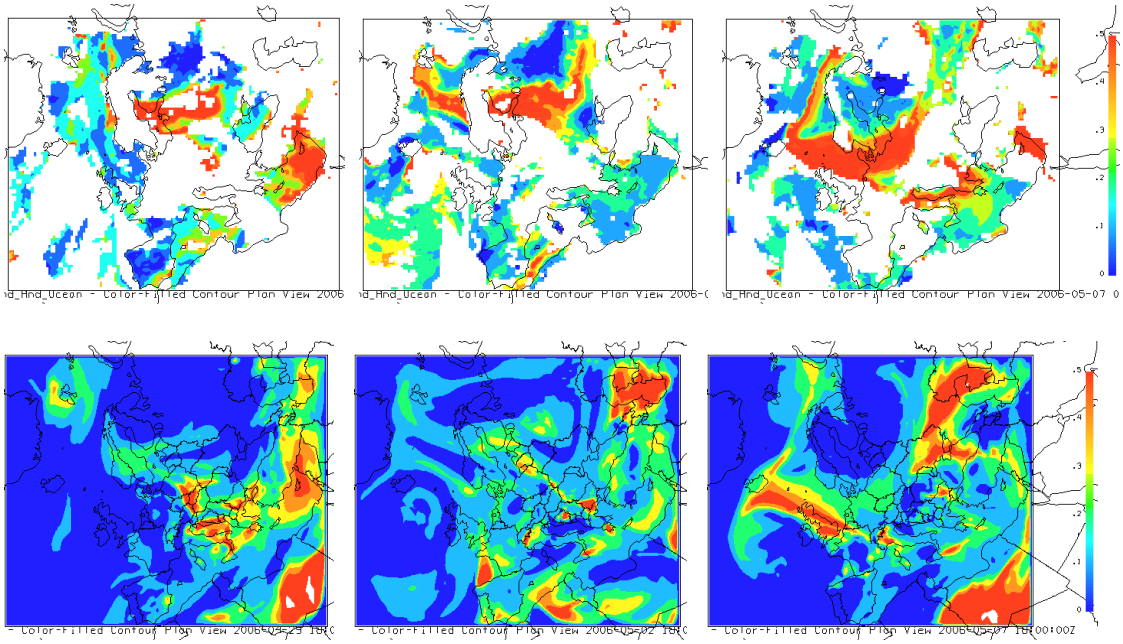

Figure 6.3: Daily mean model calculated AOD (bottom panels) and MODIS AOD data (upper panels) at 0.55 μm for the agricultural Waste burning event in eastern Europe: 29 April, 2 and 7 May 2006 (from left to right).

The model has also been used to calculate pollution episodes associated with the agricultural and forest fires in Russia and eastern Europe in spring 2006. Monthly emissions of black and organic carbon from GFED2 have been distributed over the period from 15 April to 10 May loosely based on the information about the number of fires from Stohl et al. (2007). Figure 6.3 displays the maps of MODIS AOD and model calculated AOD for three days: 29 April, 2 and 7 May 2006.

There is a fairly good resemblance between the distribution patterns of AOD retrieved from the MODIS data and that calculated with the model. On the other hand, the calculated AOD due to fire emissions are lower then those retrieved from MODIS measurements. This can partly be explained by the uncertainties in emission data and partly by the inaccuracies associated with calculating the dispersion.

6.4.3 Comparison of AOD spatial distributions

Model calculated AOD at 0.55 μm has been compared with MODIS AOD retrievals for the selected periods (July-August and November-December in 2003 and March-April and July-August in 2004). To provide a more consistent comparison, calculated AOD have been averaged for hours with sunlight and with predicted cloud cover less than 50%. Daily mean AOD values from the model and from MODIS data have been compared for grid cells of the EMEP grid.

Table 6.2 provides a summary of comparison statistics (relative bias and spatial correlation coefficient) between calculated and retrieved AOD over all cells of the EMEP grid for the actual periods. For comparison, the results from both model AOD calculations, i.e. using log-normal and monodisperse aerosol distributions in Mie scattering calculations, have been compared with MODIS AOD and are presented in Table 6.2.

Table 6.2: Relative bias and the coefficient of spatial correlation between model calculated AOD and AOD retrievals from MODIS over all cells in the EMEP grid.

		Bias (%)	R		Bias (%)	R
Mie-lognor AOD	2003			2004		
	Jul-Aug	-52	0.35	Jul-Aug	-54	0.26
	Nov-Dec	-17	0.11	Mar-Apr	-51	0.11
Mie-mono AOD	2003			2004		
	Jul-Aug	-79	0.31	Jul-Aug	-82	0.17
	Nov-Dec	-58	0.07	Mar-Apr	-77	0.11

The model calculated AOD is lower compared to MODIS retrieved AOD in both cases. The best correspondence with MODIS data is found for AOD calculated using log-normal particle size distribution. In this case, the model negative bias is in the range of -51 to -55 % for summer and spring months 2003-2004 and -11% for November-December 2003. The spatial correlation between modelled and MODIS retrieved AOD is rather poor for all seasons, being somewhat better for summer months July and August (0.35 in 2003 and 0.26 in 2004). Using the monodisperse size distribution approximation gives larger model underestimation of MODIS AOD and lower spatial correlations between calculated and retrieved AOD than using the log-normal approximation.

6.4.4 Comparison of AOD for different areas

Calculated AOD has been compared with MODIS data for grid cells representing different regions in Europe (the areas are just rectangle parts of the grid in selected geographical locations). Comparison statistics between modelled and MODIS AOD for several such areas are summarised in Table 6.3.

Table 6.3: Comparison of modelled AOD and MODIS AOD for several areas.

Area	July-Aug 2003		Nov-Dec 2003		March-April 2004		July-Aug 2004	
	Bias (%)	R	Bias (%)	R	Bias (%)	R	Bias (%)	R
Benelux	-33	0.53	-	-	-18	0.54	-41	0.50
UK	-39	0.65	*23*[*)]	*0.87*	-23	0.45	-47	0.53
central Europe	-44	0.61	33	0.48	-28	0.30	-54	0.48
south-east Europe	-37	0.66	8	0.17	-26	0.37	-29	0.41
central Russia	-59	0.67	*-14*[*)]	*0.29*	-64	0.24	-56	0.18
southern Norway	-65	0.21	-	-	-65	0.37	-71	0.44
Mediterranean Sea	-24	0.05	-18	0.0	-51	0.0	-26	0.23
southern N. Atlantic	-53	0.28	-33	0.32	-59	0.35	-59	0.0

[*)] 15-25% data coverage (periods with less than 15% data coverage are excluded)

The main findings from the comparison are:

- Over land, the model AOD underestimation tends to be larger in summer months, with the negative bias varying mostly between 30 and 70%. One of the reasons for that could be that some of aerosol sources important in summer are not accounted for in the calculations (i.e. secondary organic aerosol and bio-aerosols). In winter, the model AOD results are closer to or even slightly overestimate MODIS AOD (Note that much less MODIS AOD retrievals are available for autumn-winter season).

- With a few exceptions, the temporal correlation between calculated and MODIS AOD over land is better for the summer months (mostly between 0.4 and 0.65) than for other seasons.

- Over remote sea areas (e.g. the southern part of the North Atlantic), the model underestimates MODIS AOD by 30 to 60%. The temporal correlation for sea areas is rather poor (below 0.3) and is particular low for the Mediterranean Sea.

- For the first time model calculated aerosol properties could be compared with measurements for such regions as Russia, south-eastern Europe and the Mediterranean Sea. Examples of this are provided in Figure 6.4.

6.4.5 AOD and surface $PM_{2.5}$ at EMEP sites

To see whether there is any relation between surface PM concentrations and AOD we have looked at both calculated and measured surface $PM_{2.5}$, and calculated and retrieved AOD for the same locations.

First, we compare model calculated AOD with AOD retrieved from MODIS measurements for (the grid cells with) EMEP sites, where surface measurements of $PM_{2.5}$ are also available for 2003 and 2004.

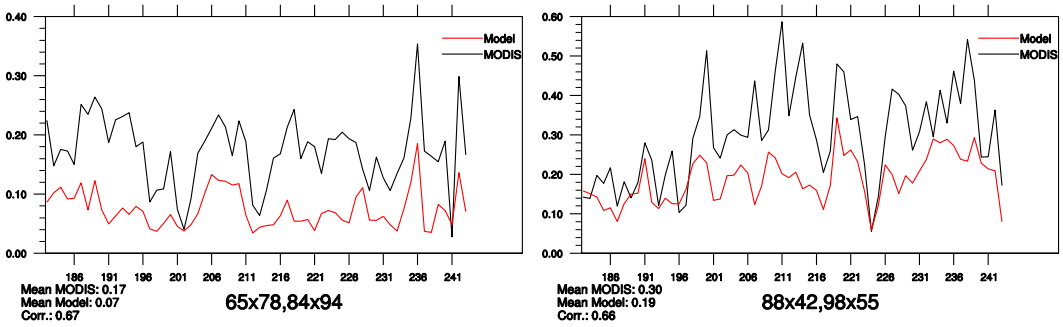

Figure 6.4: Time series of modelled and MODIS AOD for grid cells representing the European part of Russia (left panel) and southern Europe, i.e. parts of Greece, Albania and Macedonia, (right panel) for July-August 2003.

For the summer months (July - August), the model underestimation of MODIS AOD lies between 20% and 55% in 2003 and between 30% and 70% in 2004. The temporal correlation is fairly good (typically around 0.5-0.6) for central and northern Europe, but considerably worse for some Spanish sites (0.2-0.3). Somewhat better correlations are found for 2003 compared to 2004.

For the spring months (March - April 2004), fewer days with MODIS AOD are available. The model underestimates MODIS AOD by 25% to 55%. The correlation results vary considerably between sites, with the correlation coefficients ranging between 0.0 and 0.6.

For the late autumn-winter period (November-December 2003), only a limited amount of AOD retrieval data is available from MODIS for central and northern Europe, as much data was discarded due to the contamination by clouds or snow/ice surface cover. For Spanish sites, with MODIS data capture of more than 25%, the model underestimation range between 15% and 75%, whereas the correlation coefficients typically ranges between 0.2 and 0.4.

Figure 6.5 shows examples of time-series of model calculated and MODIS AOD for Birkenes (NO01), Aspvreten (SE12) and Langenbrügge (DE12) for July-August 2003, and for Cabo de Creus (ES10) for three different periods, namely July-August 2003, November-December 2003, and March-April 2004.

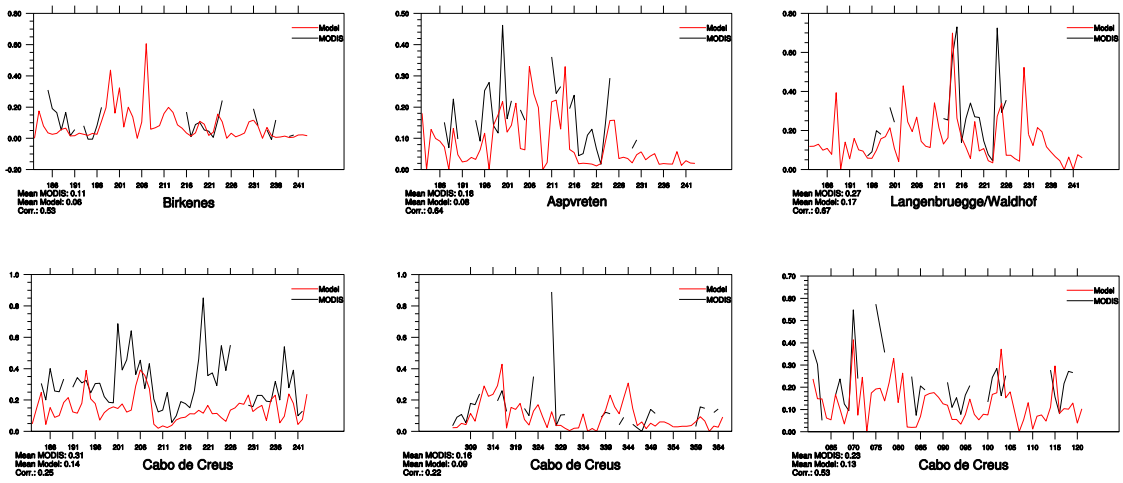

Figure 6.5: Time series of modelled AOD and MODIS AOD for selected EMEP sites: upper panel- Birkenes (NO01), Aspvreten (SE12) and Langenbrügge (DE02) for July-August 2003; lower panel – Cabo de Creus (ES10) for July-August 2003 and November-December 2003, and March-April 2004.

A joint analysis of $PM_{2.5}$ and AOD results has been carried out for the summer months, for which more MODIS retrieval aerosol data is available. Rather mixed correlation between observed surface $PM_{2.5}$ and MODIS AOD is found for the 18 stations considered. In general, the correlation between measured $PM_{2.5}$ and AOD was better for sites in southern Europe (Spain and Italy), where the correlation coefficient ranged between 0.45 and 0.7, while the corresponding range for central and northern Europe was between 0.2 and 0.5.

It is interesting to note that for many sites, the correlation between modelled and MODIS AOD is higher than the correlation between calculated and measured $PM_{2.5}$, especially for summer 2003. For instance, the respective correlations are 0.53 and 0.19 for Chaumont (CH03), 0.51 and 0.22 for Ispra (IT04), 0.46 and 0.26 for Niembro (ES08), and 0.57 and 0.47 for Els Torms (ES14) (Figure 6.6).

6.4.6 Result uncertainties

Comparison of these first simulated AOD results from the EMEP aerosol model with MODIS AOD retrieval data has in general shown a fairly good agreement in terms of bias and temporal correlations However, the spatial correlation for the whole EMEP grid is rather poor. Also, considerable discrepancies between modelled and MODIS AOD are found for some periods and regions. While analysing the results, it is important to keep in mind that there are non-negligible uncertainties in both the model AOD results and MODIS AOD retrievals.

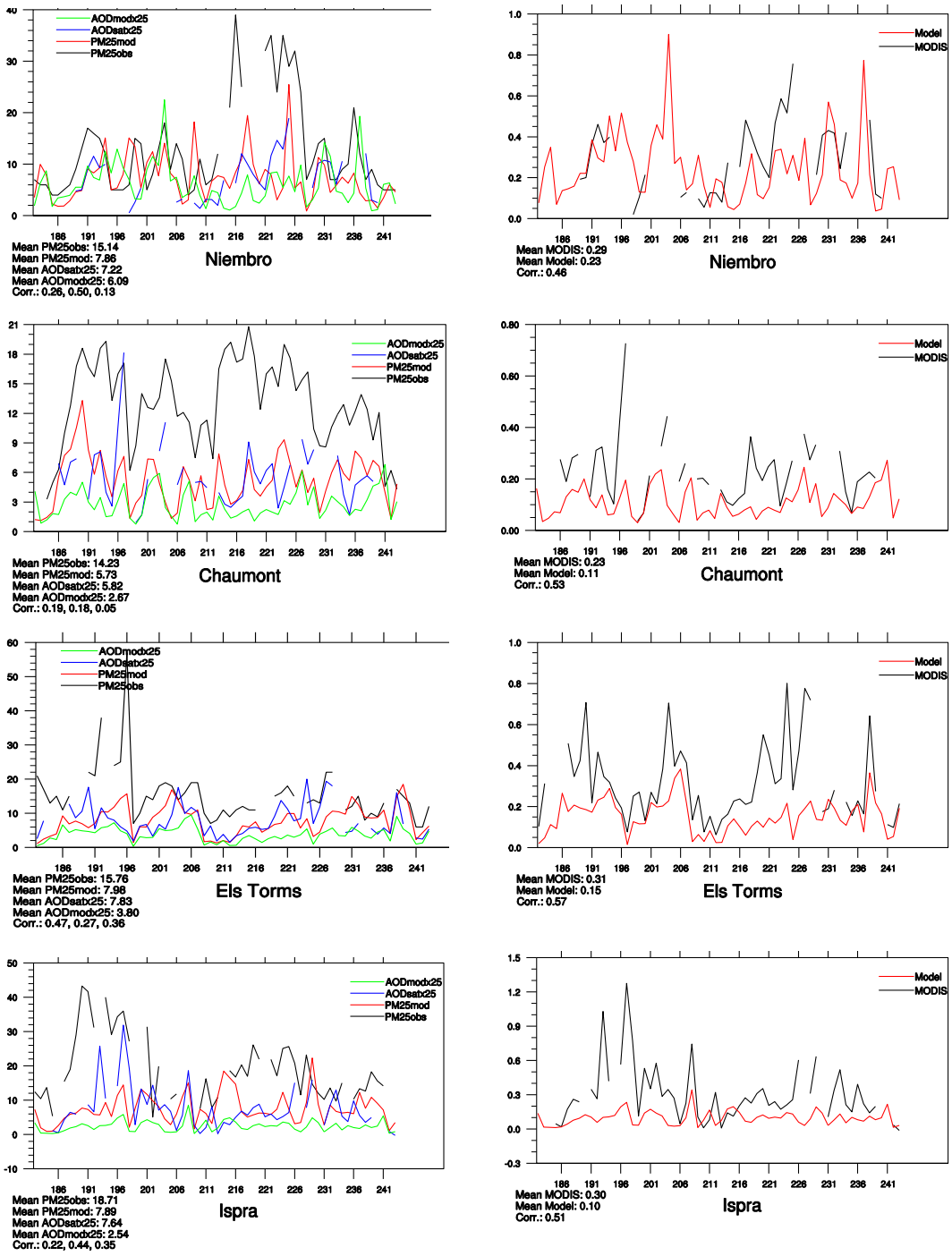

Figure 6.6: Time series for the EMEP sites Niembro (Spain), Chaumont (Switzerland) and Ispra (Italy) of: Left panels - calculated and measured $PM_{2.5}$, and calculated and MODIS AOD (multiplied by 25 to fit with PM scale); all correlations are with measured $PM_{2.5}$; Right panels - calculated and MODIS observed AOD.

6.4.7 Uncertainties in MODIS AOD data

Among the main uncertainties in MODIS AOD retrievals are those due to:

- over ocean – cloud and sun glint data contamination; dust with non-spherical geometry;
- over land – uncertainties in surface reflection; sub-pixel snow, ice or surface water; cloud data contamination.

Depending on how many contaminated pixels were discarded, each of the 50x50 km^2 EMEP grid cell may aggregate a different amount of AOD data. This means that grid cells will have varying data coverage and that the representativeness of MODIS AOD data will vary from grid cell to grid cell.

Besides, MODIS AOD retrieval algorithms rely upon prescribed aerosol types ("aerosol models"), which are assigned pre-computed optical properties, based on AERONET data. An "aerosol model" consists of one fine and one coarse aerosol mode, which are chosen from among four fine and five coarse pre-described aerosol modes in the over-ocean retrieval algorithm. The over-land retrieval uses a priori assigned fine aerosol types for four seasons, aggregated on 1° x 1° grid globally. The non-absorbing "aerosol model", representing urban/industrial pollution, is chosen for western Europe, whereas the neutral aerosol type (generic/forest fires aerosol) is assumed for the rest of the EMEP grid. This means that the ambient aerosol profiles and composition as assumed in MODIS retrievals and calculated with the EMEP model will differ.

Moreover, MODIS retrieval algorithm does not seem to take into account the dependence of aerosol optical properties on ambient relative humidity. Furthermore, the complex refractive indices for different aerosol components used in the model and in the MODIS retrievals are not necessarily the same (e.g. we have assumed somewhat smaller scattering for soluble particles and larger absorptions for black carbon than used in MODIS retrievals). Thus, the optical properties of aerosols will differ in the model and MODIS calculations. This is another likely cause of discrepancies in modelled and MODIS AOD.

6.4.8 Uncertainties in modelled AOD

The correctness of model AOD results depends, on one hand, on the model's ability to accurately calculate aerosol atmospheric concentrations and size distribution and, on the other hand, on the accuracy with respect to modelling aerosol optical properties. The latter relies on the choice of complex refractive indices for different aerosol components and on how the effective refractive indices are derived, and it depends on the representation of aerosol size distribution.

AOD modelling using Mie-dispersion algorithm for size-resolved aerosols is based on model calculated particle number concentrations and size distribution, which in turn are associated with considerable uncertainties. This is mainly because of the lack of data on the size distribution of particle emission and missing aerosol sources, but also due to uncertainties in modelling aerosol dynamic processes, i.e. nucleation, coagulation and condensation. On the other

hand, using complex refractive indices to calculate extinction efficiencies and cross-sections for size-resolved particles represent a sounder parameterisation than the mass-based one. Still, there are uncertainties in complex refractive index values for different aerosol components, uncertainties related to aerosol mixing state and thus derivation of the effective refractive index. Furthermore, particle deviation from a spherical form assumed for Mie-scattering calculations gives rise to inaccuracy in AOD modelling, especially for aerosol loading dominated by dust particles.

6.4.9 Sensitivity tests of AOD results to primary emitted particle sizes

As described in Section 3.1, there is presently no appropriate information about the size distribution of primary particles emitted from anthropogenic sources. In the EMEP model, rather crude assumptions on the size of primary particles were made in order to derive the number of particles emitted in the Aitken and the accumulation fractions from primary $PM_{2.5}$ emissions.

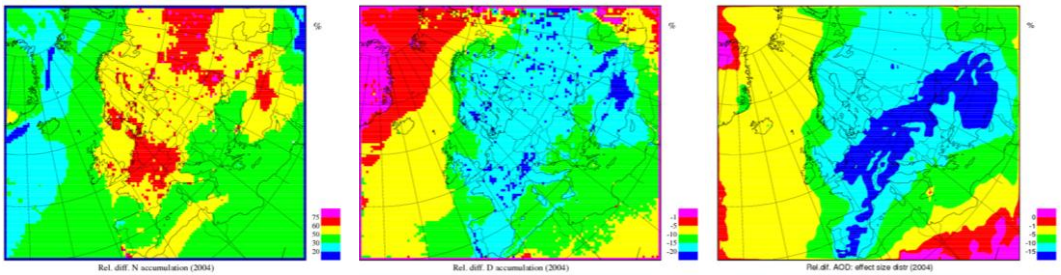

Figure 6.7: Relative changes in the annual mean number (left) and diameter (middle) of accumulation particles, and AOD (right), as the diameter of primary emitted Aitken particles decrease from 0.04 µm to 0.03 µm and the diameter of primary emitted accumulation particles is decreased from 0.4 µm to 0.3 µm. Year: 2004.

Preliminary sensitivity tests have shown that decreasing the diameters of primary emitted Aitken particles from 0.04 µm to 0.03 µm and accumulation particles from 0.4 µm to 0.3 µm leas to increases of the annual mean particle number concentrations by 75-120% in the Aitken fraction and by 35-75% in the accumulation fraction (Figure 6.7, left). At the same time, annual mean diameters of Aitken and accumulation particles have decreased respectively by 5-15% and by 10-17% (Figure 6.7, middle) (diameters of Aitken particles increased by 5-10% over ocean). The combined effect of increased particle number and decreased particles size is a general decrease of AOD by 5% to 20% over land and by 1-5% over the ocean. Thus, in this case, the effect of decreased aerosol scattering cross-sections overrides the effect of increased particle number.

6.5 Summary of modelled AOD results and MODIS data

Model calculated AOD has been compared with AOD retrieved from MODIS measurements for four 2-month periods in 2003 and 2004, representing different seasons. On average, model calculated AOD is lower compared to MODIS data for all seasons. The best correspondence with MODIS data is found for AOD calculated using log-normal representation of particle size distribution. In this

case, the model negative bias is in the range of -51% to -55 % for summer and spring months and -11% for late autumn-winter months. The spatial correlation between modelled and MODIS retrieved AOD is rather poor for all seasons, being somewhat better for summer months July and August (0.35 in 2003 and 0.26 in 2004).

Over land areas, the model AOD underestimation tends to be larger for summer months (30-70%), while for the winter months the model appears to slightly overestimate MODIS AOD. In general, the temporal correlation is better for summer months (mostly between 0.4 and 0.65) than in other seasons over land. Over remote sea areas (e.g. the southern part of North Atlantic), model underestimates MODIS AOD by 30-60%, and the temporal correlation for sea areas is rather poor.

Rather mixed correlation between observed surface $PM_{2.5}$ and MODIS AOD is found for EMEP stations. In general, the correlation between measured $PM_{2.5}$ and AOD is better for southern European sites, typically ranging between 0.45 and 0.7, while it is lower for central and northern Europe (between 0.2 and 0.5). One interesting result is that for quite a few sites, the correlation between modelled and MODIS AOD is higher than the correlation between calculated and measured $PM_{2.5}$, especially for summer 2003.

These first model calculations of AOD show quite promising results. However, it is recognised that the uncertainties in both model results and MODIS data may affect the comparison results. The main uncertainties in modelled AOD are those associated with the size distribution of primary emitted particles, with aerosol dynamics parameterisations, with the aerosol mixing state in refractive index computations, and the effect of non-spherical particles.

6.6 Use of SYNAER satellite data for aerosol monitoring in Europe

6.6.1 Aerosol retrieval from satellite and the SYNAER product

In the past few years the capability of satellite monitoring the aerosol optical depth (AOD) has increased tremendously (see e.g. Kaufman et al., 2002), and several studies have appeared that investigate the usefulness of AOD to improve the monitoring of particulate matter (PM). Examples of satellite retrieval of additional aerosol optical properties include the Angstrom coefficient (from AATSR, Veefkind et al., 1999), the separation into fine and coarse mode aerosols (from MODIS, Levy et al., 2007), aerosol characterisation based on pre-defined aerosol types (using MISR, Kahn et al., 2005) and particle number concentrations (based on MERIS, von Hoyningen-Huene et al., 2003; Kokhanovsky et al., 2006).

Several groups, mainly from the US, have performed comparisons of satellite retrieved AOD with ground-based PM values. For Ispra (IT04R), Chu et al. (2003) found that time-series of AOD and 24h average PM_{10} mass concentrations correlated well for a period of several months in 2001 experiencing stable meteorological conditions. For Europe, the first comparison of spatial and temporal variations in PM (PM_{10} and $PM_{2.5}$ data from 2003, obtained from the AIRBASE database) and AOD from MODIS was reported by Koelemeijer et al. (2006). The authors found correlation coefficients between AOD* (= AOD

divided by the boundary layer height and corrected for growth of aerosols with relative humidity) and PM_{10} and $PM_{2.5}$ of 0.5 and 0.6, respectively. These values were averages of rural and (sub) urban background stations. Their results clearly show that satellite AOD measurements can be a useful measure to improve the monitoring of PM distributions over Europe.

Another approach that has been used to extract aerosol properties (beyond AOD) is the SYNAER (SYNergetic Aerosol Retrieval product, Holzer-Popp et al., 2000, 2008) method. SYNAER data have been provided through the ESA-GSE project PROMOTE (PROtocol MoniToring for the GMES Service Element: Atmosphere, see also http://www.gse-promote.org). The SYNAER algorithm derives aerosol properties by exploiting complementary information from the Advanced Along Track Scanning Radiometer (AATSR) and the Scanning Imaging Absorption Spectrometer for Atmospheric Cartography (SCIAMACHY), both onboard the European platform ENVISAT. Daily aerosol parameters on a 60x30 km^2 resolution are provided in near-real time (approximately 12 hours after acquisition) over Europe and Africa. Due to the scan mode and swath width of the instruments full cloud-free coverage at the equator is achieved after 12 days.

The SYNAER product seems to be a valuable source of data in addition to the regular EMEP monitoring network. Its main advantage is the ability to estimate, beside AOD, aerosol composition (type of aerosols between continental, maritime, polluted, desert outbreak and biomass burning/heavily polluted air masses as mixtures of four basic aerosol components sulfate/nitrate, mineral dust, sea salt, soot) and near-surface PM concentrations (PM_{10}, $PM_{2.5}$ and PM_1).

As described in EMEP (2006) the quality of the SYNAER AOD and PM products looks very promising, but a larger validation exercise is needed to assess the product properly. Its main disadvantage is obviously the low spatial resolution and relatively low temporal data coverage of SYNAER/ENVISAT. In the following we present preliminary results from a comparison between SYNAER products and EMEP measurements/model results.

6.6.2 SYNAER measurements of Aerosol Optical Depth

The aerosol optical depth (AOD) describes the column integrated atmospheric optical extinction, i.e. the attenuation of the intensity of incoming solar radiation due to scattering and/or absorption of aerosols. AOD varies with wavelength, aerosol composition, aerosol size distribution, height distribution and total concentration. The relation to ground-based PM in Europe is currently under investigation (see discussion above).

Figure 6.8 gives an example of AOD retrieved with the SYNAER retrieval from 3 May 2006. The enhanced AOD values seen around the southern part of Finland correspond to air masses with a high aerosol load, which have been transported north-eastward from the area subject to the massive agricultural and forest fires in western Russia and eastern Europe in spring 2006 (see Chapter 4 for more details).

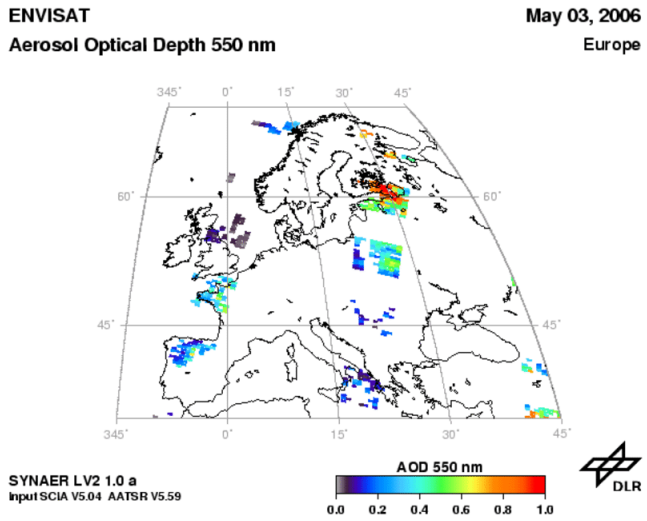

Figure 6.8: Example image of a daily SYNAER results (Aerosol Optical Depth at 550 nm) over Europe for 3 May 2006. Clearly enhanced values over southern Finland can be seen, resulting from agricultural fires in eastern Europe/western Russia.

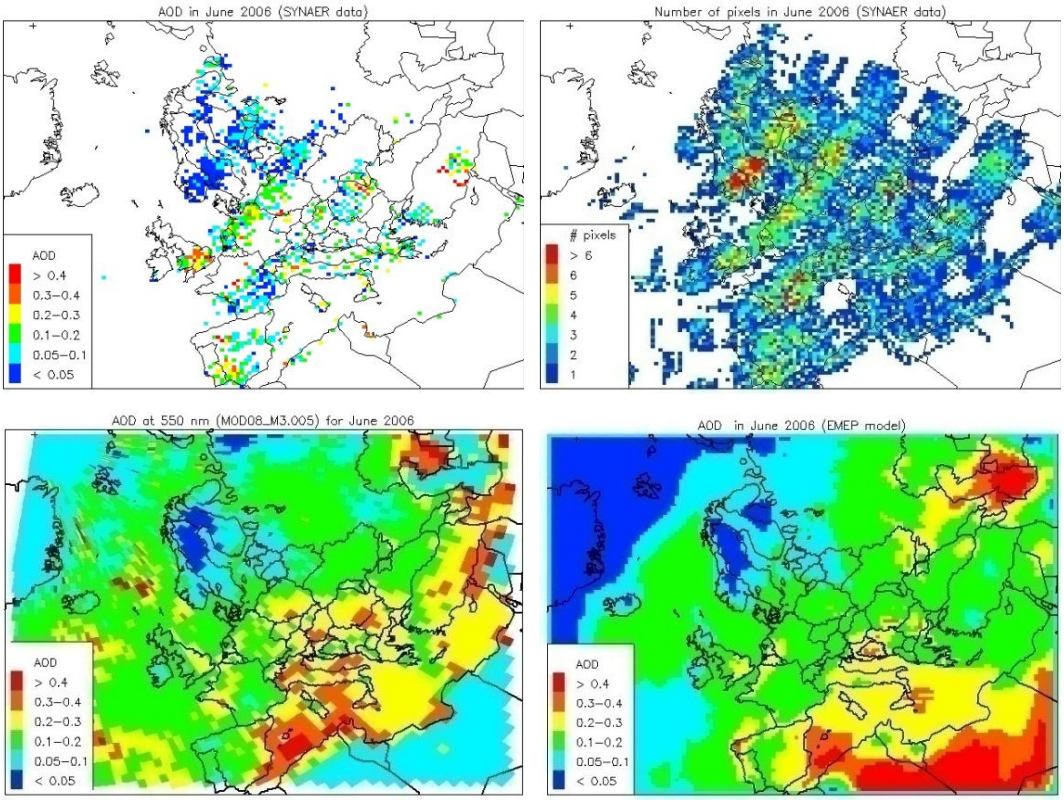

Figure 6.9: Monthly average of SYNAER Aerosol Optical Density (AOD at 550 nm) for June 2006 (upper left panel), the number of pixels available in each EMEP-grid (upper right panel), AOD from MODIS onboard TERRA (1x1 degree data, courtesy of Langley Research Centre, NASA) (lower left panel) and AOD at 550 nm calculated with the EMEP model (lower right panel).

The data availability of satellite sensors working in the UV/Vis region is better during summer. Therefore we show as an example monthly averaged data from June 2006 (64 orbits were available). The upper right panel of Figure 6.9 shows the number of SYNAER pixels (60x30km^2) that have their centers inside a particular cell in the EMEP 50x50 km grid. The uneven distribution of pixel numbers is caused by the alternation of nadir and limb viewing mode of SCIAMACHY. The 'mean' AOD for all values measured in June 2006 is shown (upper left panel of Figure 6.9) when at least four centers of SYNAER pixels were available in a grid-cell. For comparison, AOD data from the MODIS sensor onboard TERRA and the EMEP model is shown. The qualitative comparison of the data sets is satisfactory. All images show the well known typical pattern; i.e. low AOD values above Scandinavia, increased values in Belgium/the Netherlands and some parts of southern and eastern Europe. MODIS AOD versus the EMEP model AOD is studied in detail in section 6.1-6.6. First validation results of SYNAER AOD against AOD from the NASA's AEROSOL ROBOTIC NETWORK (AERONET) have been documented by Holzer-Popp et al. (2008).

6.6.3 SYNAER measurements of Particulate Matter

We have previously evaluated two earlier versions of the SYNAER/ENVISAT data product (*v1.0* and *v1.8*). In version 1.0 the conversion of AOD/type information to near surface PM concentrations was performed assuming a homogeneous 2 km boundary layer. At present (*v2.0*), this has been replaced by a vertical profile correction based on the EURAD chemistry transport model. Further improvements made for the actual version SYNAER/ENV *v2.0* and first validation are documented in detail in Holzer-Popp et al. (2008). Here, we have used a post-processing versions *v2.01*, which is – apart from correction factors introduced for insoluble solutions and desert dust outbreak mixtures - identical to the operational version 2.0.

Our earlier results were based on comparison with in-situ data from the EMEP sites Illmitz (AT0002R), Zarra (ES0012R), Payerne (CH0002R), Ispra (IT0004R) and Birkenes (NO0001R) and SYNAER PM data (*v1.0*). SYNAER *v1.0* seemed to overestimate PM_{10} and $PM_{2.5}$ on certain occasions, especially at Zarra. This may be due to Saharan dust events that occur frequently over Spain, which may increase the tropospheric aerosol load without increasing ground level PM. Similar overestimation of PM_{10} at Illmitz and Ispra could not be explained by this. At Payerne, the SYNAER product generally provided lower levels than the EMEP data. This may be due to high mountains with clean air surrounding the station, which undoubtedly is sampled by the satellite as well. It could be seen that SYNAER *v1.8* was an improved product, with generally lower PM values that were more comparable to PM measured on the surface. In particular, this could be seen at Zarra (Spain), where *v1.0* PM values were much too high. Still, slightly higher satellite values were seen at several sites.

An overview of monthly averaged SYNAER $PM_{2.5}$ data for Europe from June 2006 is given in Figure 6.10. For comparison, monthly mean $PM_{2.5}$ values for EMEP sites are shown in the panel aside. From Figure x.4 it is apparent that information obtained from satellites using the SYNAER retrieval to calculate near-surface $PM_{2.5}$ can contribute to our understanding of the aerosol distribution in Europe. This is particularly true for regions with a low or lacking coverage of

EMEP stations. Nevertheless, on has to keep in mind that due to the present low temporal coverage of the satellite sensor, the averages shown in Figure 6.10 are not a 'real' monthly average, but more a collection of individual episodes. DLR are planning to transfer the SYNAER retrieval method to GOME-2 on METOP, which has daily observations of Europe. This, and a potential application of the method using future geo-stationary missions, will overcome the existing shortcoming of Earth Observation for monitoring of air quality.

For a validation of SYNAER *v2.01*, we used daily PM values from EMEP to compare with daily averaged co-located SYNAER data. So far we have mainly used the rejection criteria of bad pixels provided by the data provider. Data with large a spectral fit error, large AOD type ambiguity over bright land and ocean albedo, large cloud fraction, and bright ocean albedo were excluded. The validation work is still ongoing, so only preliminary results are shown. Using daily EMEP data (12h-12h) for comparison with satellite "snap-shots" from morning/midday hours can only give quality indications. The aim of our work is not only to determine the quality of the data product, but also to make a contribution to determine thresholds for good/bad pixel criteria.

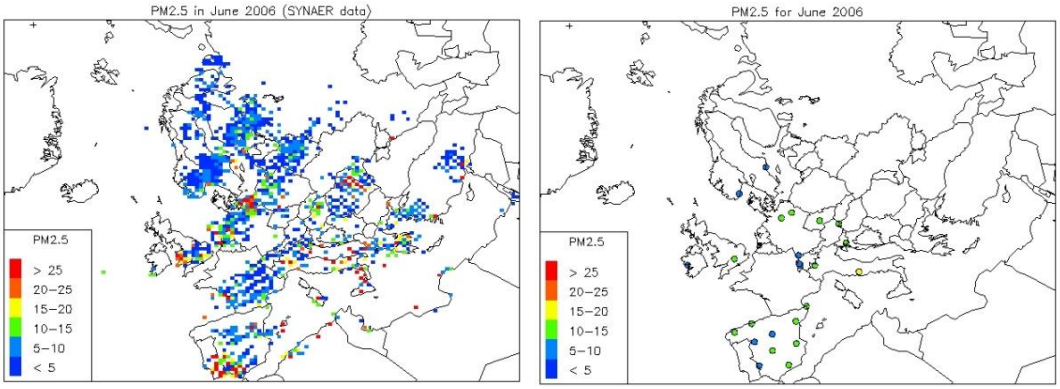

Figure 6.10: Monthly averaged $PM_{2.5}$ values from SYNAER (left panel) and EMEP (right panel) for June 2006. SYNAER data are shown as averages when more than four centers of SYNAER pixels were found in the 50x50 EMEP grid-cells.

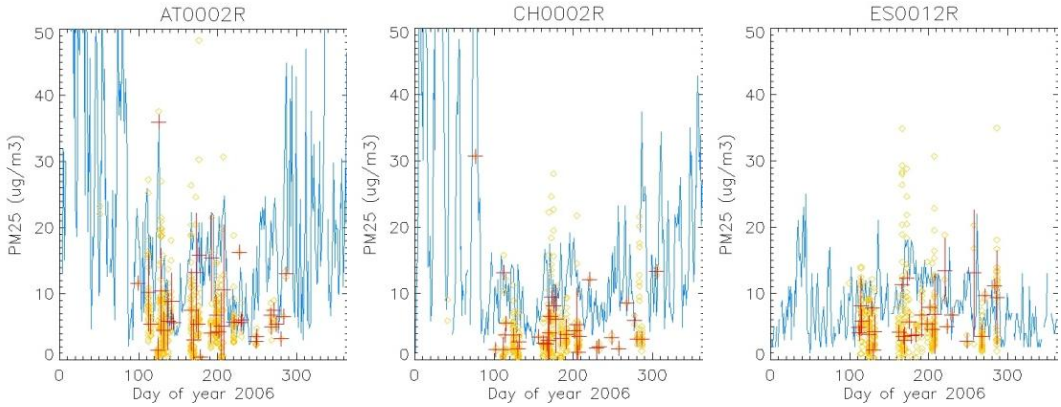

Figure 6.11: Time-series of daily $PM_{2.5}$ values for Illmitz (AT0002R), Payerne (CH0002R) and Zarra (ES0012R) in 2006 (in blue). Overlaid are $PM_{2.5}$ values measured at co-located SYNAER pixels (in orange). Daily mean satellite $PM_{2.5}$ data are shown as red crosses.

As examples, time-series of daily $PM_{2.5}$ values for Illmitz (AT0002R), Payerne (CH0002R) and Zarra (ES0012R) from 2006 are shown in Figure 6.11. Overlaid are individual co-located satellite $PM_{2.5}$ (measured at the same day and within 2 degrees distance from the EMEP site) and the daily mean satellite $PM_{2.5}$. It can be seen that co-located satellite overpasses mainly are from the summer months. SYNAER $PM_{2.5}$ values are slightly lower than ground-based $PM_{2.5}$ values. Preliminary validation results are shown in Table 6.4.

Table 6.4: Preliminary validation results of SYNAER particulate matter (PM_{10}, $PM_{2.5}$ and PM_1) values using daily EMEP PM values for comparison. As spatial co-location criteria, 2° have been chosen and the maximum allowed cloud-cover within the SYNAER pixel has been set to 20%.

Code	# co. loc.	PM_{10} emep	PM_{10} Synaer	Std. Synaer	Dev. %	Corr.	# co. loc.	$PM_{2.5}$ Emep	$PM_{2.5}$ synaer	Std. Synaer	Dev. %	Corr.
AT0002R	35	24.3	11.0	11.8	-55	0.37	35	17.7	8.0	6.3	-55	0.39
CH0002R	25	15.5	18.7	15.3	21	-0.21	34	12.9	5.5	5.5	-57	0.59
CH0004R	28	12.6	9.4	14.7	-26	0.19	38	9.3	8.5	8.0	-8	0.30
CZ0003R	11	16.6	11.6	6.1	-30	-0.41	20	16.9	4.4	2.3	-74	-0.10
DE0002R	30	23.7	8.3	5.0	-65	0.01	25	15.3	11.8	10.0	-23	0.59
DE0003R	26	11.2	17.0	13.0	52	0.11	27	6.4	8.4	10.6	32	-0.11
DE0044R	25	27.1	6.9	4.2	-75	-0.22	27	16.3	6.5	8.4	-60	0.23
ES0007R	29	23.8	8.0	5.5	-66	-0.16	25	12.5	4.3	3.4	-66	-0.09
ES0008R	25	20.3	15.0	12.1	-26	-0.08	25	11.2	5.6	5.3	-51	0.31
ES0009R	26	15.9	9.8	7.7	-38	-0.33	26	9.2	4.5	4.5	-50	0.12
ES0010R	24	19.2	14.8	12.6	-23	-0.18	20	11.5	10.0	5.5	-13	-0.43
ES0011R	26	20.0	16.5	13.6	-18	-0.25	31	10.7	6.7	4.0	-37	-0.05
ES0012R	51	15.9	14.5	10.1	-9	0.14	30	10.3	6.5	3.3	-37	-0.06
ES0013R	39	14.1	14.1	11.2	0	0.03	26	8.2	11.5	7.2	40	-0.22
ES0014R	43	18.0	12.0	9.1	-33	-0.02	24	10.0	6.9	5.3	-31	0.19
ES0015R	46	15.0	11.7	9.6	-22	0.28	24	9.7	4.5	3.5	-54	-0.14
ES0016R	54	15.4	18.9	17.8	23	0.25	19	11.6	6.2	3.5	-47	0.18
GB0036R	48	21.9	14.1	9.7	-36	0.1	23	13.5	5.9	3.5	-57	-0.36
IT0001R	46	28.3	14.2	12.3	-50	0.16	27	16.9	5.5	4.6	-67	0.37
NO0001R	12	8.6	16.1	12.9	88	-0.25	11	7.4	7.5	4.5	2	-0.22
SE0011R	15	17.4	15.4	10.4	-12	0.27	4	22.1	11.0	7.5	-50	-0.01
SE0012R	46	13.3	9.7	7.5	-27	0.2	12	9.8	8.7	5.4	-11	0.51

Code	# co. loc.	PM_1 emep	PM_1 Synaer	Std. Synaer	Dev. %	Corr.
AT0002R	35	13.9	6.4	4.8	-54	0.41
CH0002R	35	9.9	4.8	4.2	-52	0.55
CH0004R	38	6.7	7.1	6.4	7	0.17
DE0002R	30	10.9	4.0	2.0	-63	0.07
NO0001R	11	5.1	10.0	5.5	99	0.32

The estimation of the linear correlation coefficient *r* is still very preliminary. The value is strongly depending on the criteria, which we have been chosen for good/bad data points. For example, changing the criteria from 1 degree to 2 degrees and the criteria for cloud-fraction from 35% to 20%, decrease the linear correlation coefficient for $PM_{2.5}$ at Illmitz from 0.54 to 0.39, respectively. The correlation at Payerne increases from 0.31 (1°) to 0.60 (2°), and changed to 0.59 (cloud-fraction < 0.2). Using median data instead of mean daily averages changes *r* to 0.5 at Illmitz and 0.73 for Payerne. We expect that by replacing simply linear correlation by more advanced approaches, and by taking into account errors/standard-deviations of averages, more conclusive results will be obtained.
Nevertheless, a few preliminary conclusions can be drawn: There seems to be a clear negative bias of SYNAER/ENV *v2.01* seen at a majority of EMEP sites (contrary to previous versions). The SYNAER PM data show variable correlation at different EMEP sites. The correlation between SYNAER and EMEP PM seems to be better for PM_1 than for $PM_{2.5}$ and PM_{10}. Relatively high correlation coefficients can be seen at some stations, while there seems to be no correlation at other sites. The reason for the apparent bias and the correlation/lack of correlation this is still under investigation.

6.6.4 Conclusions and future work

We have performed a study on the utilization of the SYNAER data product (SYNergetic Aerosol Retrieval product) for monitoring of aerosols in Europe from satellite sensors. The main advantage of SYNAER is its ability to calculate aerosol composition and concentrations of particulate matter. It is clear that information obtained from satellites using the SYNAER retrieval to calculate near-surface PM can contribute to our understanding of PM distribution in Europe, in particular in regions with low or lacking coverage of EMEP stations.

The overall quality of the SYNAER AOD and PM products looks promising, but to understand the observed bias and correlation/lack of correlation, further studies have to be performed. The optimization of the rejection criteria for bad pixels is to be studied in more detail and the representativeness of EMEP stations (e.g. topography, population density) with respect to satellite ground pixel needs to be given more attention. We plan to use EMEP data with higher time resolution (hourly averages) and campaign data, perform validation of the chemical characterization obtained by SYNAIR (mixtures of 4 basic aerosol components sulfate/nitrate, mineral dust, sea salt, soot), with emphasis on the quality of the correction factors for the dust outbreak mixtures. In addition, the techniques for calculating monthly and seasonal averages/maps of SYNAER data need to be refined (e.g. using more advanced interpolation techniques 'krieging', error-weighted values).

In addition, the SYNAER product itself will be further improved by DLR. Besides algorithm development, this includes adaptation of the method to use METOP GOME-2/AVHRR data to significantly improve the spatial coverage and enable daily observations of Europe (for cloud-free pixels) instead of 1 observation every 12 days (with ENVISAT AATSR/SCIAMACHY). Data will become available on 10 km x 10 km grid to exploit the 1 km resolution of the radiometer.

Acknowledgements. This work was supported by the Norwegian Space Centre/ESA through the Norwegian PRODEX project “SatLuft” and the ESA-GSE project PROMOTE. MODIS data are obtained courtesy from Langley Research Centre, NASA.

7 References

Bauer, H., Giebl, H., Hitzenberger ,R., Kasper-Giebl, A., Reischl, G., Zibuschka, F. and Puxbaum, H. (2003) Airborne bacteria as cloud condensation nuclei. *J. Geophys. Res.*, *108*, D21, 4658, doi: 10.1029/2003JD003545.

Bauer, H., Kasper-Giebl, A., Löflund, M., Giebl, H., Hitzenberger, R., Zibuschka, F. and Puxbaum, H. (2002) The contribution of bacteria and fungal spores to the organic carbon content of cloud water, precipitation and aerosols, *Atmos. Res.*, *64*, 109-119.

Bauer, H., Schueller, E., Weinke, G., Berger, A., Hitzenberger, R., Marr, I.L. and Puxbaum, H. (2008) Significant contributions of fungal spores to the organic carbon and to the aerosol mass balance of the urban atmospheric aerosol. *Atmos. Environ.*, *42*, 5542-5549.

Bond, T.C. and Bergstrom, R.W. (2006) Light absorption by carbonaceous particles: an investigative review. *Aerosol Sci. Technol.*, *40*, 27-67.

Chan, Y.C., Simpson, R.W., McTainsh, G.H. and Vowles, P.D. (1997) Characterization of chemical species in $PM_{2.5}$ and PM_{10} aerosols in Brisbane, Australia. *Atmos. Environ.*, *31*, 3773-3785.

Chu, D.A., Kaufman, Y.J., Zibordi, G., Chern, J.D., Mao, J., Li, C. and Holben, B.N. (2003) Global monitoring of air pollution over land from the Earth Observing System-Terra Moderate Resolution Imaging Spectroradiometer (MODIS). *J. Geophys. Res.*, *108*, D21, 4661, doi: 10.1029/2002JD003179.

Chýlek, P. and Wong, J.G.D. (1998) Erroneous use of the modified Kohler equation in cloud and aerosol physics applications. *J. Atmos. Sci.*, *55*, 1473-1477.

Cofala, J., Klimont, Z., Amann, M., Bertok, I., Heyes, C., Shöpp, W. and Wagner, F. (2006) Draft input data for projections of air pollutant emissions and their sources in the non-EU countries up to 2020. Laxenburg, IIASA (EMEP/CIAM Report 1/2006).

Cofala, J., Amann, M., Heyes, C., Wagner, F., Klimont, Z., Posch, M., Shöpp, W., Tarrasón, L., Jonson, J.E., Whall, C. and Stavraki, A. (2007) Analysis of policy measures to reduce ship emissions in the context of the revision of the National Emissions Ceiling Directive, final report. Laxenburg, IIASA (IIASA Contract No. 06-107).

EC (2008) Directive 2008/50/EC of the European Parliament and the council of 21 May 2008 on ambient air quality and cleaner air for Europe. *Off. J. Eur. Com.*, *L152*, 11/06/2008, 1-44.

EC JRC (2004) Forest fires in Europe: 2003 fire campaign. Report 4. Brussels, European Communities (S.P.I.04.124EN).

EMEP (2003) The EMEP monitoring strategy 2004–2009. Background document with justification and specification of the EMEP monitoring programme 2004-2009. Ed. By K. Tørseth and Ø. Hov. Kjeller (EMEP/CCC-Report 9/2003).

EMEP (2004) Transboundary acidification, eutrophication and ground level ozone in Europe. Status report 1/2004. Oslo, Norwegian Meteorological Institute (EMEP Report 1/04).

EMEP (2005) Transboundary acidification, eutrophication and ground level ozone in Europe in 2003. Status report 1/2005. Oslo, Norwegian Meteorological Institute (EMEP Report 1/05).

EMEP (2006a) Measurements of particulate matter. Status report 2006. Kjeller, Norwegian Institute for Air Research (EMEP/CCC-Report 3/2006).

EMEP (2006b) Transboundary particulate matter in Europe. Status report 4/2006. Kjeller, Norwegian Institute for Air Research (EMEP Report 4/2006)

EMEP (2007) Transboundary particulate matter in Europe. Status report 4/2007. Kjeller, Norwegian Institute for Air Research (EMEP Report 4/2007) URL: http://www.nilu.no/projects/ccc/reports.html.

Hale, G.M. and Querry, M.R. (1973) Optical constants of water in the 200-nm to 200-mm wavelength region. *Appl. Opt.*, *12*, 555-563.

Holben, B.N., Eck, T.F., Slutsker, I., Tanré, D., Buis, J.P., Setzer, A., Vermote, E., Reagan, J.A., Kaufman, Y.J., Nakajirma, T., Lavenu, F., Jankowiak, I. and Smirnov, A. (1998) AERONET – A federated instrument network and data archive for aerosol characterization. *Remote Sens. Environ., 66,* 1-16.

Holzer-Popp, T., Schroedter, M. and Gesell, G. (2000) High resolution aerosol maps exploiting the synergy of ATSR-2 and GOME. *Earth Obs. Q., 65,* 19-24.

Holzer-Popp, T., Schroedter-Homscheidt, M., Breitkreuz, H., Martynenko, D. and Klüser, L. (2008) Synergetic aerosol retrieval from SCIAMACHY and AATSR onboard ENVISAT. *Atmos. Chem. Phys. Discuss., 8,* 2903-2951.

IIASA (2005) RAINS Europe database. Accessible at http://www.iiasa.ac.at/rains.

Jaenicke, R. (2005) Abundance of cellular material and proteins in the atmosphere. *Science, 308,* 73.

Kahn, R.A., Gaitley, B.J. and Martonchik, J.V. (2005) Multiangle Imaging Spectroradiometer (MISR) global aerosol optical depth validation based on 2 years of coincident Aerosol Robotic Network (AERONET) observations. *J. Geophys. Res., 110,* D10S04, doi: 10.1029/2004JD004706.

Kahnert, M., Lazaridis, M., Tsyro, S. and Tørseth, K. (2004) Requirements for developing a regional monitoring capacity for aerosols in Europe within EMEP. *J. Environ. Monit., 6,* 646-655.

Kaufman, Y.J., Tanre, D. and Boucher, O. (2002) A satellite view of aerosols in the climate system. *Nature, 419,* 215 – 223.

Kirkevåg, A., Iversen, T., Seland, Ø. and Kristjánsson, J.E. (2005) Revised schemes for aerosol optical parameters and cloud condensation nuclei in CCM-Oslo. Oslo, University of Oslo (Institute Report series, 128).

Kiss, G., Varga, B., Galambos, I. and Ganszky, I. (2002) Characterization of water-soluble organic matter isolated from atmospheric fine aerosol. *J. Geophys. Res., 107D,* 8339, doi: 10.1029/2001JD000603.

Koelemeijer, R.B.A., Homan, C.D. and Matthijsen, J. (2006) Comparison of spatial and temporal variations of aerosol optical thickness and particulate matter over Europe. *Atmos. Environ., 40,* 5304-5315.

Kokhanovsky, A.A., von Hoyningen-Huene, W. and Burrows, J.P. (2006) Atmospheric aerosol load as derived from space. *Atmos. Res., 81,* 176-185.

Köpke, P., Anwender, D., Mech, M., Oppenrieder, A., Reuder, J., Ruggaber, A., Schreier, M., Schwander, H. and Schween, J. (2006) Actual state of the UV radiation transfer model package STAR. In: *IRS2004: Current problems in atmospheric radiation.* Ed. by Fischer and Sohn. Hampton, A. Deepak Publ., pp. 71-74.

Kupiainen, K. and Klimont, Z. (2004) Primary emissions of submicron and carbonaceous particles in Europe and the potential for their control. Laxenburg, IIASA (Interim report IR-04-079).

Levy, R.C., Remer, L.A., Mattoo, S., Vermote, E.F. and Kaufman, Y.J. (2007) Second-generation operational algorithm: Retrieval of aerosol properties over land from inversion of Moderate Resolution Imaging Spectroradiometer spectral reflectance. *J. Geophys. Res., 112,* doi:10.1029/2006JD007811.

Mahowald, N.M., Artaxo, P., Baker, A.R., Jickells, T.D., Okin, G.S., Randerson, J.T. and Townsend, A.R. (2005) Impacts of biomass burning emissions and land use change on Amazonian atmospheric phosphorus cycling and deposition. *Global Biogeochem. Cycles, 19,* GB4030.

Mareckova, K., Wankmüller, R., Wiesser, M., Poupa, S., Muik, B. and Anderl, M. (2008) Inventory review 2008 stage 1 and 2 and review of gridded data. Vienna, EEA (EEA/CEIP Report) (under preparation).

McDow, S.R. and Huntzicker, J.J. (1990) Vapor adsorption artifact in the sampling of organic aerosol: face velocity effects. *Atmos. Environ., 24A,* 2563-2571.

Meteorologisk institutt (2006) Climatological Monthly reports (www.met.no).

Mishchenko, M.I. and Travis, L.D. (2008) Electromagnetic scattering by particles and surfaces. http://www.giss.nasa.gov/~crmim. [Accessed 20080812].

Mishchenko, M.I., Travis, L.D. and Lacis, A.A. (2002) Scattering, absorption, and emission of light by small particles. Cambridge, Cambridge University Press.

Myhre, C.L., Toledano, C., Myhre, G., Stebel, K., Yttri, K.E., Aaltonen, V., Johnsrud, M., Frioud, M., Cachorro, V., de Frutos, A., Lihavainen, H., Campbell, J.R., Chaikovsky, A.P., Shiobara, M., Welton, E.J. and Tørseth, K. (2007) Regional aerosol optical properties and radiative impact of the extreme smoke event in the European Arctic in spring 2006. *Atmos. Chem. Phys., 7,* 5899-5915. http://www.atmos-chem-phys.net/7/5899/2007/acp-7-5899-2007.pdf

Penner, J.P., et al. (2001) Aerosols, their direct and indirect effects. In: *Climate Change 2001: The Scientific Basis. Contribution of Working Group I to the Third Assessment Report of the Intergovernmental Panel on Climate Change.* Ed. by J.T. Houghton et al. Cambridge, Cambridge Univ. Press. pp. 289–348.

Pio, C.A., Legrand, M., Oliveira, T., Afonso, J., Santos, C., Caseiro, A., Fialho, P., Barata, F., Puxbaum, H., Sánchez-Ochoa, A., Kasper-Giebl, A., Gelencsér, A., Preunkert, S. and Schock, M. (2007) Climatology of aerosol composition (organic versus inorganic) at non-urban sites on a west-east transect across Europe. J. *Geophys. Res., 112*, D23S02, doi: 10.1029/2006JD008080.

Puxbaum, H. and Tenze-Kunit, M. (2003) Size distribution and seasonal variation of atmospheric cellulose. *Atmos. Environ., 37*, 3693-3699.

Puxbaum, H., Caseiro, A., Sánchez-Ochoa, A., Kasper-Giebl, A., Caseiro, A., Claeys, M., Gelencser, A., Legrand, M., Preunkert, S. and Pio, C. (2007) Levoglucosan levels at background sites in Europe for assessing the impact of biomass combustion on the European aerosol background. *J. Geophys. Res., 112*, D23S05, doi: 10.1029/2006JD008114.

Remer, L.A., Tanré, D. and Kaufman, Y.J. (2006) Algorithm for remote sensing of tropospheric aerosol from MODIS: Collection 5. Product ID: MOD04/MYD04). NASA Goddard Space Flight Center, Code 913, Greenbelt, MD 20771, USA. http://modis.gsfc.nasa.gov/data/atbd/atbd_mod02.pdf

Saarikoski, S., Sillanpää, M., Sofiev, M., Timonen, H., Saarnio, K., Teinilä, K., Karppinen, A., Kukkonen, J. and Hillamo, R. (2007) Chemical composition of aerosols during a major biomass burning episode over nothern Europe in spring 2006: Experimental and modelling assessments. *Atmos. Environ, 41*, 3577-3589.

Sánchez-Ochoa, A., Kasper-Giebl, A., Puxbaum, H., Gelencsér, A., Legrand, M. and Pio, C.A. (2007) Concentrations of atmospheric cellulose, a proxy for plant debris, across a west-east transect over Europe. *J. Geophys. Res., 112*, D23S08, doi: 10.1029/2006JD008180.

Sattler, B., Puxbaum, H. and Psenner, R. (2001) Bacterial growth in supercooled cloud droplets. *Geophys. Res. Lett., 28,* 239-242.

Schmid, H., Laskus, L., Abraham, H.J., Baltensperger, U., Lavanchy, V., Bizjak, M., Burba, P., Cachier, H., Crow, D., Chow, J., Gnauk, T., Even, A., ten Brink, H.M., Giesen, K.-P., Hitzenberger, R., Hueglin, C., Maenhaut, W., Pio, C., Carvalho, A., Putaud, J.-P. and Toom-Sauntry, D. (2001) Results of the "carbon conference "international aerosol carbon round robin test stage I. *Atmos. Environ., 35,* 2111–2121.

Simpson, D., Yttri, K.E., Klimont, Z., Kupiainen, K., Caseiro, A., Gelencsér, A., Pio, C., Puxbaum, H. and Legrand, M. (2007) Modeling carbonaceous aerosol over Europe: Analysis of the CARBOSOL and EMEP EC/OC campaigns. *J. Geophys. Res., 112*, D23S14, doi:10.1029/2006JD008158.

Sokolik, I.N. and Toon, O.B. (1999) Incorporation of mineralogical composition into models of the radiative properties of mineral aerosol from UV to IR wavelengths. *J. Geophys. Res*., *104D*, 9423-9444.

Stohl, A., Berg, T., Burkhart, J.F., Fjæraa, A.M., Forster, C., Herber, A., Hov, Ø., Lunder, C., McMillan, W.W., Oltmans, S., Shiobara, M., Simpson, D., Solberg, S., Stebel, K., Ström, J., Tørseth, K., Treffeisen, R., Virkkunen, K. and Yttri, K.E. (2007) Arctic smoke – record high air pollution levels in the European Arctic due to agricultural fires in Eastern Europe. *Atmos. Chem. Phys., 7*, 511-534.

Tarrasón, L., Benedictow, A., Aas, W., Klein, H. and Vestreng, V. (2007) Transboundary pollution in 2005: an overview. In: *Transboundary acidification, eutrophication and ground level ozone in Europe.* Oslo, The Norwegian Meteorological Institute (EMEP Status report 1/2007). pp. 13-32.

Tsyro, S. (2005) To what extent can aerosol water explain the discrepancy between model calculated and gravimetric PM_{10} and $PM_{2.5}$? *Atmos. Chem. Phys., 5*, 602, 1-8.

Turpin. B. and Lim, H.-J. (2001) Species contributions to $PM_{2.5}$ mass: concentrations: Revisiting common assumptions for estimating organic mass. *Aerosol Sci. Technol., 35*, 602-610.

Veefkind, J.P., de Leeuw, G., Durkee, P.A., Russell, P.B., Hobbs, P.V. and Livingston, J.M. (1999) Aerosol optical depth retrieval using ATSR-2 data and AVHRR data during TARFOX. *J. Geophys. Res., 104D*, 2253-2260.

von Hoyningen-Huene, W., Freitag, M. and Burrows, J.B. (2003) Retrieval of aerosol optical thickness over land surfaces from top-of-atmosphere radiance. *J. Geophys. Res., 108*, D4260, doi: 10.1029/2001JD002018.

WHO (2005) WHO air quality guidelines global update. Report on working group meeting, Bonn, Germany, 18-20 October 2005. Copenhagen, World Health Organisation.

Winiwarter, W., Bauer, H., Caseiro, A. and Puxbaum H. (2008) Quantifying emissions of primary biological aerosol particle mass in Europe. *Atmos. Environ.*, doi: 10.1016/j.atmosenv.2008.01.037, in press.

Wittmaack, K., Wehnes, H., Heinzmann, U. and Agerer, R. (2005) An overview on bioaerosols viewed by scanning electron microscopy. *Sci. Total Environ.*, *346*, 244–255.

Yttri, K.E., Aas, W., Bjerke, A., Cape, J.N., Cavalli, F., Ceburnis, D., Dye, C., Emblico, L., Facchini, M.C., Forster, C., Hanssen, J.E., Hansson, H.C., Jennings, S.G., Maenhaut, W., Putaud, J.P. and Tørseth, K. (2007a) Elemental and organic carbon in PM_{10}: a one year measurement campaign within the European Monitoring and Evaluation Programme EMEP. *Atmos. Chem. Phys.*, *7*, 5711–5725, www.atmos-chem-phys.net/7/5711/2007/.

Yttri, K.E., Dye, C. and Kiss, G. (2007b) Ambient aerosol concentrations of sugars and sugar-alcohols at four different sites in Norway. *Atmos. Chem. Phys.*, *7*, 4267-4279, www.atmos-chem-phys.net/7/4267/2007/.

APPENDIX A

Figures to Chapter 5

Time-series of the concentrations of PM_{10}, $PM_{2.5}$ and their components as calculated with the EMEP model and measured during EMEP intensive periods in June 2006 and January 2007

Birkenes (NO01) June 2006

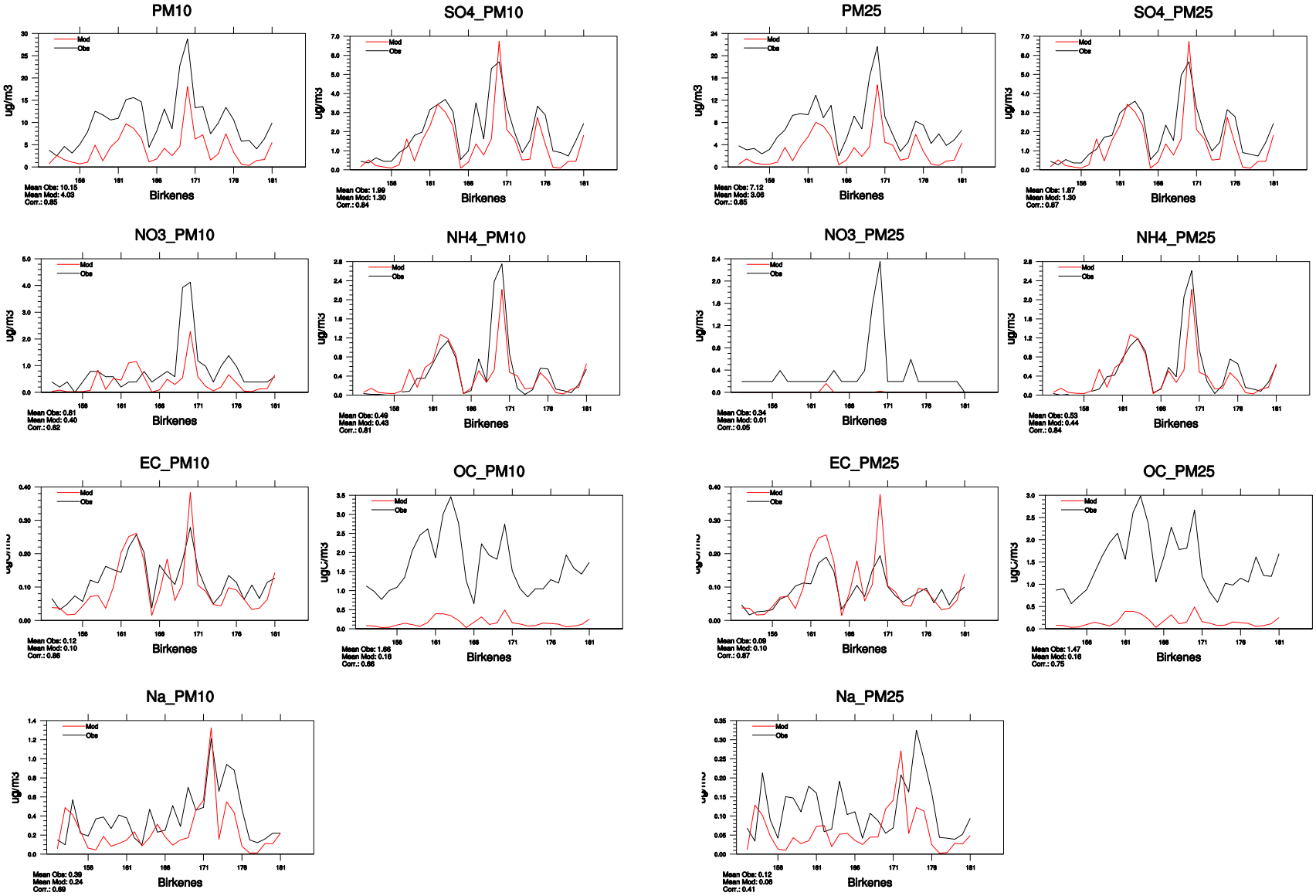

Birkenes (NO01) January 2007

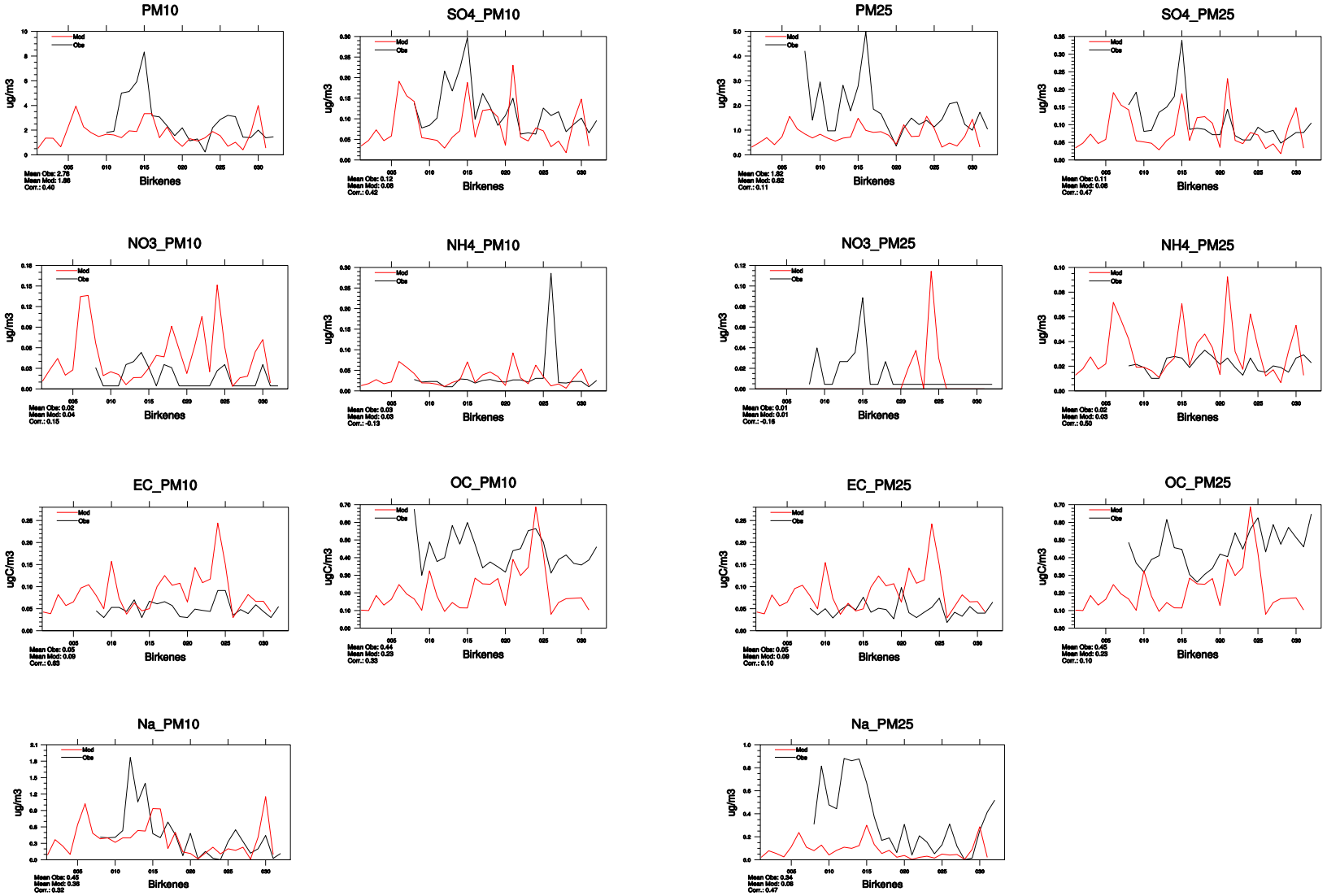

Melpitz (DE44) June 2006

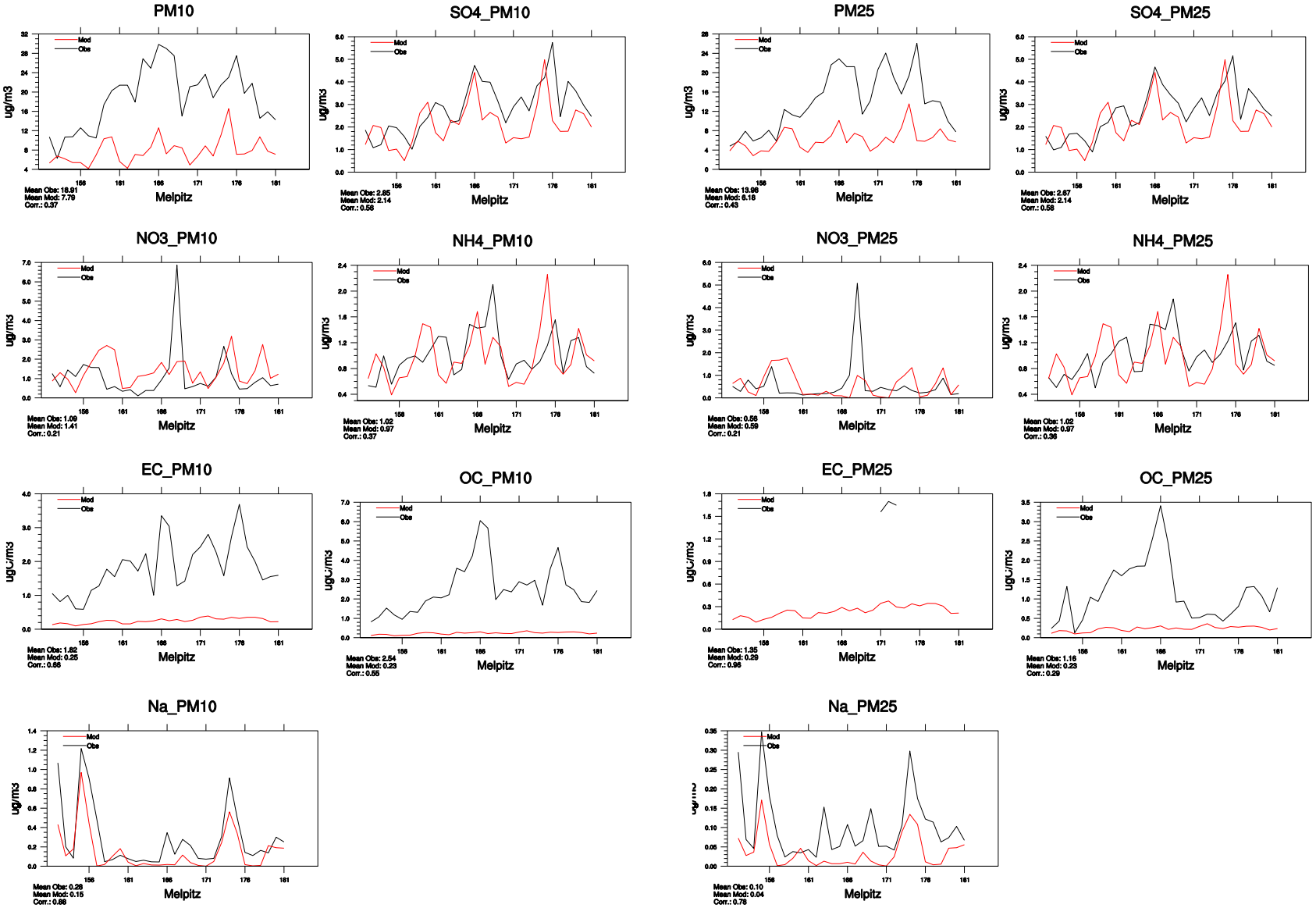

Melpitz (DE44) January 2007

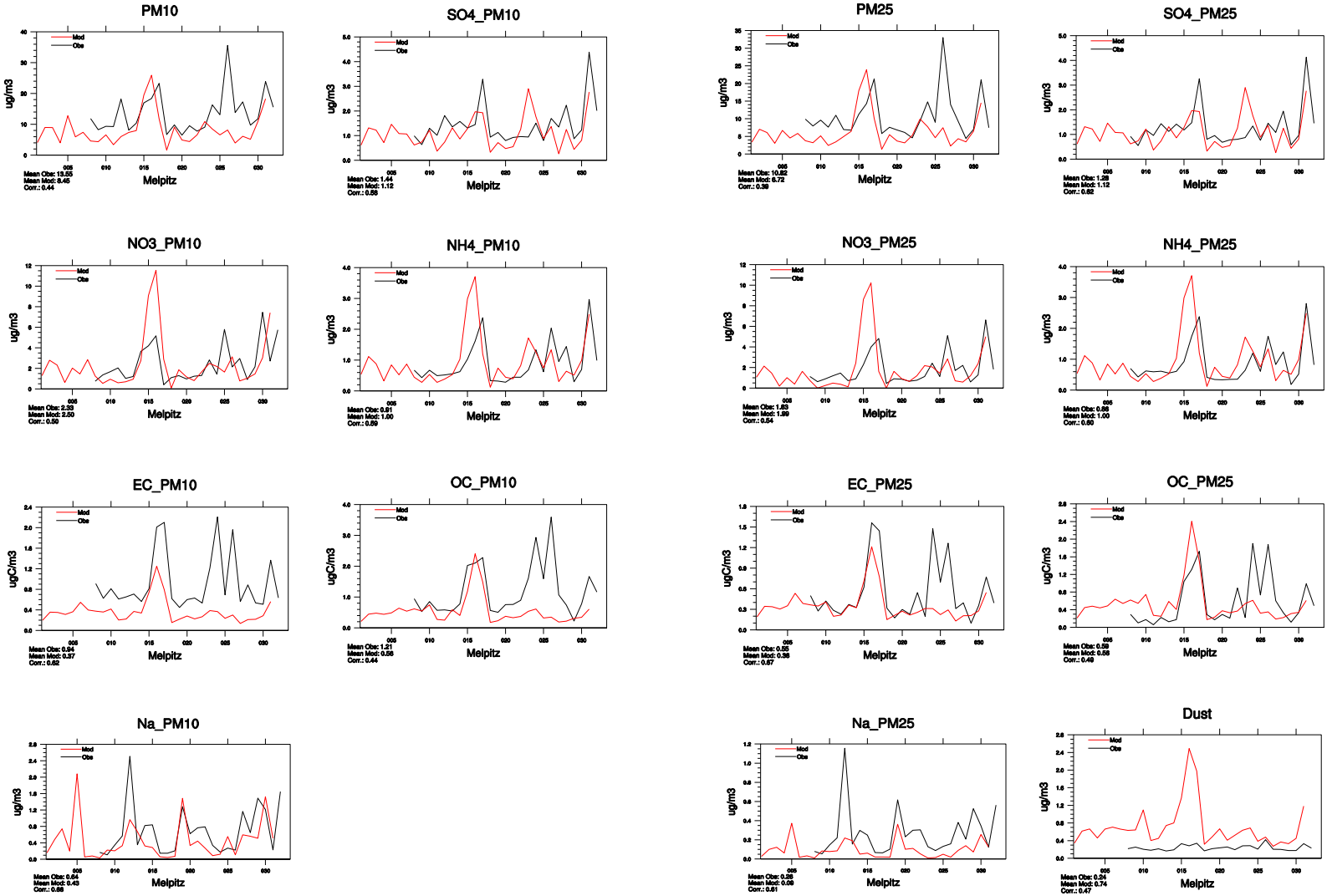

Montelibretti (IT01) June 2006

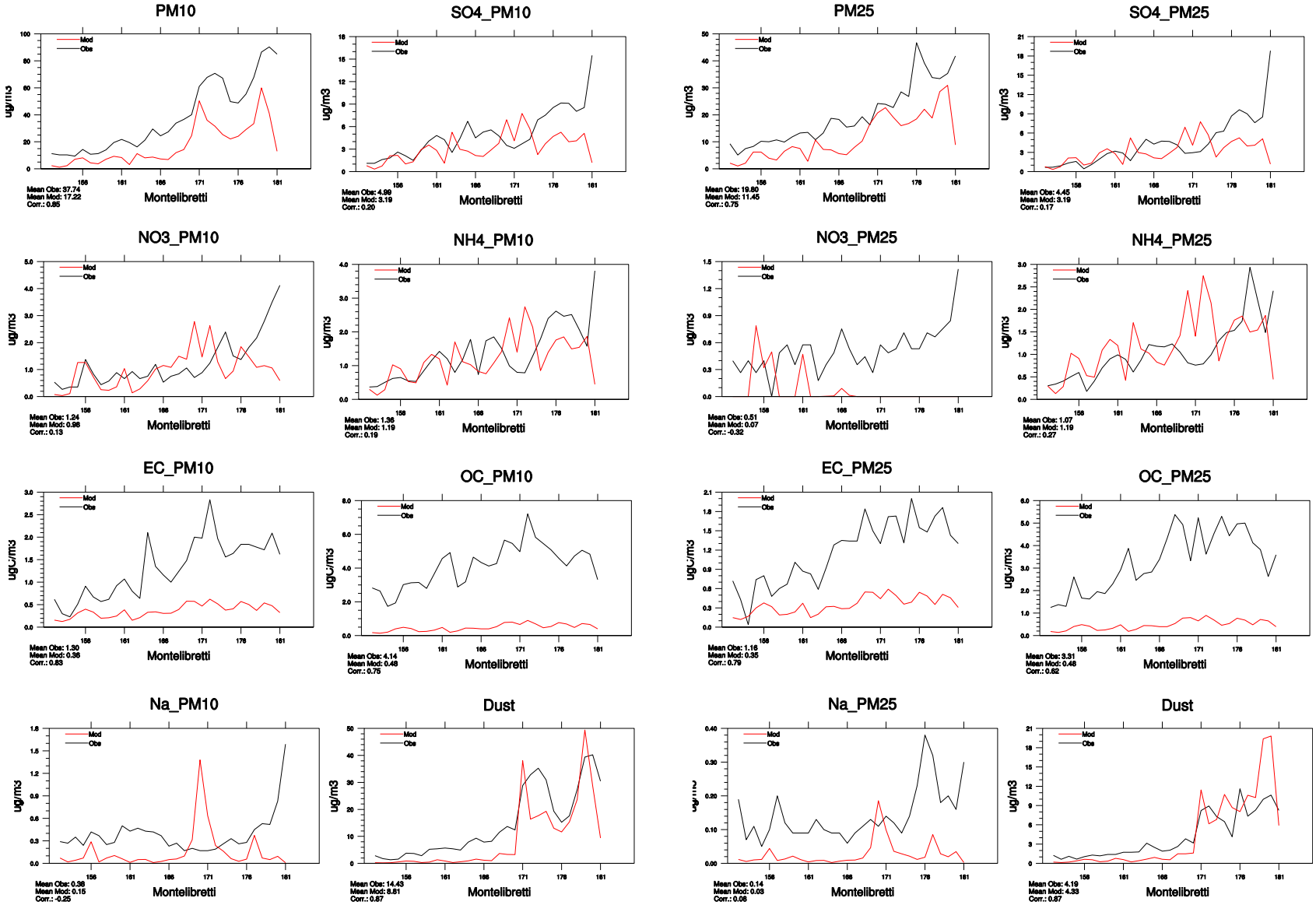

Montelibretti (IT01) January 2007

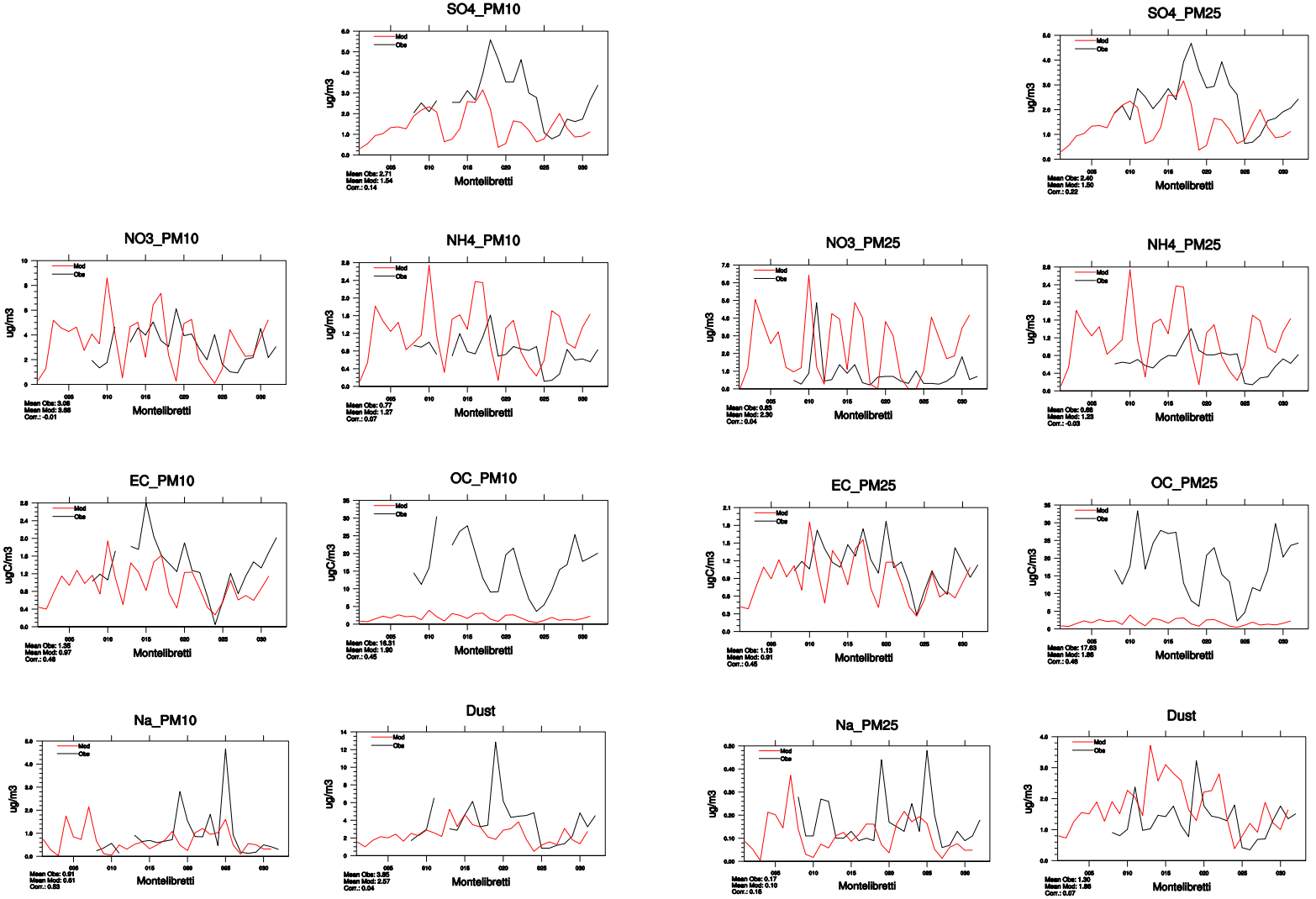

Virolahti (FI17) June 2006

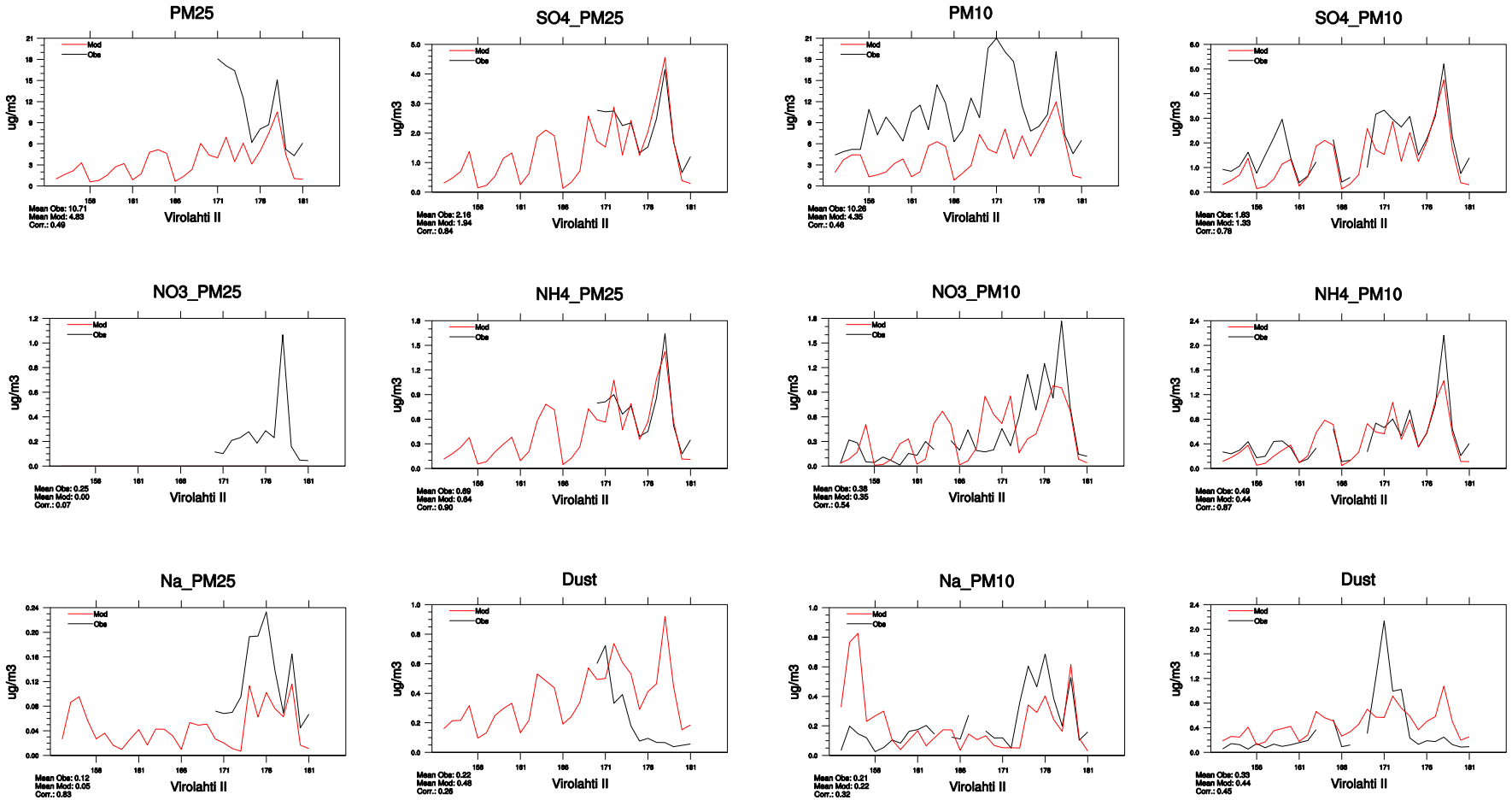

Virolahti (FI17) January 2007

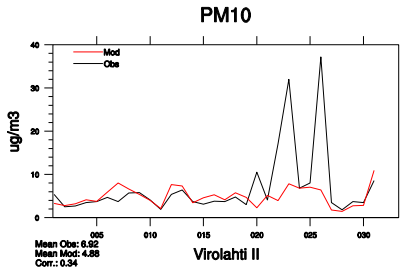

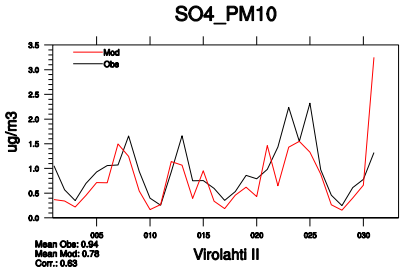

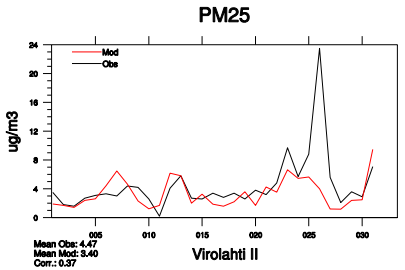

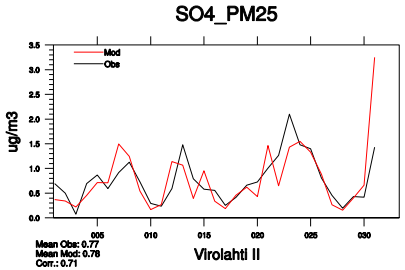

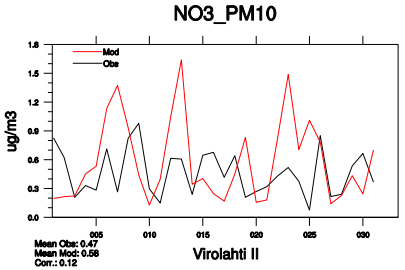

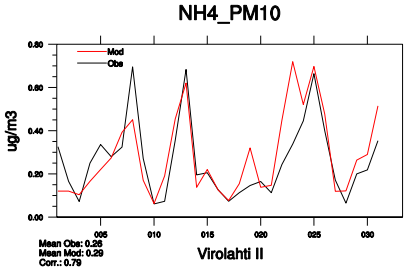

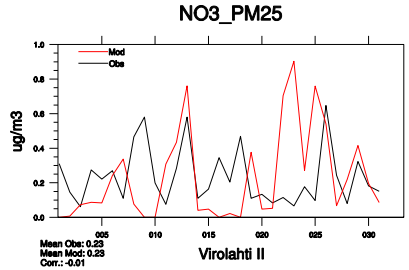

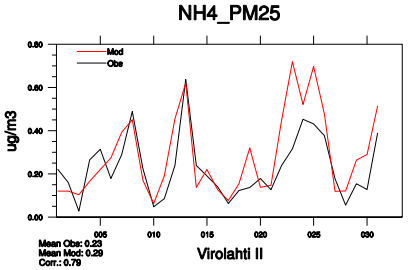

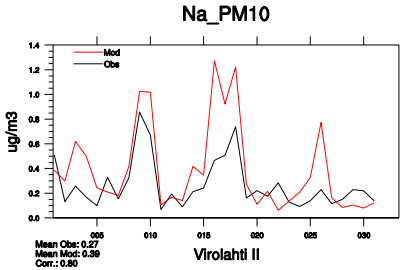

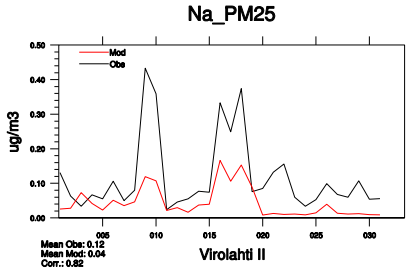

Montseny (ES17) June 2006

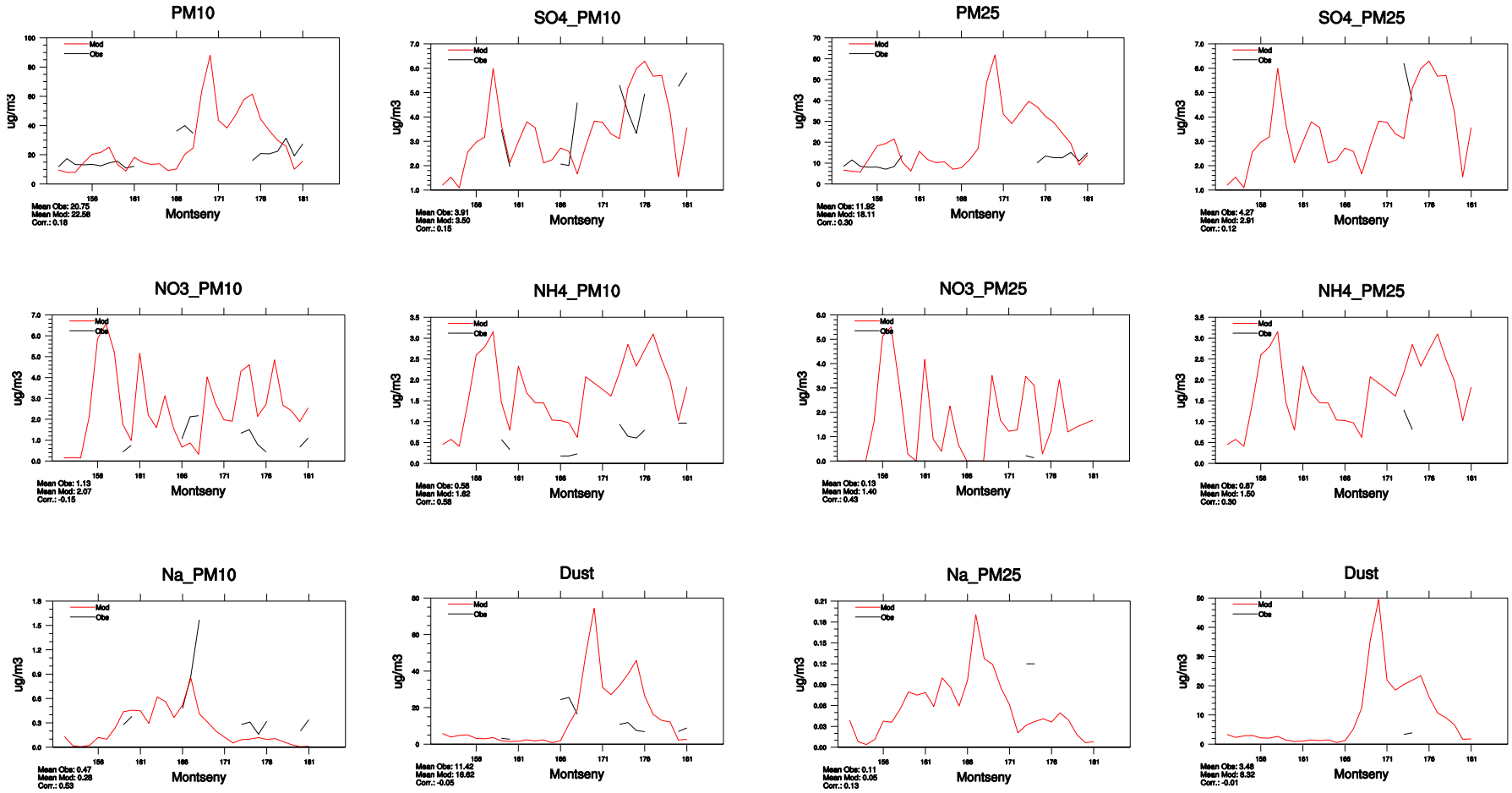

Montseny (ES17) January 2007

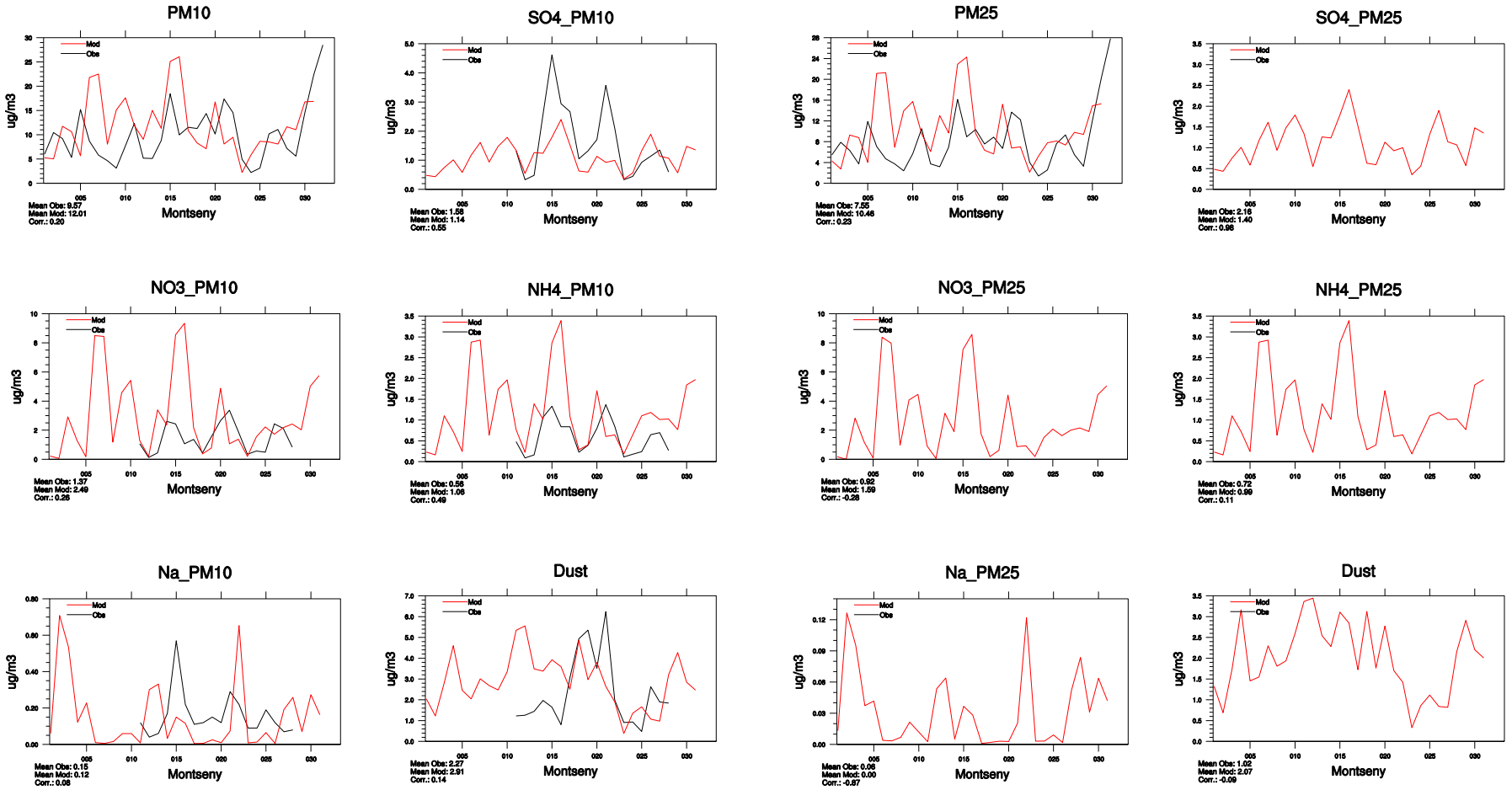

Ispra (IT04)

June 2006 January 2007 June 2006 January 2007

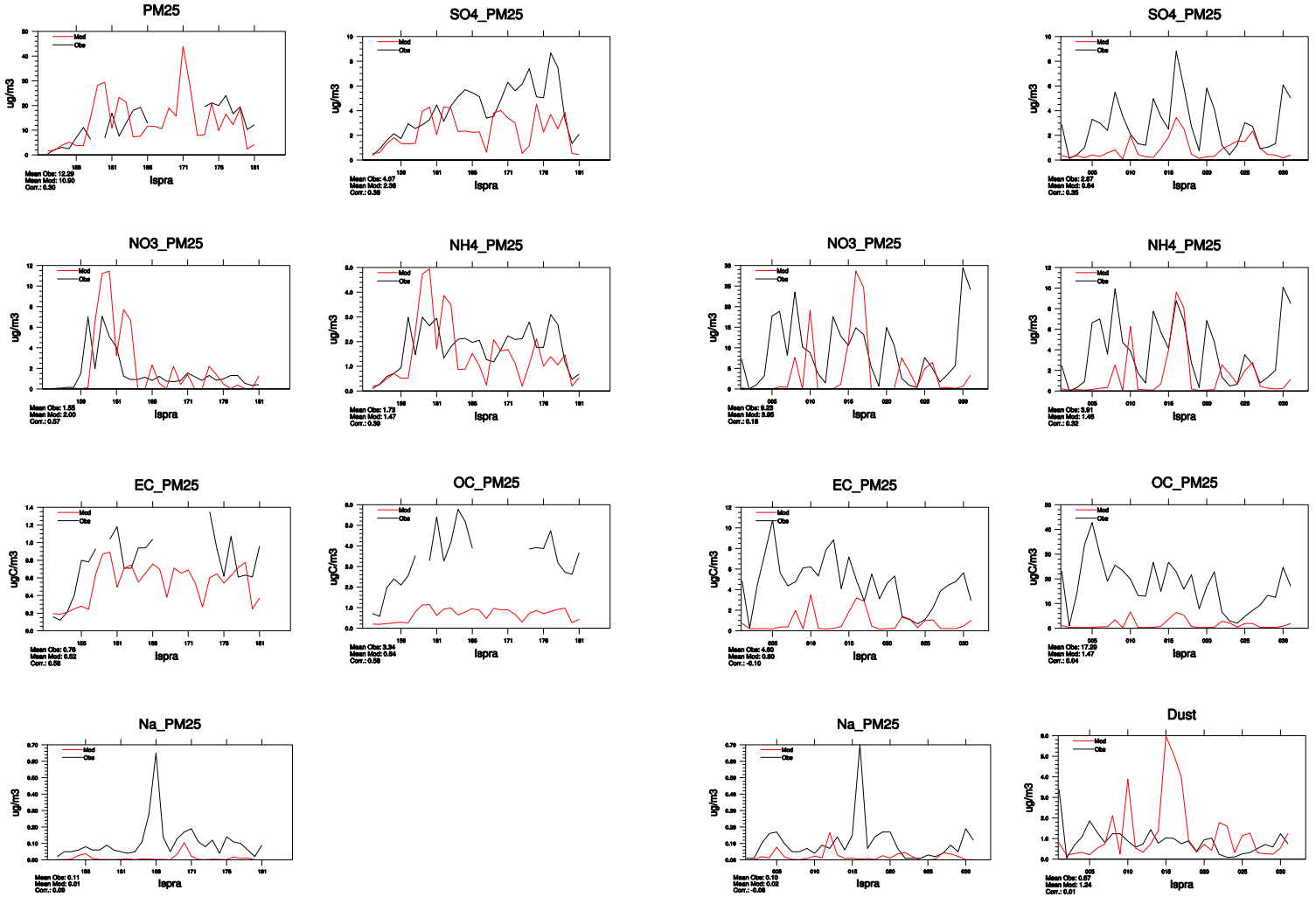

Payerne (CH02)

June 2006

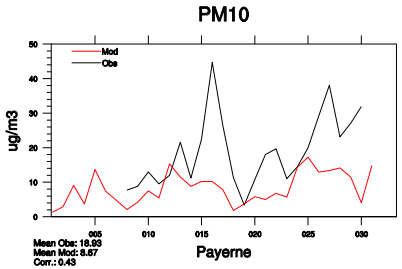

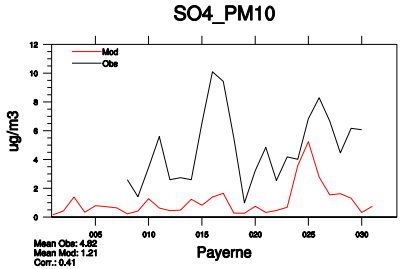

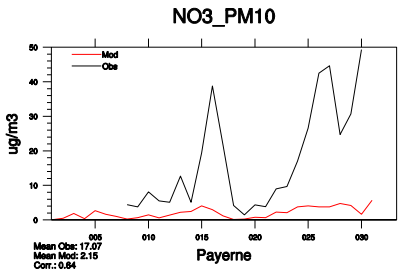

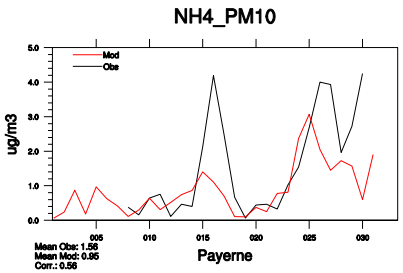

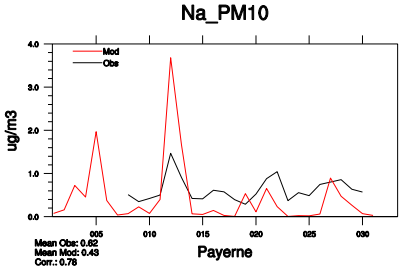

January 2007

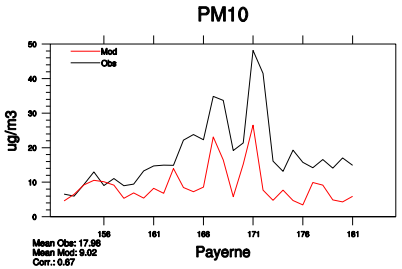

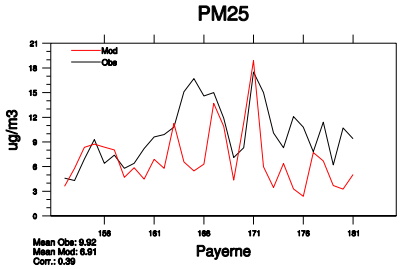

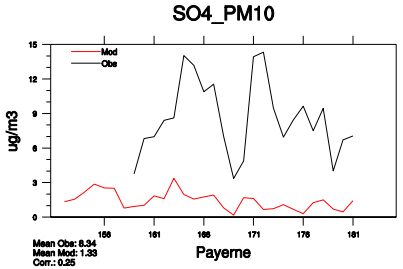

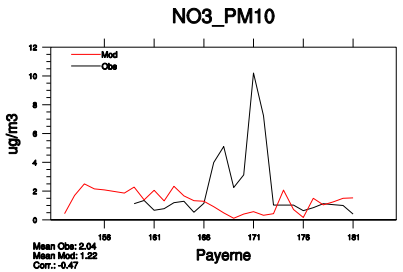

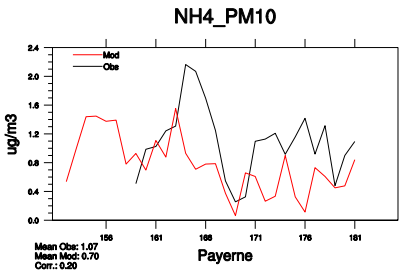

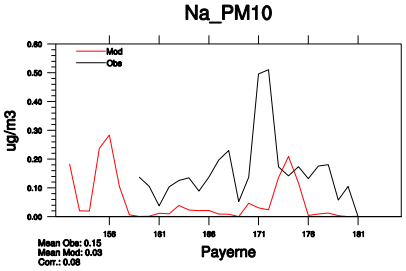

Illmitz (AT02)

June 2006 January 2007

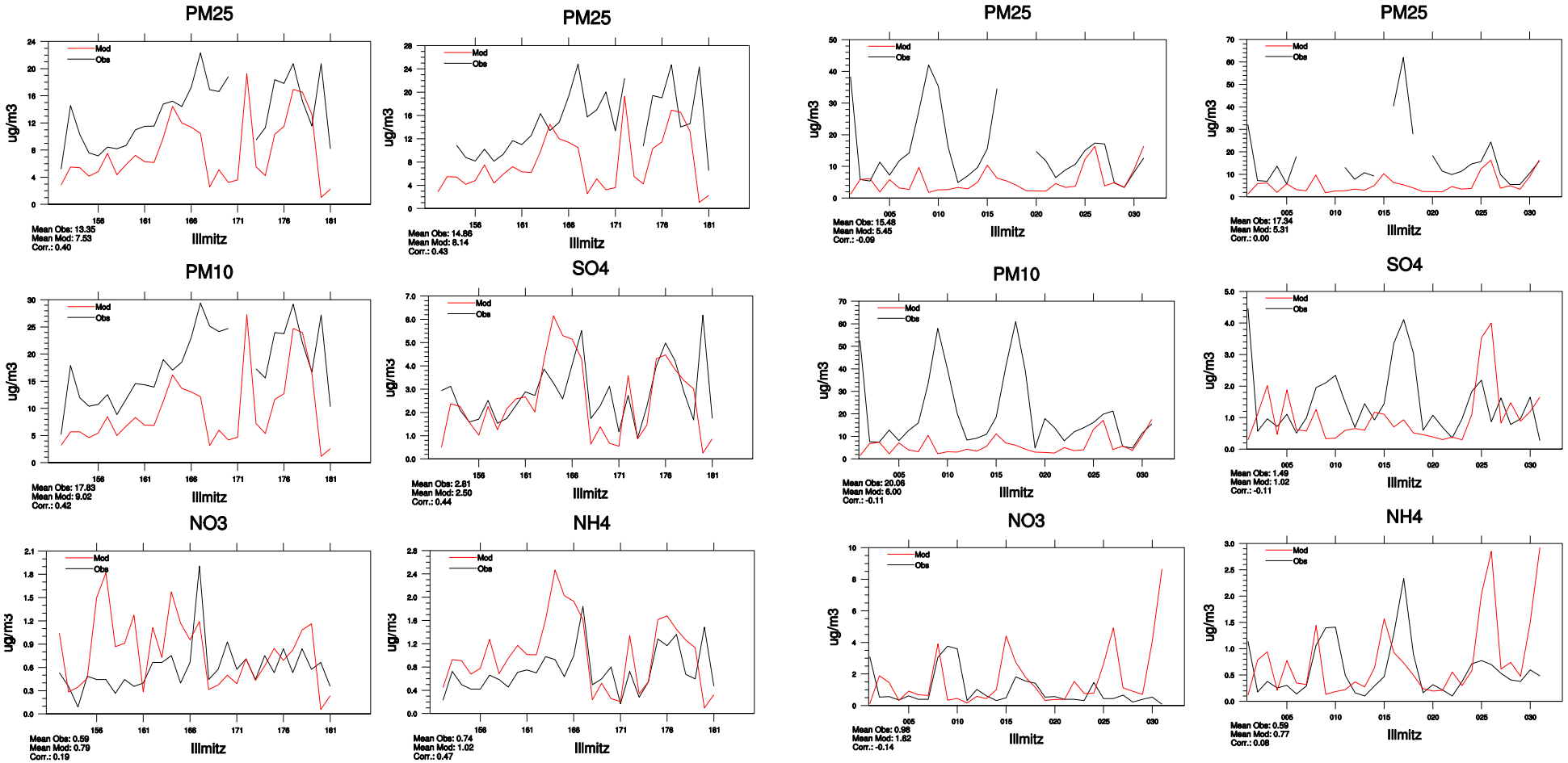

Note: Daily time series of $PM_{2.5}$ on the right hand side are based on hourly measurements for both June 2006 and January 2007

Coarse NO_3^-

June 2006

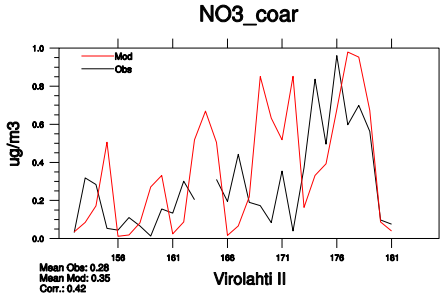

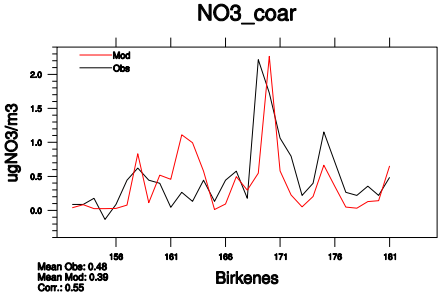

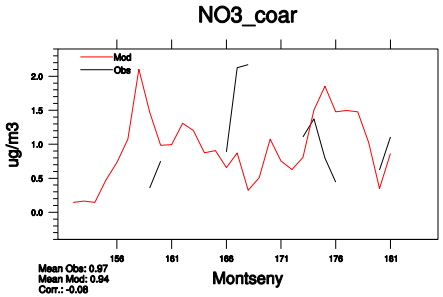

January 2007

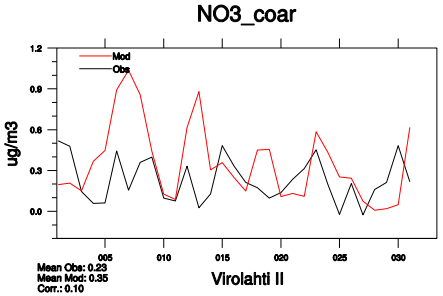

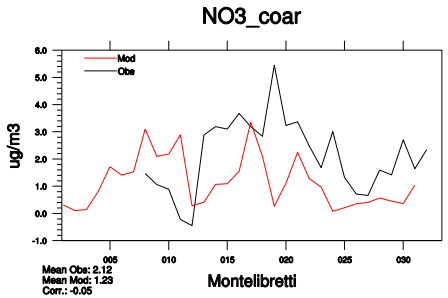

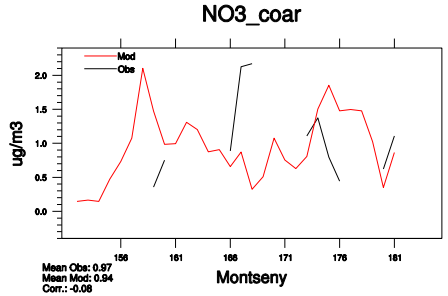

Coarse Na^+

June 2006 | January 2007 | June 2006 | January 2007

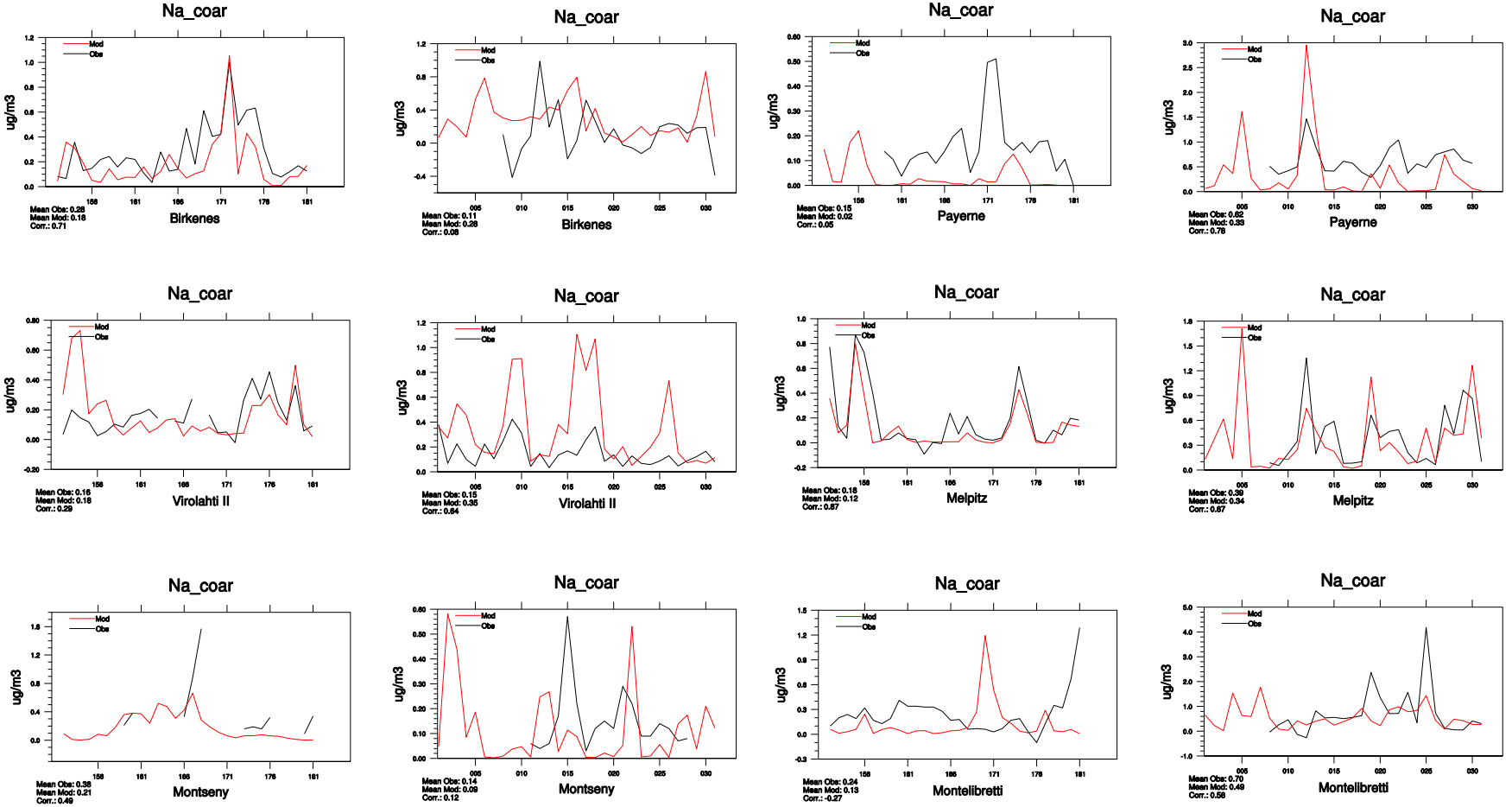

emep

Meteorological Synthesizing Centre – West
Norwegian Meteorological Institute
P.O.Box 43 – Blindern, N-0313 Oslo, Norway

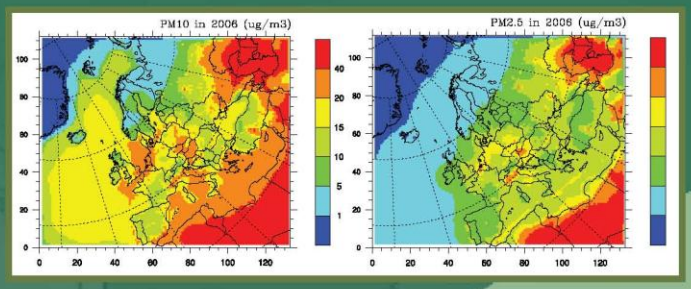

ccc
Norwegian Institute
for Air Research (NILU)
P.O. Box 100
NO-2027 Kjeller
Norway
Phone: +47 63 89 80 00
Fax: +47 63 89 80 50
E-mail: kjetil.torseth@nilu.no
Internet: www.nilu.no

ciam
International Institute for
Applied Systems Analysis
(IIASA)
A-2361 Laxenburg
Austria
Phone: +43 2236 80 70
Fax: +43 2236 71 31
E-mail: amann@iiasa.ac.at
Internet: www.iiasa.ac.at

ceip
Umweltbundesamt GmbH
Spittelauer Lände 5
1090 Wien
Austria
Phone: +43-(0)1-313 04
Fax: +43-(0)1-313 04/5400
E-mail:
emep.emissions@umweltbundesamt.at
Internet:
www.umweltbundesamt.at/

msc-e
Meteorological Synthesizing
Centre-East
Krasina pereulok, 16/1
123056 Moscow
Russia
Phone: +7 495 981 15 66
Fax: +7 495 981 15 67
E-mail: msce@msceast.org
Internet: www.msceast.org

msc-w
Norwegian Meteorological
Institute (met.no)
P.O. Box 43 Blindern
NO-0313 OSLO
Norway
Phone: +47 22 96 30 00
Fax: +47 22 96 30 50
E-mail: emep.mscw@met.no
Internet: www.emep.int